Stochastische modellering van draadloze sensornetwerken

Stochastic modelling of wireless sensor networks

Kishor Patil

Promotoren: prof. dr. ing. D. Fiems, dr. ir. K. De Turck
Proefschrift ingediend tot het behalen van de graad van
Doctor in de Ingenieurswetenschappen

UNIVERSITEIT
GENT

Vakgroep Telecommunicatie en Informatieverwerking
Faculteit Ingenieurswetenschappen
Academiejaar 2018 – 2019

ISBN 978-94-6355-280-6
NUR 919, 986
Wettelijk depot: D/2019/10.500/88

Examination committee:
Chairman: prof. dr. ir. Gert de Cooman
Promoters: prof. dr. ing. Dieter Fiems
dr. ir. Koen De Turck
prof. dr. ir. Urtzi Ayesta
prof. dr. Dieter Claeys
prof. dr. ir. Tuan Phung-Duc
prof. dr. ir. Heidi Steendam
prof. dr. ir. Joris Walraevens

Acknowledgements

This dissertation would not have been possible without the guidance of my advisers, support of my friends and the love of my family. First, I would like to thank my advisers prof. Dieter Fiems and dr. Koen De Turck for guiding me through this dissertation and also through the last four years of graduate studies. Especially, I would like to express my gratitude and respect towards prof. Fiems for giving his valuable time to discuss my dissertation, during office hours, non-office hours, holidays and even during his leave through emails. His constructive criticism has been the key to bring the report to its current form.

I thank Ghent University and the Department of Telecommunications and Information Processing (TELIN) for providing all the academic facilities that were required during the course of the research. I would also like to thank the fellow graduate students of the TELIN Department; Bo Bo and Mohammad for always creating a nice atmosphere in the office, my former colleague Katia for helping me with all the practical arrangements when I first arrived in Belgium and Apoorv, Joachim and Sofian for snooker games and tournaments in the department. I would also like to thank my friends at other Departments of the University - Harish, Kannaki and Renu for making my stay a truly wonderful experience.

I deeply appreciate the faith and encouragement shown by my family without which the work could have never been possible. I am especially grateful to my parents for their support and love throughout my life.

Kishor Patil

Contents

List of Figures

Samenvatting

In onze fysieke omgeving kan men veel verschillende soorten ruimtelijk verspreide informatie meten. Enkele typische voorbeelden zijn temperatuur, vochtigheid, druk, trillingen, geluid, enz. Draadloze sensornetwerken (Wireless Sensor Networks, WSN's) zijn ontwikkeld om deze informatie uit de fysieke wereld te verzamelen en door te geven aan de digitale wereld voor verdere verwerking. WSN's kunnen verschillende praktische toepassingen ondersteunen, zoals de bescherming van civiele infrastructuren, habitatmonitoring, precisielandbouw, detectie van giftige gassen of gezondheidsmonitoring op afstand. Een typisch WSN bestaat uit een verzameling uiterst kleine sensoren, verspreid over een bepaald gebied, die informatie in hun onmiddellijke omgeving verzamelen, en uitgerust zijn met zender-ontvangers om de informatie door te zenden. Daarenboven is elke sensor uitgerust met een geheugenchip en een kleine batterij. De geheugenchip kan de sensorinformatie tijdelijk opslaan en alle vermogen die nodig is voor het detecteren, verwerken en doorgeven van deze informatie wordt onttrokken aan de batterij. Omdat sensoren doorgaans ruimtelijk worden verspreid, is het duur, of zelfs onmogelijk, om batterijen te vervangen eenmaal de sensoren verspreid zijn. Een onmiddellijk gevolg hiervan is dat de capaciteit van de batterij de levensduur van de sensor beperkt. De sensor is nu eenmaal niet langer operationeel als de batterij leeg is. In sommige gevallen wordt daarom de communicatie geoptimaliseerd met betrekking tot energieverbruik. In veel andere toepassingen worden sensoren voorzien van een hernieuwbare energiebron zodat bijkomende energie kan onttrokken worden aan omgevingsbronnen, zoals bijvoorbeeld de zon, de wind of warmte. Zowel het scenario met als het scenario zonder energiebron legt extra beperkingen en enorme uitdagingen op bij het ontwerp en de modellering van draadloze sensornetwerken. Energiebronnen zoals wind, zon en warmte fluctueren in de loop van de tijd, zodat de hoeveelheid energie die kan onttrokken worden ook fluctueert. Dergelijk tijdsvariërend gedrag kan de prestaties van het netwerk sterk beïnvloeden.

In dit proefschrift onderzoeken we de prestaties van draadloze sensornetwerken aan de hand van een aantal stochastische modellen. Deze modellen leggen de belangrijkste onzekerheden vast die de dynamiek van de WSNs bepalen, zoals bijvoorbeeld het onttrekken van energie, het energieverbruik, en de gegevensoverdracht. Het belangrijkste doel van het netwerk is om zoveel mogelijk informatie te verzamelen en tegelijkertijd het energieverbruik tot een minimum te beperken. Over het algemeen wordt een aanzienlijke hoeveelheid energie verbruikt om verschillende WSN-operaties uit te voeren, zoals detectie, verwerking en transmissie. De hoeveelheid energieverbruik is echter niet voor elke operatie gelijk. Transmis-

sies vereisen bijvoorbeeld aanzienlijk meer energie dan waarnemingen. Bovendien kunnen voor een optimaal ontworpen WSN beslissingen om al dan niet te verzenden worden beïnvloed door verschillende attributen van de informatie, inclusief de kwaliteit en de waarde van de informatie. De kwaliteit van informatie (quality of information, QoI) houdt rekening met de nauwkeurigheid, consistentie, volledigheid en tijdigheid van de informatie. De waarde van informatie (value of information, VoI) beschrijft daarentegen het belang van de informatie. Elke keer dat een sensor iets detecteert, verzamelt het informatie die al dan niet belangrijk kan zijn. We modelleren de evolutie van de VoI onder verschillende assumpties en onderzoeken de impact van deze assumpties op de algemene prestaties van het netwerk.

In het eerste deel introduceren we stochastische modellen die een statische sensorknoop isoleren van de rest van het netwerk, en bestuderen we de interactie tussen gegevensverzameling, energieopname en energieverbruik. Afhankelijk van de aard van de waarde van het informatieproces, stellen we verschillende modellen voor. Aanvankelijk gaan we ervan uit dat de waarde van informatie additief is, d.w.z. dat we nieuw gemeten sensorwaarde kunnen optellen bij de reeds gevatte waarde in de knoop. Het model voorziet in een redelijk algemeen proces om de sensorwaarden doorheen de tijd te beschrijven: we veronderstellen een stationair ergodisch maar niet noodzakelijk Markoviaans model voor om de prestaties van een statische sensorknoop te evalueren. Het basisraamwerk stelt ons in staat om de evolutie van het batterijniveau en de VoI te schrijven in termen van een stelsel van recursieve vergelijkingen voor de stationaire ergodische rij. We maken gebruik van de lineariteit van de vergelijkingen om het gedrag op lange termijn van de verschillende netwerkprocessen te analyseren. We bewijzen in het bijzonder het bestaan van een stationair ergodisch proces voor de batterijniveaus en de VoI. De ergodiciteit stelt ons verder in staat om het lange-termijngemiddelde gedrag van het systeem af te leiden. Hierbij berekenen we verschillende prestatiematen zoals de stationaire verdeling van het batterijniveau en de gemiddelde waarde van informatie verzameld door een mobiele knoop. We berekenen ook het tweede moment om de spreiding van de waarde van informatie van zijn gemiddelde waarde in te kunnen schatten. Een andere uitbreiding van het basismodel vat het gecorreleerde gedrag van de energiecaptatie in meer detail. We includeren deze tijdscorrelatie door de energiecaptatie te modelleren aan de hand van een Markov-gemoduleerd proces. Enkele numerieke voorbeelden illusteren dat tijdcorrelatie een aanzienlijke invloed heeft op de algehele prestaties van de sensor.

In sommige toepassingen wordt informatie gewaardeerd op basis van de leeftijd van de informatie, i.e., hoe recenter hoe waardevoller. In dergelijke gevallen wordt de informatie in de sensorknoop vervangen als de knoop nieuwe waardevollere informatie ontvangt, hetzij vanuit de omgeving of van een naburige sensor. Dit motiveerde ons om VoI met een niet-additieve karakter te beschouwen, dat bekend staat als de “age of information” of de leeftijd van de informatie. Om de prestaties van een dergelijk netwerk te onderzoeken, ontwikkelen we een stochastisch model dat steunt op het kader van de Markov-beslissingsprocessen (Markov decision processes, MDPs). In tegenstelling tot de modellen in de vorige paragraaf, laat dit

raamwerk niet alleen toe om de prestaties van sensoren te bepalen, maar kan het ook de optimale controle vinden zodat mogelijks verschillende ontwerpdoelstellingen met elkaar kunnen verzoend worden. Men kan bijvoorbeeld streven naar het minimaliseren van het energieverbruik of het maximaliseren van de waargenomen informatie. In het bijzonder richten we ons op het bepalen van de optimale transmissiecontrole zodat de maximale VoI een (mobiele) centrale knoop bereikt. Bovendien maken we gebruik van de quasi-birth-death-structuur van het probleem en gebruiken we het policy-iteratie algoritme om de optimale controle te bepalen. De oplossing laat zien dat de beslissing om te zenden enkel afhangt van een VoI-drempelwaarde, zodat de controle in de praktijk zeer eenvoudig te implementeren is.

In tegenstelling tot de modellen voor een geïsoleerde knoop in het eerste deel, breiden we het controleraamwerk uit naar grootschalige draadloze sensornetwerken in het tweede deel. We bestuderen netwerken waarbij een groot aantal sensoren met elkaar interageren om de informatie door te geven aan een bepaalde eindknoop, mogelijks in meerdere stappen. De interactie tussen sensoren heeft meerdere voordelen, zoals een lager energieverbruik, het afdekken van een groter gebied en een verbeterde connectiviteit met de eindknoop. Vanuit wiskundig oogpunt zijn stochastische modellen voor dergelijke netwerken een uitdaging en vaak te complex om exact op te lossen. Hoewel het mogelijk is om een Markov-proces formeel te introduceren voor het volledige netwerk, is het numeriek evalueren van het Markov-proces (d.w.z. het oplossen van de zogenaamde balansvergelijkingen) rekenkundig zwaar en enkel praktisch haalbaar voor netwerken met slechts een paar knooppunten. Deze Markoviaanse modellen hebben meestal een multidimensionale toestandsruimte (één dimensie per sensor) en hebben daarom last van wat bekend staat als het probleem van de toestand-ruimte-explosie. Schalingstechnieken, zoals vloeistoflimieten en diffusiebenaderingen, bieden een manier om een dergelijk probleem gedeeltelijk te ondervangen. Daarom evalueren we de prestaties van ons grootschalige WSN-model binnen het zogenaamde mean-field-limietraamwerk. Door de waarnemings- en interactiesnelheden op de juiste manier te schalen, kunnen we de evolutie van het WSN beschrijven aan de hand van een set gewone differentiaalvergelijkijgen (ODE), althans wanneer het aantal sensorknooppunten groot is. Dit is een belangrijk voordeel: in de limiet kunnen we het stochastische controleprobleem vervangen door een deterministisch controleprobleem dat aanzienlijk gemakkelijker is op te lossen. We bewijzen formeel de convergentie van het Markoviaans netwerkmodel naar de oplossing van de set differentiaalvergelijkingen en vinden het optimale controlebeleid in deze limiet. In de pre-limiet kan men dan verwachten dat de gevonden controle zo goed als optimaal is. Om deze aanpak te illustreren, onderzoeken we verder een systeem waarbij de sensoren in drie toestanden kunnen zijn en onderzoeken we zowel theoretisch als numeriek de optimale transmissiecontrole. Bovendien valideren we de mean-fieldbenadering door middel van Monte-Carlo-simulaties door de prestaties van het willekeurige systeem te vergelijken met de mean-fieldlimiet.

In een laatste deel concentreren we ons op een specifiek type WSN, namelijk onderwater-WSN's (underwater WSN, UWSN). In dit deel ontwikkelen we een

numeriek traceerbaar stochastisch model om de prestaties van het depth-based-routeringsprotocol in UWSN's te beoordelen, wat één van de belangrijkste routeringsprotocollen is voor dergelijke netwerken. De snelheid van het akoestische signaal in UWSNs verschilt erg van de snelheid van de signalen voor land-WSNs. De tijd die een pakket nodig heeft om van de ene naar de andere sensor te reizen is dan ook significant. Naast de gemiddelde bron-tot-oppervlaktetransmissietijd, verkrijgen we ook uitdrukkingen voor andere prestatiematen zoals de distributie van het aantal hops en het gemiddelde energieverbruik. We valideren ons stochastische model door de berekende prestatiematen te vergelijken met schattingen die zijn verkregen door stochastische simulatie. We vergelijken ook nog de computationele complexiteit van het model en de simulatie en tonen aan dat het stochastische model de prestatie veel sneller kan inschatten.

Summary

Our physical environment exhibits many diverse types of spatially distributed information. This information can be anything like temperature, humidity, pressure, vibration, sound, etc. Wireless sensor networks (WSNs) are developed to collect this information from the physical world and provide it to the digital world for further processing. WSNs can support various practical applications, like the protection of civil infrastructures, habitat monitoring, precision agriculture, toxic gas detection and remote health monitoring. A typical WSN is formed by a collection of tiny sensor nodes, equipped with transceivers and distributed over some area of interest that collect data from their environment. In particular, each sensor node is equipped with on-board memory and a small battery. The on-board memory stores the information that is sensed from the environment and all the power required for sensing, processing and relaying this information is drawn from the battery. As sensor nodes are typically spatially deployed, it is expensive if not impossible to replace batteries once the nodes are deployed. As a consequence, the battery capacity limits the lifetime of the sensor node as the sensor node fails once it is out of energy. In some cases, the communication is optimised with respect to energy consumption, whereas many other applications rely on energy harvesting sensors which extract the energy from ambient sources such as solar, wind or heat. Both scenarios with and without energy harvesting impose additional constraints and formidable challenges in the design and modelling of wireless sensor networks. For example, external conditions from which the harvesting circuitry draws its energy fluctuate over time, so the amount of energy that can be harvested fluctuates as well. Such time-varying behaviour can greatly affect the performance of the network and thus extra care is needed while designing such networks.

In this dissertation, we investigate the performance of a wireless sensor network through a number of stochastic models. These models capture the key uncertainties that determine the dynamics of the WSN, like energy harvesting and consumption, and data transmissions. The main goal of the network is to gather as much information as possible while keeping the energy expenditure at a minimum. In general, a significant amount of energy is consumed to perform various WSN operations such as sensing, processing and transmitting. However, the amount of energy consumption is not the same for each operation. For example, transmissions require considerably more energy than sensing and processing. Moreover, for an optimally designed WSN, transmission decisions can be influenced by different attributes of the information like the quality or the value of information. The quality of information (QoI) accounts for accuracy, consistency, completeness, and

timeliness of the information whereas the value of information (VoI) describes the importance of the information. Each time a node senses, it gathers information that may or may not be important. We model the evolution of the VoI by two different processes and investigate the impact of their nature on the overall performance of the network.

In the first part, we propose stochastic models for a sensor node in isolation that assess the interaction between data collection, energy harvesting and energy expenditure. Depending on the particular nature of the value of information process, we propose different models. Initially, we assume that the value of information is additive and propose a stationary ergodic but not necessarily Markovian model to evaluate the performance of a sensor node. The basic framework allows us to write the battery level and VoI in terms of a set of recursions, which define a stationary ergodic sequence. We take advantage of the linearity of the equations to analyse the long term behaviour of the different network processes. We prove the existence of a stationary ergodic process consisting of battery levels and VoI. The ergodicity further allows us to derive the long-term average performance of the system in terms of the model parameters. Performance measures include the stationary distribution of the battery levels and the mean value of information collected by a mobile sink at a particular battery level. We also calculate the second moment to investigate the spread of the value of information from its average value. Another extension of the basic model is inspired by the correlated behaviour of the harvesting process. We capture the time correlation by modelling the energy harvesting process by a Markov modulated process and show that time correlation has a significant impact on the overall performance of the sensor node.

In some applications, information is valued on the basis of its freshness. In such cases, information is not additive, but replaced if the node receives updated information either from the environment or from a neighbouring node. This motivates us to consider the non-additive nature of the VoI, which is widely known as the age of information. To investigate the performance of such a network, we develop a stochastic model within the framework of Markov decision processes. Unlike the previous models, this framework not only calculates the performance of a static control policy of the sensor node, but also allows for finding the optimal control policy that balances possibly different design objectives. For example, one may aim at minimising the energy consumption or at maximising the sensed information. In particular, we focus on obtaining the optimal transmission policy that achieves the maximum collection of VoI at a mobile sink. Furthermore, we exploit the quasi-birth-death structure of the problem and use the policy iteration algorithm to obtain the optimal control. The solution reveals that the optimal policy is a threshold policy that is very easy to implement in practice.

While the first part assesses performance of sensor nodes, we extend the control framework to large-scale wireless sensor networks in the second part. In this part we focus on networks where a large number of sensor nodes interact with each other to pass on the information to a dedicated sink in multiple hops. The interaction among nodes has multiple benefits such as reduced energy expenditure, coverage of a larger area and improved connectivity to the sink. From a math-

ematical point of view, stochastic models for such networks are challenging and often too complex to allow for obtaining an exact solution. While it is possible to formally introduce the Markov process that models the complete network, assessing the Markov process numerically (i.e., solving the so-called balance equations) is computationally expensive, and only practically feasible for networks with but a few nodes. These Markovian models typically have a multidimensional state space (one dimension per node) and therefore suffer from what is known as the state-space-explosion problem. Scaling techniques like fluid limits and mean-field approximations offer a way to partially overcome the state-space-explosion problem. Therefore, we evaluate the performance of our large scale WSN model within the framework of mean-field limits. By properly scaling the sensing and interaction rates, we find that the evolution of the WSN model can be described by a set of ordinary differential (ODE) equations when the number of sensor nodes is large. This is a key advantage: in the limit the stochastic control problem reduces to a deterministic control problem that is considerably easier to solve. We formally prove the convergence of the network model to the solution of the ODE and find the optimal control policy in this limit. We then also obtain a good approximation of the optimal control policy in the pre-limit. To illustrate the approach, we further investigate a system where the sensor nodes can be in three states and investigate the optimal transmission policy theoretically as well as numerically. Moreover, we validate the mean-field approximation through Monte-Carlo simulations by comparing the performance of the random system to the mean-field limit.

In a last part, we focus on a particular type of WSN, namely underwater WSNs. In this part, we develop a numerically tractable stochastic model to assess the performance of the depth-based routing protocol in UWSNs, which is one of the main routing protocols for such networks. The major difference between terrestrial and underwater networks lies in the speed of the signal. The speed is much lower in underwater acoustic channels, compared to their terrestrial counterparts. Thus, the delay for a packet to reach from one node to another node is significant. In addition to the mean end-to-end delay, we obtain expressions for other performance metrics like the number-of-hops distribution and the mean energy consumption. We validate our stochastic model by comparing the average performance indices obtained by our analysis with the estimates obtained by stochastic simulation. Moreover, we compare the computational complexity of both model and simulation and it turns out that the stochastic model is much faster than the simulations in assessing the performance of depth-based routing.

1

Introduction

Sensor networks gather spatially distributed information and transfer it to a central location. These networks capture real-world phenomena and convert them into a suitable digital form that can be processed, stored, and analysed further on. Sensors, typically being tiny, can be integrated into numerous devices and the information they collect can provide an essential aid to decision making. The information gathered by sensors spans a wide range including temperature, humidity, pressure, position, vibration, sound, etc. Such measurements can help to avoid or mitigate the effects of catastrophic infrastructure failures caused by intensive natural events like floods or earthquakes, conserve natural resources, and enhance home and national security. Often, the collection of the information is essential for our understanding of physio-chemical and biological processes and, in most cases, can provide the basis for predictive modelling. For example, weather forecasting largely relies on accurate measurements of the current atmospheric conditions. Such predictions in turn can help farmers, exterior painters, tour guides, teachers and students to plan their activities accordingly. Some other instances of wireless sensor network applications include the detection and prediction of floods so that timely warnings can be issued for the affected areas, health and safety monitoring activities, fire detection in forests, etc. In all these cases, the availability of information is key for making informed decisions and it is of utmost importance that the available information is error-free and up-to-date as much as possible. Moreover, the information is spatially distributed, making it necessary to collect information from multiple sources.

To facilitate the collection and transfer of information over large distances, many network applications require hundreds or even thousands of sensor nodes. These nodes then make up the sensor network, the nodes being connected to each other by mostly wireless transmission channels. The nodes use these channels to transfer the information towards a particular destination node for further processing. In general, not all sensor nodes have a direct channel to the final destination node. If the sensor network covers a considerable area, directly connecting to a central node would require a powerful transmitter which would drain the sensor node's battery quickly. Instead, the information that is collected by the nodes is

relayed by other nodes to the final destination. In other words, a long distance transmission is replaced by a number of short distance transmissions.

These sensor nodes are usually battery-operated devices. Their lifetime after deployment is heavily dependent on the capacity of the small on-board battery. In general, it is not possible to replace or recharge this battery due to terrestrial challenges. Many research works have been devoted to extending the lifetime of the network. Some researchers use efficient energy-saving mechanisms or power optimisation tools such as duty cycling while others use energy harvesting nodes to extract the necessary energy from ambient energy sources available to the sensor node. Each approach comes with advantages and limitations. For example, the use of harvesting techniques can mitigate the dependency on the batteries but the uncertain nature of the energy source can affect the performance of the network significantly. Similarly, the other processes such as sensing the information or availability of the sink to transmit the data are also not deterministic and appropriate techniques are needed to model these phenomena to understand the overall system's behaviour with respect to its parameters. In this dissertation, we investigate the performance of a wireless sensor network through several stochastic models. These models capture the behaviour of different environmental processes and support optimising the transmission strategies of the sensor nodes. These strategies can vary according to the need of applications. Moreover, the detailed investigation of these models allow us to provide strong insights on network design. We use different modelling and performance evaluation techniques, such as queueing networks, Markov models, the asymptotic analysis of networks through mean-field limits, and numerical simulations. These methodologies help us answer questions about either the transient or steady-state behaviour of the network. A detailed discussion on stochastic modelling is presented later in this chapter in subsection 1.2.

The remainder of this introductory chapter is organised as follows. In the next section we discuss sensor networks in more detail, including some key characteristics for modelling such networks. Section 1.2 then briefly introduces the key tools from probability theory that will be used throughout the dissertation. Finally, 1.3 outlines the main contributions of the following chapters.

1.1 Wireless sensor networks

A wireless sensor network (WSN) is a group of spatially dispersed, dedicated interconnected sensors for monitoring and recording the physical conditions of the environment. A WSN can be comprised of only a few devices or sensor nodes (SN), but can equally well consist of several thousands of these SNs. The SNs extract information from their environment and transmit the information wirelessly to a centralised station (or user). WSNs mainly consist of three components: gateways, relay nodes, and sensors. Gateways act as an interface between the wireless sensor nodes and the application platform, where the collected data is processed. Relay nodes, sometimes referred to as routers, are used to extend the coverage

area of the sensor network. Finally, sensors can sense, measure and collect the information from the environment. Some nodes may both act as relay and sensor as well.

The information sensed at a sensor node is analysed and the node can then decide whether to transmit the data or not. In addition to sensing, the wireless sensor has on-board processing, communication, and storage capabilities. However, the capabilities of the sensor nodes can vary widely depending on the particular application. For example, some simple sensors only collect and transfer information whereas more powerful devices can also perform extensive preprocessing, including data compression and aggregation.

WSNs can be used in many applications that require close monitoring of the physical world. They provide a cost-effective and energy efficient solution for a wide range of applications including health care, utilities, remote monitoring and diverse industrial contexts. Among the principal WSN applications, we count surveillance (e.g., real-time highway traffic surveillance), environmental monitoring to detect biological or chemical threats, and ecosystem monitoring in forests to get information on populations of exotic plants and/or animals [1]. Moreover, WSN technology is one of the key enabling technologies of the Internet of Things (IoT) [2, 3]. For more details on the applications of WSNs, we refer to [4, 5].

1.1.1 Communication in a WSN

For many areas in which WSNs are applied, it is common that the sensor nodes have to operate without the support of infrastructure or the possibility of maintenance and repair. In some applications such as highway traffic monitoring and flood forecasting, sensor nodes are fixed at predetermined locations while in disaster management applications such as volcano monitoring and earthquake detection, nodes are thrown out of a plane in the area of interest. In such applications, a sensor node can detect the earthquake event based on the seismic frequency spectrum. The efficient measurement from the sensor nodes can be used to reduce the loss of life and property. Furthermore, these measurements can also be used to establish a more optimal search and rescue system, saving many lives. Having knowledge of the disaster area can help in deploying resources (e.g., food trucks) for meeting the needs of the maximum number of people. The SN must autonomously perform a number of operations including setting up the communication with other nodes, determining its own location and initiating its sensing and transmission activities.

The communication between nodes can be categorised mainly into two topologies as shown in Figure 1.1. When the transmission range of each sensor node is large enough to send data directly to the sink or base station, they form a star topology. In this case, remote nodes do not send data to each other. This means the sink must be within the transmission range of each individual node. Therefore many sensor nodes may require considerable transmitting power to transfer the information in one hop to the sink. The use of a mobile sink can mitigate this problem by moving the sink along a designated path to collect the information at each node. While the nodes can send the information with less power, they will sometimes

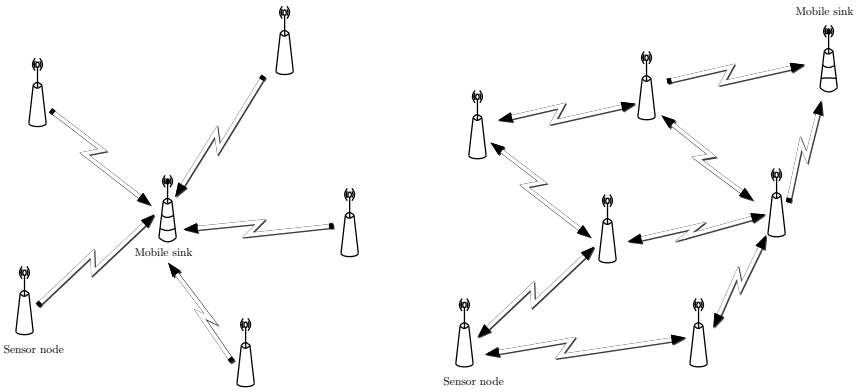

(a) One hop Communication (Star) (b) Multi-hop Communication (Mesh)

Figure 1.1: Communication topologies

have to wait for a transmission opportunity as the sink may not be in range. In many other applications, the network allows transmitting data from one node to another node to cover a larger area. This allows for what is known as multi-hop communication forming a mesh topology. Here, sensor nodes not only capture the data from the environment but also serve as relays for other nodes. They collaborate to propagate the sensor data towards the sink. The main advantages of this topology are redundancy and scalability. If some node fails to communicate with neighbouring nodes, the other nodes are still able to forward the message to the desired location through an alternate path. Although a mesh topology can achieve a considerable reduction in energy expenditure, it also requires efficiently designed routing protocols.

1.1.2 Key Processes

A sensor node is the main component of a WSN through which sensing, processing and communication take place. It is a small electronic device, equipped with a small battery and on-board memory. The primary objective of the sensor node is to gather as much information as possible while keeping the energy expenditure at a minimum. The main power source for sensor nodes is a small on-board battery that limits the lifetime of sensors. Since they are often installed in hostile terrain, it is very expensive and difficult, if not impossible, to replace or recharge the battery due to environmental and terrestrial challenges. To increase the lifetime, one can opt to increase the battery size, but this incurs an additional cost and increases the weight and size of the SN that makes this solution less attractive [6]. To overcome this problem, one can either efficiently manage energy consumption or harvest the energy from the environment. Each approach has its advantages and limitations.

To study the operation of a sensor node over time, we identify three important

processes: the consumption of energy, the harvesting of energy and the sensing of information that are explained in detail below.

Energy consumption

The energy consumption in a sensor node is mostly due to SN operations like sensing, computing, switching and transmitting. In the conventional view, the energy consumption is mostly dominated by radio communications. Moreover, the amount of energy consumed for data transmission normally depends on the volume of data to be transmitted in the network and the duration the sensor node has the opportunity to transmit. In most cases, the energy cost is due to computing is insignificant compared to the energy cost associated with communication. For example, Pottie et al. [7] mention that the energy required to transmit one bit of information is approximately equal to that needed to perform a thousand processor operations. Therefore, data compression can be used to minimise energy consumption and extend the overall lifetime of the network, see e.g. [8] where the authors investigate optimal algorithms for the compression of sensed data, communication and sensing in WSNs.

An alternative approach focuses on optimising the energy expenditure of the SN. If less energy is used over time, the SN remains operative for a longer time with the same initial energy budget [9, 10]. In particular, controlling the communication subsystem of the SN can be very useful to reduce energy consumption [11]. The control can be based on computing the redundancy of nodes in the WSN [12] or include duty cycling [13]. For example, as there is still significant energy consumption when the sensor node is idle, switching off the sensor node can save the battery and therefore extend the lifetime of the SN. In such strategies, the sensor node periodically wakes up to transmit the data and then sleeps by powering off to conserve the energy. WSN technology must efficiently manage the frequency of ON and OFF times of the node. In addition to the energy requirement, WSNs also need to have efficient routing protocols for relaying the information from source to sink.

Energy harvesting

Even though energy consumption is optimised, the lifetime of a SN is still determined by the limited energy budget on deployment. To overcome this dependency, one promising solution is to use sensor nodes that scavenge the necessary energy from the environment, see [14]. Such sensor nodes are referred to as energy harvesting sensor nodes (EH-SN). The provisioning of harvesting capability (e.g. solar, wind or heat harvesting) and a rechargeable battery removes the fixed upper limit on the energy budget. An EH-SN can constantly recharge during its lifetime. However, energy management is still required to balance energy harvesting and energy expenditure.

In general, the behaviour of the energy harvesting source is dynamic in nature. It can affect the amount and rate of energy being harvested over time. For exam-

ple, solar or wind based harvesting sources are predictable but non-controllable in nature. In such cases, one can forecast the availability of the source, but a careful mechanism is needed to decide how to spend the available energy and how much to store for future operations. There are considerable research efforts in the area of predictive models for energy harvesting and we refer to a comprehensive review [15] for further reference.

Value of information

Sensor networks are built and deployed mainly for the purpose of providing particular information to their users. This information may, for example, pertain to the temperature distribution in a building whose environmental conditions need to be controlled; the vital signs and location of a patient whose health needs to be remotely monitored; the stress levels of a bridge whose structural health needs to be monitored; or the position, capabilities, and intentions of enemy troops, insurgents, etc., so that adequate military and/or civilian preparations can be made. There are two important aspects related to the information: the quality of the information (QoI) and the value of information (VoI). The QoI takes into account the quality attributes, such as accuracy, consistency, completeness, and timeliness of the information [16, 17, 18] whereas the VoI tells us how well the values of these attributes reflect and accommodate the information needs of applications that consume it.

The information gathered by the nodes can be comprised of a predefined set of attributes, which take up the same amount of bytes. However, the quantity of the data not necessarily reflects its importance. For example, information on a fire in a forest or on an intruder in a military area carries more importance than regular weather updates. Similar differences in importance can be attributed in landslide detection, agricultural area monitoring as well as structural monitoring and control [19, 20, 21, 22]. In environmental monitoring, we can associate the VoI to the age of information. It acts as the measure for the freshness of the information. The sensor node updates the information if its age is less than that of the current information. Thus, outdated information is dropped from the network as it is of less or no importance to the user. Throughout this dissertation, we make use of the VoI concept and keep track of the value of information that is stored in the sensor node. As we will see later, the value of information significantly impacts the transmission decision and the performance of the network.

1.1.3 Uncertainties in these processes

Due to the recent advancements in sensor technology and wireless networking, mobile devices are revolutionising the way that information from the physical world is collected and used. However, some constraints like varying and hostile environments, ever-changing network topologies, untrustworthy communications, etc. point to what is known as *uncertainty* in the operation of networks. The presence of uncertainty can have a devastating impact on standard protocols, and disturb implicit structural assumptions. Moreover, they propagate throughout the

network and eventually lead to overall performance degradation. Therefore, uncertainty should be properly identified and accounted for with priority in the design of sensor networks. Below, we list a number of important sources of uncertainty in WSNs.

Sensing uncertainty

The sensing of data from the environment depends on the coverage area of the sensor node, which is an essential determinant of the sensing quality of a WSN. From a stochastic point of view, uncertainty in the sensing process can occur due to the interference caused by node mobility or environmental interference such as noise. Quantifying sensing uncertainty (e.g., uncertainty in sensor range) can help to facilitate effective sensor (re-)deployment strategies for mobile as well as static sensor networks. Some recent studies [23, 24] suggest to use probabilistic models to capture sensor behaviour since the phenomena being sensed, the sensor design, and the environmental conditions are all stochastic in nature. For instance, noise and interference in the environment can be modelled by stochastic processes.

Energy harvesting uncertainty

The most common problem in WSN is known as the *node death* which follows from energy depletion either caused by battery discharge or due to short circuits. Low batteries not only lead to fail-stop behaviour of a node but also causes the node to show random behaviour (e.g., wrong sensor readings [25]). As discussed earlier, energy harvesting provides a promising solution to avoid the node death problem. However, external conditions from which the harvesting circuitry draws its energy fluctuate over time, so that the amount of energy that can be harvested fluctuates as well. Specifically, harvesting circuitry can be highly sensitive to uncertainties, arising from the imprecise characterisation of the host environment or, alternatively, from manufacturing defects and tolerances. From a performance evaluation point of view, the harvesting process is an additional source of uncertainty that can greatly affect performance. Hence, accurate models of WSNs should take into account the random nature of the harvesting process. Moreover, there is a need for efficient power management in energy-harvesting wireless sensor networks (EH-WSN) due to the heavy dependence of the harvesting process on environmental factors.

Communication uncertainty

Wireless links are most often susceptible to transmission loss due to node mobility, dynamic obstacles, fading, limited energy resources, and spectrum allocation regulations. Sensor node mobility or a dynamic WSN environment result in intermittent connectivity. For instance, in WSNs with a mobile sink, the sink may not always be in range and thus the data transmissions have to be postponed till the sink comes in range. In some other cases, environmental interference or data

collision when two nodes want to send the data at the same time through the same link leads to transmission loss. Quantifying the communication uncertainty (e.g., the availability, quality and connection patterns of communication links) can support network algorithms for better routing decisions. Many network communication protocols and applications are built upon global static knowledge of network connectivity derived from collected traces [26]. Here, capturing the dynamically evolving relationship between nodes and the intermittent connectivity among sensor nodes is an important challenge.

1.1.4 Modelling perspective

As discussed earlier, the dynamics of WSNs are usually influenced by several dynamic environmental processes. These processes are often (i) very complex and (ii) highly unpredictable. It therefore does not suffice to describe these processes by some deterministic functions of time. Indeed, when the sensor nodes have to act upon their environment, they can at most make some predictions on the future dynamics of the environment based on past observations. That is, they know some statistics of the future evolution but not the exact evolution. As slight deviations from a prescribed evolution can have a profound impact on performance, it often does not suffice to replace the uncertain evolution by the predicted average evolution. In other words, as having perfect foreknowledge about every process is impossible to obtain, uncertainty should be accounted for and these processes should be modelled as *stochastic* processes in order to understand the dynamics of the system.

Stochastic models offer an accurate portrayal of real-world processes that can account for the different types of uncertainties as listed above. In particular, they can be used to predict how systems will behave under specified stochastic conditions. These predictions further provide powerful insights into the design of the systems under study. Stochastic modelling is used to cast the observed phenomenon from the dynamic environment into a probabilistic description such that tools from probability theory can be used to investigate the dynamics of the system. Most often, the systems are far too complicated to model in their entirety. Hence, the stochastic model only gives us a simplified view of the real system that can be tackled by the above mentioned probabilistic tools.

It is, however, important to note that modelling is as much an art as it is a science. Specifically, it is of utmost importance to include the right level of detail. On the one hand, adding details can make models more realistic and enable us to make useful predictions with high accuracy, while on the other hand, too many details make the model highly complex and difficult to solve as small changes in the structure of the equations may require enormous changes in the mathematical methods. Thus, we first have to identify the most important parts of the system and then find an appropriate mathematical technique to solve the model. In other words, we need to focus on reducing the complexities of real systems, isolating the important components, and then develop models that characterise the impact of the design decisions. In many research works, the model accuracy can be veri-

fied by conducting experiments to compare model predictions with what actually happens in practice. However, in some situations, experimentation is impossible due to ethical or financial reasons. In these circumstances, the model can only be tested less formally, for example by seeking an expert opinion or through computer simulations. We also make use of stochastic simulations to verify some of our models in this dissertation.

In a broader sense, the stochastic models can also provide answers to some additional questions. For example, what is the probability that the node runs out of energy, or how fast does the mobile sink have to travel in order to collect maximum information. Considering the dynamic nature of the WSN environment, we provide the appropriate framework to describe each process and evaluate the performance of the network using a wide range of mathematical techniques. These techniques can range from recursive difference equations and simple matrix operations to the complex asymptotic analysis of large scale systems.

1.2 Stochastic modelling

Wireless sensor networks are continuously evolving in terms of technology, implementation and deployment. As a result, they have become increasingly complex, with many interacting effects from the viewpoint of the system architecture and the application management. This trend is likely to persist in the future and thus, performance evaluation is playing a crucial role in network design to ensure a successful deployment and operation. It allows researchers to understand the impact of the network parameters on the system's performance in a rigorous way. Moreover, the stochastic modelling effort allows for directly expressing the behaviour of the system and its performance metrics in terms of the system's parameters. This in terms is the key for studying various trade-offs in the system's design, or for finding the set of parameters that ensures some target performance objective.

In this dissertation, we discuss different modelling and performance evaluation techniques, such as queueing networks, Markov models, the asymptotic analysis of networks through appropriate scalings, and numerical simulations. These methodologies have been applied to various problems and scenarios of data-aware WSNs and allow for investigating the effects of the different environmental factors on data collection, for obtaining the optimal sink trajectory, for improving power-saving and throughput, etc.

We study wireless sensor networks with a specific focus on the value of information and the energy harvesting dynamics. The stochastic models help us to capture the dynamics of harvesting and data collection accurately. For example, the detailed analyses of the models can answer questions such as how the restriction on battery capacity impacts the performance of the network. One can naturally assume that battery capacity should yield better performance, but, as we will see later, the performance evaluation shows that the gain of increasing the battery capacity quickly disappears due to the complex interaction between different network processes.

The remainder of this section introduces the main mathematical tools that are used throughout this dissertation. We mainly focus on the evaluation of the performance of the sensor network by means of Markov processes. We can only provide a basic introduction to the mathematical techniques to frame the remaining chapters. The application of these techniques for particular WSN scenarios of interest most often requires one to overcome one or several particular technical difficulties. These are discussed in the subsequent chapters whenever they appear. We start with discrete-time countable Markov chains and their control and subsequently turn our attention to continuous-time Markov chains and their deterministic approximations.

1.2.1 Markov chains

For many applications in communication systems, Markov chains with a discrete state space serve as a popular probabilistic model for network processes and algorithms. For instance, random processes like energy harvesting or data arrivals at a sensor node can be well characterised by Markov chains.

In general, a discrete-time stochastic process is a family (a sequence) of random variables $\{X_k, k \in \mathbb{Z}^+\}$ defined on a common probability space $(\Omega, \mathscr{F}, \mathsf{P})$. Here Ω is the set of outcomes of the probabilistic experiment, $\mathscr{F}$ is a σ-algebra[1] of subsets (events) of Ω, and P is a probability measure defined on $\mathscr{F}$. The random variables $X_k : \Omega \to S$ take values in some space S, which in our case will be finite or countable.

For a process with a countable state space, the process is characterised by the family of finite-dimensional probability mass functions,

$$\mathsf{P}(X_k = i_k, X_{k-1} = i_{k-1}, \ldots X_0 = i_0,), \qquad i_0, \ldots i_k \in S, k \geq 0.$$

In the simplest case, the random variables are independent and the joint probability above can be expressed as a simple product of probabilities. In many practical situations however, these processes are most interesting when the random variables are not independent, i.e., when there is some dependence structure between them. An elementary, but highly useful stochastic process that is important in the remainder is the discrete-time Markov chain (DTMC) with countable state space. It is defined as follows.

Definition 1.1. *A stochastic process $X = \{X_k : k \geq 0\}$ on a countable set S is called a (time-homogeneous) discrete-time Markov chain if, for any i, $j \in S$ and $k \geq 0$,*

$$\mathsf{P}(X_{k+1} = j | X_k = i_k, \ldots, X_0 = i_0) = \mathsf{P}(X_{k+1} = j | X_k = i_k) \doteq p_{ij}\,. \tag{1.1}$$

Here, p_{ij} is the probability that the Markov chain jumps from state i to state j and the set S is referred to as the state space of the Markov chain.

[1] a σ-algebra on a set A is a collection of subsets of A that includes A itself, and is closed under complements and countable unions.

The property 1.1 means that the DTMC is *memoryless*. That is, the probability of future outcomes does not depend on the steps that led up to the present state. This property is commonly known as the *Markov property*. The theory of Markov chains is precisely important as many processes in real life satisfy the Markov property. Even if the process of interest itself is not a Markov process, it is often possible to extend the states so that the extended process is Markovian. Note that the last term in (1.1) says that the process is time-homogeneous meaning the transition probabilities are independent of k. More precisely,

$$\mathsf{P}(X_{k+1} = j | X_k = i) = P(X_1 = j | X_0 = i) = p_{ij}. \tag{1.2}$$

If the transition probability did depend on the time index, then the Markov chain is called non-time-homogeneous, which we will not be addressing throughout this dissertation. To this point, let us define the matrix $\mathcal{P}$ with elements p_{ij} ($i, j \in S$) that describes the evolution of the system. The matrix $\mathcal{P}$ is called transition probability matrix and satisfies,

$$\sum_{j \in S} p_{ij} = 1 \quad \forall i, \tag{1.3}$$

as each row is a probability mass function, and therefore satisfies the normalisation condition.

Simulation of Markov chains

While our main focus lies on solving the Markov processes either analytically or numerically, we sometimes need to make simplifying assumptions, as the exact solution may either be analytically or numerically intractable. To evaluate the effect of such simplifications, we can compare with simulation results.

We here briefly summarise how trajectories of Markov chains with a given transition matrix can be constructed by evaluating a stochastic recursion. Vice versa, we also show how the transition matrix of the Markov chain can be constructed for a given stochastic recursion.

Let $\{X_k : k \geq 0\}$ be an S-valued Markov chain, where S is countable and ordered. Then for fixed $i \in S$, $\{p_{ij}, j \in S\}$ is a probability mass function. Therefore, let $f(x,y)$ be the function,

$$f(x,y) = \sum_{j \in S} j 1_{\{\sum_{j<x} p_{xj} < y \leq \sum_{j \leq x} p_{xj}\}}$$

for $x \in S$ and $y \in [0,1]$. Here $1_{\{\cdot\}}$ is the indicator function which evaluates to one if its argument is true and to zero if this is not the case. Now, one can generate a trajectory of the Markov chain by the stochastic recursion,

$$X_k = f(X_{k-1}, U_k),$$

where U_k is a sequence of independent random variables, uniformly distributed on $[0,1]$. Indeed, it is easy to check that $f(i,U)$ is an S-valued random variable with

probability mass function $\{p_{ij},\ j \in S\}$, see [27] for more details. While this expression holds for any Markov chain with countable state space, in most practical cases, there exist simpler and more intuitive recursions, which express the evolution of the Markovian state in terms of the input processes that drive these state changes.

Consider now an S-valued stochastic process $\{X_k : k \geq 0\}$, where S is a countable set and assume the random variables X_k are related by the stochastic recursive equation,

$$X_k = f(X_{k-1}, Z_k), \quad k \geq 1\,. \tag{1.4}$$

Here $f : S \times S' \to S$ is an arbitrary measurable function and $Z_1, Z_2, \ldots Z_k$ is a sequence of independent and identically distributed random variables with values in some general space S'. Now, if X_0 is independent of $Z_1, Z_2, \ldots, Z_k$, then X_k is a Markov chain.

It is indeed easy to verify this from definition of Markov chain. Recall that, for any $i, j \in S$ and $k > 0$, we have

$$\begin{aligned}
\mathsf{P}(X_k = j | X_{k-1} = i, \ldots, X_0) &= \mathsf{P}(f(X_{k-1}, Z_k) = j | X_{k-1} = i, \ldots, X_0) \\
&= \mathsf{P}(f(i, Z_k) = j | X_{k-1} = i, \ldots, X_0) \\
&= \mathsf{P}(f(i, Z_k) = j)\,,
\end{aligned}$$

where the last equality is due to the fact that the random variables $X_0, \ldots, X_{k-1}$ are functions of $Z_1, \ldots, Z_{k-1}$ only. In other words, $f(i, Z_k)$ is independent of $X_0, \ldots, X_{k-1}$. We can conclude that the stochastic process given by (1.4) is a Markov chain with transition probabilities $p_{ij} = \mathsf{P}(f(i, Z_k) = j)$.

Remark 1.1. *The recursive characterisation of Markov chains can also illustrate how a process can be fit into a Markovian framework by extending the state space of the Markov chain. For example, consider two functions f and g such that,*

$$X_k = f(X_{k-1}, Y_{k-1}), \quad \textit{and} \quad Y_k = g(Y_{k-1}, Z_k), \quad k \geq 1.$$

Then the process $\{X_k, k \geq 0\}$ does not constitute a Markov chain as the random variables Y_k are not independent and identically distributed. However, the process $\{(X_k, Y_k), k \geq 0\}$ is a Markov chain, as (X_k, Y_k) can be expressed in terms of (X_{k-1}, Y_{k-1}) and Z_k, the latter being an independent random variable.

Classification of states and ergodicity

When we refer to having solved a Markov chain, we most often mean that we have found the stationary distribution of the Markov chain. The existence of a unique stationary distribution of a Markov chain can be expressed in terms of the probabilities that the process returns to the different states, as well as on the mean time to return to the same state. We here briefly discuss how the states can be classified, and what this means for the existence of a stationary distribution of the Markov chain.

Two states of a Markov chain communicate if one can have a transition from one state to the other (and back) with positive probability in a finite number of steps. Let

$$p_{ij}^{(n)} = \mathsf{P}(X_n = j | X_0 = i)$$

denote the n-step transition probability from state i to state j. Note that $p_{ij}^{(n)}$ is the (i,j)th element of the matrix P^n. Then, states i and j communicate if $m > 0$ and $n > 0$ so that $p_{ij}^{(n)} > 0$ and $p_{ji}^{(n)} > 0$. Communication partitions the state space of the Markov chain into communicating classes, the most important case being Markov chains that have a single communicating class. These Markov chains are said to be *irreducible*.

A state i is said to have period d_i, if d_i is the greatest common divisor of all n that satisfy $p_{i,i}^{(n)} > 0$. In general, we are not so interested in periodic behaviour and it is beneficial to notice that if $p_{i,i} > 0$ for all states i, then the Markov chain is guaranteed to be non-periodic. Moreover, one easily verifies that two communicating states have the same period.

A state i is said to be *recurrent* if the chain returns to this state i with probability 1, while state i is said to be *transient* if this is not the case. For recurrent states, if the expected time until the process returns to the recurrent state i is finite, then state i is said to be *positive recurrent*, if this is not the case the state is *null recurrent*. As for periodicity, if a positive recurrent (null recurrent, transient) communicates with another state, then the other state is positive recurrent (null recurrent, transient) as well.

We are often interested in the behaviour of $\{X_k : k \geq 0\}$ over long time periods. In applied mathematics, infinitely long periods offer a good approximation for *long* periods, and *ergodic theory* offers a mathematical means to study the long-term average behaviour of complex systems. In particular, if we have only one sample function of a stochastic process instead of the entire ensemble, ergodicity allows us to derive all statistical information from that one sample function. More precisely, the process is ergodic if its time averages equal its ensemble averages. For Markov chains, ergodicity means that the Markov chain is irreducible, aperiodic and positive recurrent.

The long-run or limiting behaviour of a Markov chain is characterised by its stationary distribution, which is defined as follows.

Definition 1.2. *A probability measure π on S is a stationary distribution for the Markov chain X_n if*

$$\pi_j = \sum_i \pi_i \, p_{ij}^{(n)} \quad j \in S.$$

This equation reads $\pi = \pi P$ in matrix notation, where $\pi = (\pi_i : i \in S)$ is a row vector. Moreover, if we start with a stationary distribution i.e., $X_0 \sim \pi$, then the distribution of all future states remains the same, $X_n \sim \pi$ for all $n \geq 0$.

For ergodic Markov chains (or more general, for Markov chains that have at most one ergodic class), the existence and uniqueness of a stationary distribution

is guaranteed. If there is more than one positive recurrent class, then there are infinitely many stationary distributions, since all convex combinations of stationary vectors are stationary as well.

We can also study the limiting distribution of a Markov chain, the limiting distribution being $\pi_i = \lim_{n\to\infty} \mathsf{P}(X_n = i)$ for $i \in S$. For an ergodic Markov chain, the limiting distribution coincides with the stationary distribution and is independent of the initial distribution $\mathsf{P}(X_0 = i)$, $i \in S$. This is stated in detail in the following theorem from Ross [28] about the existence of the limit of the n-step transition probabilities.

Theorem 1.1. *For an irreducible, ergodic Markov chain,* $\lim_{n\to\infty} p_{ij}^{(n)}$ *exists and is independent of i. Furthermore, letting*

$$\pi_j = \lim_{n\to\infty} p_{ij}^{(n)}, \quad j \geq 0.$$

then π_j *is the unique non-negative solution of*

$$\pi_j = \sum_i \pi_i \, p_{ij} \quad j \geq 0,$$

with,

$$\sum_i \pi_i = 1.$$

In other words, it also tells us that the limiting probability of the process being in state j at time n is equal to the fraction of the total time that the process will be in state j. The proof of the theorem is out of the scope for this dissertation and we refer interested readers to [28]. In the remainder of the dissertation, we will assume that all DTMCs, whenever mentioned, are ergodic, and irreducible and refer to limiting or stationary distribution π as the equilibrium distribution. In matrix form, it is compactly written with π taken as a row vector, with $\mathbf{1}$ a column vector of $1's$, and with $\mathcal{I}$ the identity matrix,

$$\pi P = \pi, \text{ and } \pi\mathbf{1} = 1\,, \tag{1.5}$$

or equivalently as,

$$\pi(P + \mathbf{1}\mathbf{1}^T - \mathcal{I}) = \mathbf{1}^T\,.$$

1.2.2 Markov Decision Processes

WSNs are driven by random events, the sensor nodes need to act upon events under uncertainty. For example, a sensor node may choose not to transmit the data even if it has opportunity to transmit. Sensor nodes in WSN are generally resource-limited devices and static decisions like "always transmit" may lead to inefficient energy usage. The optimal decision not only depends on the value of the data it holds but also on the amount of energy as a transmission takes considerable energy. The decision to transmit now may impact the possibility to transmit later,

and therefore the node needs to assess whether or not it is best to wait till there is a higher value of information at the node. Similarly, the channel conditions can be accounted for. If the channel conditions are bad, considerably more energy is required to guarantee that the data can be transmitted correctly (or at least with a high probability). Hence, dynamically optimising the network operations to fit the physical channel conditions may result in significantly improved resource utilisation and overall performance.

Formally, in such scenarios, the sensor nodes need to adopt a certain policy, which leads to optimal performance over time in terms of a number of predefined design goals. As we model sensor nodes by means of Markov chains, the framework of Markov decision processes (MDP) can be used to study the optimal control of sensor nodes. MDPs entail that the system description possesses the Markov property, and add a set of possible actions to each state. Solving the MDP problem corresponds to finding the best action for each state. The MDP model allows for a balanced design of different objectives like, for example, minimising the energy consumption and maximising the data collection.

At this point, we formally define the MDP framework and its solution method. Assume that we have an ordinary Markov chain with state space S. At each time-step k, this process makes the decision to move according to some transition probability distribution as described in the previous section. Now the difference here is that we introduce a set of actions to be taken before this transition happens at each time-step with a probability distribution for each possible action. Thus, instead of having a process that makes the transition by itself, we now have a decision-making agent moving through the process. After action $A_k = a$ has been chosen by the agent in state $X_k = s_k$ at time k, the process moves to a new state $X_{k+1} = s_{k+1}$ according to some probability distribution $\mathsf{P}(X_{k+1} = s_{k+1} | X_k = s_k, A_k = a_k)$, for which the Markov property hold, i.e.,

$$\begin{aligned} p_k(s_{k+1}|s_k,a) &= \mathsf{P}(X_{k+1} = s_{k+1} | X_k = s_k, A_k = a_k, \ldots, X_0 = s_0, A_0 = a_0) \\ &= \mathsf{P}(S_{k+1} = s_{k+1} | S_k = s_k, A_k = a_k)\,. \end{aligned}$$

The actions define the transition distributions, but no criterion is yet introduced for indicating the award that is given to take a certain action in a state. Therefore, we introduce the reward function $r_k(s,a)$ for taking action a in state s at time k. We will always assume that $r_k(s,a)$ is bounded. This is the immediate reward at time k. As the action determines the transition and therefore also future rewards, one needs to account for both the immediate and future rewards. Depending on the length of the future (horizon) for the problem, there are two main types of MDPs — finite horizon and infinite horizon problems. We particularly consider the second type of problems where we do not have a fixed predetermined number of time steps, these can vary and in principle could be infinite. This type of MDPs are often useful in the applications where the total operation time of the system is unknown.

Value function and policy evaluation

Each subset of actions through the states from starting state to terminal state forms a *policy*, denoted by $\mu = (\mu_1, \mu_2, \ldots, \mu_k)$ for $k \leq \infty$, where $\mu_k : S \to A$ specifies the set of decision rules to be used at time steps k. I.e., μ_k associates an action with each possible state for time step k. Moreover, a policy is called *stationary* if the action only depends on the state but not on time, $\mu_k = \bar{\mu}$ for all k. These policies are fundamental to the theory of infinite horizon Markov decision processes. Now, the problem for the agent comes down to finding a path that maximises the rewards received while following this policy. The agent aims to find a policy that is better or equally good, with respect to some given objective, than all the other feasible policies. Such a policy is called the optimal policy and denoted by μ^*. Note that the policy fully defines the behaviour of an agent and depends only on the current state (not the history).

In infinite horizon MDPs, each policy μ induces a bivariate discrete-time reward process, $\{(X_k, R_k); k = 1, 2, \ldots\}$, where X_k represents the state of the system at time k and R_k represents the reward at time k, i.e., $R_k = r_k(X_k, A_k)$ with A_k the action taken at time k. The expected total discounted reward of policy μ is then defined as,

$$v_\mu(s) = \lim_{N\to\infty} v_\mu^N(s) = \lim_{N\to\infty} \mathsf{E}_s^\mu \left[\sum_{k=1}^{N} \alpha^{k-1} r_k(s,a) \right]. \tag{1.6}$$

for $0 \leq \alpha \leq 1$. The parameter α is known as the discount factor, higher α meaning that rewards in the further future are more important. The limit in 1.6 exists when the rewards R_k are bounded, $\sup_{s\in S, a\in A} |r_k(s,a)| < \infty$. Moreover, when the limit exists and interchanging the limit and expectation is valid, we have,

$$v_\mu(s) = \mathsf{E}_s^\mu \left[\sum_{k=1}^{\infty} \alpha^{k-1} r_k(s,a) \right]. \tag{1.7}$$

We now introduce some vector notation for MDPs for the description of the *policy iteration* algorithm below. Let P_{μ_k} be the $|S| \times |S|$ matrix with (s,s')th entry given by $p_{\mu_k}(s'|s) = \mathsf{P}(X_{k+1} = s' | X_k = s, A_k = \mu_k(X_k))$. Under policy $\mu = (\mu_1, \mu_2, \ldots)$, we can similarly define the k-step transition probability matrix P_μ^k with entries $p_\mu^k(s'|s) = \mathsf{P}_\mu(S_{k+1} = s' | S_1 = s)$. Here, the subscript μ indicates that these entries are the transition probabilities for policy μ. This matrix can then be expressed in terms of the one-step transition matrices P_{μ_k} as follows,

$$P_\mu^k = P_{\mu_k} P_{\mu_{k-1}} \ldots P_{\mu_1}.$$

Let v_μ be the column vector with entries $v_\mu(s)$. In view of the definition of $v_\mu(s)$, we can express v_μ as follows,

$$v_\mu = \sum_{k=1}^{\infty} \alpha^{k-1} P_\mu^{k-1} r_{\mu_k}, \tag{1.8}$$

where r_{μ_k} is the column vector with entries $r_k(s,\mu_k(s))$. For ease of notation, let $P_\mu^0 = I$ be the identity matrix, then we have,

$$\begin{aligned} v_\mu &= r_{\mu_1} + \alpha P_{\mu_1} r_{\mu_2} + \alpha^2 P_{\mu_1} P_{\mu_2} r_{\mu_3} + \dots \\ &= r_{\mu_1} + \alpha P_{\mu_1} \left(r_{\mu_2} + \alpha P_{\mu_2} r_{\mu_3} + \dots \right) \\ &= r_{\mu_1} + \alpha P_{\mu_1} v_{\mu'}. \end{aligned}$$

where $\mu' = (\mu_2, \mu_3, \dots)$. For a stationary policy μ, we have $\mu = \mu' = (\bar{\mu}, \bar{\mu}, \dots)$, and therefore,

$$v_\mu = r_\mu + \alpha P_\mu v_\mu \,. \tag{1.9}$$

One can show that that there is a unique solution v_μ if $0 \leq \alpha < 1$, see [29] for the proof.

Solving MDPs

There are three basic methods for solving MDPs - value iteration, policy iteration and linear programming. As the name suggests, the first two approaches solve the problem iteratively while the third approach transforms the problem into a linear program which can be then solved using the simplex method. We particularly focus on policy iteration as the WSN problems we address have large state and action space and solving the model with policy iteration is more efficient in such cases, compared to value iteration or linear programming.

The rewards for our models are bounded and positive. Moreover, we assume that the transition probabilities and rewards do not vary with time. That is, we have $p_k(s'|s,a) \doteq p(s'|s,a)$ and $r(s,a) \doteq r_k(s,a)$, for all k. With these assumptions, the limit $\lim_{k\to\infty} v_\mu^k(s)$ exists. Restricting our attention to stationary policies when seeking for optimal policies, we have the following expression for the value function $v^*(s)$ that characterises the optimal policy,

$$v^*(s) = \max_{a\in A} \left[r(s,a) + \alpha \sum_{s'\in S} p(s'|s,a)\, v^*(s') \right] . \tag{1.10}$$

The above system of equations is called the system of *optimality* or *Bellman* equations. It now remains to find the policy that maximises the above expected reward. Let $\mu^*(s)$ be the optimal policy that satisfies following the Bellman equation,

$$\mu^*(s) = \arg\max_{a\in A} v^*(s) = \arg\max_{a\in A} \left[r(s,a) + \alpha \sum_{s'\in S} \mathsf{P}(s'|s,a)\, v^*(s') \right] . \tag{1.11}$$

Policy iteration

The basic idea behind policy iteration is to generate a sequence of policies that gradually increase the value function. In particular, the algorithm alternates between a value determination step where the current policy is evaluated, and a policy

improvement step that aims to improve the current policy based on its evaluation. The policy is improved by selecting an action for each state that increases the total expected discounted reward. The algorithm is summarised below.

1. *Initialisation* : set $k = 0$ and consider an arbitrary decision rule μ_0.
2. *Policy evaluation* : Obtain v^k by solving the linear system,
$$v^k = (I - \alpha P_{\mu_k})^{-1} r_{\mu_k}.$$
3. *Policy improvement* : update the policy as follows,
$$\mu_{k+1} \leftarrow \arg\max_{\mu} \left[r_\mu + \alpha P_\mu v^k \right].$$
4. If $\mu_{k+1} = \mu_k$, stop and set $\mu_{k+1} = \mu^*$ otherwise increment k by 1 and return to 2.

Since we consider systems with a finite number of states and a finite number of actions in each state, policy iteration is guaranteed to stop in a finite number of steps. Although policy iteration is computationally efficient as it often takes a considerably fewer number of iterations to converge, each iteration can be computationally expensive as it involves solving a linear system. We defer a further discussion on the complexity of policy iteration as well ways to execute policy evaluation efficiently to Chapter 3, where we present an MDP model for a wireless sensor node.

1.2.3 Mean field approximation

A WSN consists of a large (several hundred to thousand) number of sensor nodes. These nodes can continuously interact with each other in order to achieve a common goal such as maximising information transfer from the sensors to a designated sink node. Developing stochastic models and analysing such a network using mathematical techniques is quite challenging. The first reason is their high complexity, which makes them difficult to solve. Secondly, the complexity of the analysis is highly sensitivity to the mathematical assumptions. Small changes in the modelling assumptions may require gigantic changes in the mathematical formulations. Stochastic scaling techniques like fluid limits and mean field approximations help to study the performance of such large-scale systems. We particularly focus on the mean field approximations and give a basic introduction to the framework in this chapter.

Curse of dimensionality

Markov chains are often characterised by their state space and by the transitions that can be taken from any of these states. In general, the Markovian system may

be described by an arbitrarily large number of state variables that introduces additional challenges in assessing the performance of the system and in obtaining the optimal control policy of the system. The main motivation of using approximation techniques in control theory is to address one of the challenges related to large state spaces, often referred to as the curse of dimensionality. The curse of dimensionality relates to the observation that as the dimension of the system (number of state variables) grows, it becomes increasingly difficult to solve the problem using standard numerical methods. In particular, iterative solutions become computationally expensive because they involve matrix operations that grow in size with the size of the state space. This motivates us to look for approximation techniques that can accurately capture the dynamics of the original system.

Mean Field approximations originate from statistical physics [30] and are a technique developed within the field of probability theory. This technique is useful to study the behaviour of stochastic processes with highly-dimensional (and hence a very large) state space. Classical applications of this technique generally require two levels of abstraction. The first is to assume that all the interacting objects are indistinguishable from each other and take away their individual identities. Instead of capturing the behaviour of each instance, the system's behaviour is observed at the population level. The second level of abstraction ignores the spatial distribution of the agents across the system and the objects are assumed to be uniformly distributed across the system space. Applying mean-field analysis involves describing how the population evolves through the system of differential equations, finding the deterministic behaviour of the system by solving these differential equations and analysing properties of this behaviour. Depending on the system under analysis, each of these steps may become challenging and modifications of the general idea are needed in order to obtain desired results.

Continuous time Markov chains

In order to understand the mean field framework, one needs to know a fair amount of mathematical techniques. We need a deterministic approximation in continuous time and hence we start by introducing continuous-time Markov chains (CTMC). In essence, a continuous-time Markov chain is a discrete-time Markov chain with the modification that, instead of spending one time unit in a state, the chain remains in a state for an exponentially distributed amount of time whose rate depends on the state. A continuous-time Markov process $X = \{X(t) : t \geq 0\}$ on a countable state space S satisfies the Markov property i.e., for integers (states) i, j, k and for all time instants s, t, u with $t \geq 0$, $s \geq 0$, and $0 \leq u \leq s$, we have,

$$\begin{aligned}\mathsf{P}(X(t+s) = k | X(s) = j, X(u) = i) &= \mathsf{P}(X(t+s) = k | X(s) = j) \\ &= \mathsf{P}(X(t) = k | X(0) = j).\end{aligned}$$

The definition above defines a time-homogeneous process because the last probability does not depend on s.

In general, a CTMC is completely characterised by the so-called generator

matrix $\mathbf{Q}$ with elements,

$$q_{ij} = \lim_{\Delta t \to 0} \frac{\mathsf{P}(X(t+\Delta t) = j | X(t) = i)}{\Delta t}, \quad i \neq j, i, j \in S.$$

The parameter q_{ij} is known as the transition rate from state i to state j, for $i \neq j$. The diagonal elements of the $\mathbf{Q}$ are defined as $q_{ii} = -\sum_{j \neq i} q_{ij}$, which is notationally convenient. Similar to DTMCs, we have a unique stationary distribution for the CTMC if it is finite and irreducible. Let π denote the stationary distribution of CTMC. The solution can be found by solving $\pi\mathbf{Q} = 0$ and $\pi\mathbf{1} = 1$, where $\mathbf{1}$ denotes a column vector of appropriate dimension.

The key concept in obtaining a deterministic approximation is a sequence of Markov processes for which the magnitude of both jumps and the average time between consecutive jumps goes to zero. In such a situation, the fluctuations become negligible and we can approximate a process with discrete jumps by a continuous process that satisfies (a set of) ordinary differential equations.

Population model and deterministic approximation

Consider a process with N different entities, the state of each entity being described by some state vector. The entities can interact, resulting in a CTMC where the state is described by the state variables of all entities. If each entity is in one out of K states, the state space of the population process is K^N. Even for moderate K and N, direct analysis of such systems by classic numerical techniques quickly becomes computationally prohibitive.

In order to construct the mean field model, we take away the individual identities of the interacting entities. We then only need to count the number of entities in each of the different states. This introduces a new Markov chain, with a reduced state space. The number of dimensions in the new state space is equal to the number of states an individual object can take. More importantly, the new representation allows for studying what happens when N grows to infinity. To this end, we study a sequence of models for increasing system size N. We normalise the models in order to bring them to the same scale (e.g., divide each variable by size N) and study relevant dynamics. In particular, we require proper scaling and regularity assumptions on transition rates. We only consider models that satisfy a *density dependence* condition. In simple terms, this condition requires that the transition rates are scaled together with the population size so that they are independent of the population size in the normalised model. The transition rates are Lipschitz continuous in such cases. Additionally, if we have convergence of initial conditions, the behaviour of the normalised system can be characterised by a set of ordinary differential equations whose solution gives an accurate approximation of the normalised system. We defer technical discussions on scaling and convergence to the deterministic approximation of the normalised system to Chapter 4. To illustrate the idea of the mean field, we provide a simple example below.

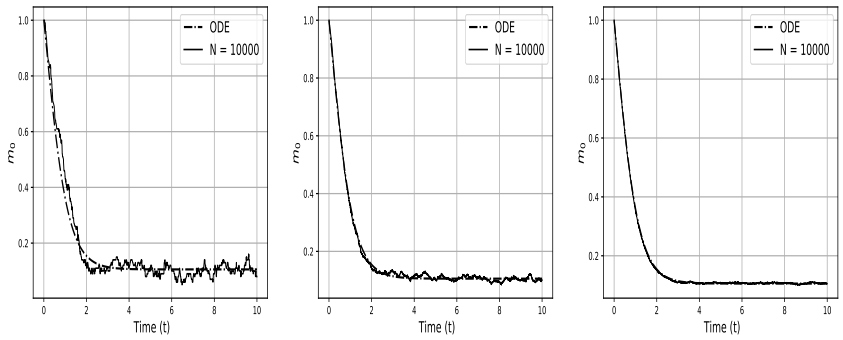

Figure 1.2: Comparison of solution of ODE and trajectories for different population of network CTMC model

Example

Consider a network with N nodes. Each node can be in two possible states, say state 1 if the node carries information and state 0 if this is not the case. Let $X_n^N(t)$ denote the state of the nth node in the model with N nodes. The nodes can either get information from their environment with rate ℓ_1^N or from the neighbouring node through an exchange process. Let γ^N be the rate at which nodes in the network meet each other. When two nodes meet each other information is only exchanged if the receiving node has no information while the sending node has something to send. Let ℓ_0^N be the rate at which a node loses its information and returns to state 0. Thus, the overall state of the network is described by the vector $\mathbf{X}^N(t) = (X_1^N(t), \ldots, X_N^N(t))$. The process $\mathbf{X}^N(t)$ constitutes a Markov process and we immediately see that the state space of the overall network is 2^N. Thus, analysing such a network becomes very difficult.

We now introduce the reduced Markovian description, by applying a counting abstraction. Let $M^N(t) = \left[M_0^N(t) M_1^N(t)\right]$, where $M_i^N(t)$ counts the number of nodes in state i. We have sequence of models $M^N(t)$ with increasing system size and we normalise them with system size N. Let $m_j^N(t) = N^{-1} M_j^N(Nt)$ and assume that the rates are scaled as follows: $\ell_j^N = \ell_j/N, \gamma^N = \gamma$. We can then show that for $N \to \infty$ the process $m_j^N(t)$ converges to a deterministic process $m_j(t)$ (almost surely) which is described by the system of ordinary differential equations,

$$m_0'(t) = \ell_0 m_1(t) - \ell_1 m_0(t) - \gamma m_0(t) m_1(t)\,, \tag{1.12}$$

and $m_1(t) = 1 - m_0(t)$. The first term on the right-hand side of (1.12) represents the loss of information of a node (so the number of nodes without information increases), while the second term represents the arrival of new information. The last term relates to an information exchange between nodes. The proof of convergence of the scaled process is discussed in chapter 4 in a broader context.

To understand how well this ordinary differential equation (ODE) represents the system, we simulate a number of trajectories of the continuous time Markov chain of the system for different values of N and compare it with the solution of equation 1.12.We set the rates as $\ell_0 = 0.2, \ell_1 = 0.8$ and $\gamma = 1$. We assume that all nodes have zero VoI initially and plot the solution of ODE and trajectory of continuous time population model. Figure 1.2 depicts the comparison between the solution of the ODE and some trajectories of the stochastic process for different population levels. As we can see, as N increases, the trajectories can no longer be distinguished from the limiting deterministic solution.

1.3 Dissertation Outline

We now provide a general overview of the dissertation and explain how the chapters of this dissertation are interconnected. We also take advantage of this moment to highlight the publications that resulted from our work. Stochastic modelling of wireless sensor networks is the main theme of this dissertation. We mainly focus on terrestrial WSNs covering two main objectives. Each objective addresses the performance issues of wireless sensor networks at different levels of abstraction and detail. The first objective is to develop models for isolated energy harvesting sensor nodes. These models provide important insights on how different environment processes affect the performance of the sensor node. The second objective is to consider the interactions between (a large number of) sensor nodes, under the assumption that they cooperate towards common goals. Such models are highly complex and we use stochastic scaling techniques to provide closed form solutions. Lastly, we also provide a short analysis of stochastic modelling of the depth-based routing protocol in an underwater wireless sensor network.

Chapter 2 and 3 mainly address the first objective i.e., the analysis of a static sensor node in isolation. The models in these chapters are mainly useful in one-hop communication applications. The work in chapter 2 has resulted into two journal publications [31, 32]. This chapter mostly relies on discrete time Markov chain theory and the sensor nodes are modelled as systems of two interacting buffers: a data buffer and an energy buffer. The key assumption is that the VoI is additive in nature. This can be true in many practical applications where information gets accumulated at the sensor node until transmission. In such cases, the VoI denotes the amount of sensed information. We investigate the long term behaviour of the different network processes such as the amount of energy in the system and the mean value of information collected from the node. In particular, we start with a basic model that captures the most important dynamics of WSNs and then add more complicated assumptions in order to generalise the model for more applications. We provide the stability analysis of the value of the information process and calculate the first two moments of VoI theoretically [31]. We then extend this model by allowing energy consumption for sensing the information. Moreover, we provide an additional analysis of the behaviour of the node when it is aware of the presence of information at a particular time [33]. Finally, we introduce time

correlation in the energy harvesting process to capture its bursty nature and study the trade-off between the cost of frequent data collection and timely data delivery in this setting [32]. We illustrate each model with the help of numerical examples and provide powerful insights on the impact of the different parameters on the network design.

The use of a controlled framework for WSNs starts in Chapter 3. In contrast to chapter 2, we now assume that the nature of the VoI process is non-additive. This is highly important in WSN applications where the age of information is more important than the amount of information. This work has resulted into a journal article in performance evaluation [34]. We introduce a two-dimensional Markov decision process and rely on the Quasi-Birth-Death (QBD) structure of the transition matrices to facilitate finding the optimal control of the energy-harvesting sensor node. We further investigate the structure of the optimal policy and provide interesting properties of the value function. We evaluate a policy with the linear level reduction method and obtain the exact solution with the policy iteration algorithm. The optimal control policy turns out to be the threshold in nature. We investigate the sensitivity of this threshold by means of numerical experiments.

Chapter 4 mainly addresses the second objective: we investigate large-scale WSNs where a high number of nodes interact with each other. Unlike Chapter 3, the control problem in this chapter is a finite-horizon problem and the state of the system is one dimensional, denoting only the VoI. That is, energy harvesting is not accounted for. The nodes in the network now can gain the information either from the environment or from a neighbouring node. However, an exchange of information between nodes costs a significant amount of energy, compared to sensing from the environment. The network tries to keep the maximum value of information while keeping the exchange process at a minimum. We use a continuous-time deterministic approximation and obtain the limit of the population process in terms of ordinary differential equations as the number of nodes in the network grows to infinity. Then, we use the Hamilton-Jacobi-Bellman (HJB) equation, which is based on Bellman's principle of optimality. We evaluate the control problem through Pontryagin's minimum principle and establish some interesting properties of the optimal policies. Finally, we illustrate our approach by providing a close form solution for the three state system.

We consider the underwater wireless sensor network in Chapter 5. Like their terrestrial counterparts, UWSNs adopt multi-hop routing protocols that aim at delivering the harvested data packets to on-surface sink nodes. We particularly limit our attention to Depth based routing (DBR) which is one of the most important routing strategies for underwater networks, due to its simple implementation and robustness against node mobility. This work has led to a journal article in AdHoc networks [35]. In particular, we use a decomposition approach to study depth-based routing in underwater sensor networks, and evaluate the performance of the system in terms of the end-to-end delay, the packet delivery probability, the distribution of the number of hops to reach the surface and the energy consumption. We observe that the performance evaluation of the model is far less time consuming than that of simulations.

Finally, in Chapter 6, we summarise our contributions and draw some overall conclusions from the work done in this dissertation. We also provide an outlook on possible future direction.

2

Modelling and analysis of an isolated sensor node

As the key constituent of the Internet of Things (IoT), WSNs have attracted considerable research interest in the past years. They enable fast data-to-decision applications that act in real time on collected data. In this chapter, we develop analytical models for static energy harvesting sensor nodes in isolation, which collect the information from their environment and pass it on to a mobile sink. The models quantify the value of the data that is collected by the sink. Such models are very useful in one hop communication applications like highway traffic surveillance. In particular, our analytical models assess the interaction between data collection, energy harvesting and energy expenditure. The decisions made by a node most often depend on the quality as well as on the timeliness of the information. Therefore, we consider the concept of "value of information" which covers both aspects.

The typical sensor node (SN) can be modelled as a system of two interacting buffers, i.e. a data buffer to store the collected information, and an energy buffer to store the energy harvested from the environment. Each buffer is generally fed by an input process that is typically bursty. While burstiness in data buffers is a well-studied subject, the interaction of two such buffers holds interesting questions, for example in terms of optimal control and dimensions. We assume that the sensor node under consideration operates energy neutral; all energy for sensing and transmissions is harvested from the environment. The energy buffer is in fact a small on-board battery for temporary energy storage. As the node solely depends on harvested energy, it may run out of energy. As a result, the sensor node at hand can only transmit when the mobile sink is in range and the sensor has sufficient energy for transmitting its data.

We focus on optimal data collection, adopting the hybrid WSN of Zhou et al. [36], which consists of static sensors responsible for sensing environmental variables, and mobile sensors called IoT mobile sinks that move to designated sink locations where they gather data sensed by static sensors. Mobile sinks were introduced to overcome the hot-spot effect in sensor networks [37]. Both static and mobile sink nodes (or base terminals) collect data from sensor nodes and some-

times act as gateways to other users by processing and sending relevant information. If all sensor data is relayed by the sensor nodes to a (static) sink, nodes closer to the static sink are more heavily loaded as they need to relay more packets to the static sink in comparison with nodes further away. As a result, they consume more energy and may die at an early stage, or will frequently run out of energy if they can harvest energy. Mobile sinks overcome this problem by moving the sink around. See e.g. [38] for a discussion on design issues and challenges in existing distributed protocols for mobile sinks. Although mobility increases the network lifetime by balanced utilisation of power [39], it also introduces new challenges as minimising the delay in packet delivery [40].

Finally, we mention some applications of hybrid WSNs. Ren et al. [1] optimise the data collection scheduling of a hybrid WSN, and propose such WSN for highway traffic surveillance and ecosystem monitoring . In the highway traffic scenario, sensors are deployed along a highway and collect traffic information such as the number of vehicles and their speeds, the types of vehicles, etc. The ecosystem scenario includes monitoring of exotic plant growth or endangered animals. In a typical ecosystem monitoring scenario, humans or vehicles can only access the system via limited roads, while the exact sensor locations in the forest are not easily reached. In unmanned agriculture, Huang and Chang [41] propose a wireless sensor network with a mobile sink for collecting image data. The mobile sink mitigates the need to relay large amounts of data or to transmit large amounts over a long distance. In either case, considerable energy is required that cannot be delivered by the sensors. Similarly, Yang and Miao [42] propose a mobile sink to solve the problem of poor scalability and unbalanced energy consumption in farmland WSNs. Finally, motivated by energy constraints for the sensor nodes, Taherian et al. [43] propose a WSN with a mobile sink for monitoring a railway transportation system.

The remainder of this chapter is organised as follows. In the next section, we give an overview of closely related literature. Sections 2.2 to 2.4 then introduce increasingly complex models for a sensor node in isolation in a hybrid sensor network. Finally, we summarise our findings in section 2.5.

2.1 Related work

As we focus on a stochastic model for an EH-WSN, we now discuss some related stochastic models. The first set of models consider the battery dynamics of a wireless sensor node, without data buffering. The battery state is usually discretised, meaning that the battery provides chunks of energy, rather than a continuous stream of energy. The simplest Markovian model of the battery is a continuous or discrete-time (quasi-) birth-death Markov process, where births and deaths correspond to energy harvesting and energy expenditure respectively, see e.g. [44] where harvesting and recharging are combined and [45] where the harvesting process exhibits time correlation. The latter authors model the energy harvesting process as a two-state Markov modulated model, i.e., a node either harvests energy

leading to a random increase of the amount of energy or is unable to harvest any energy. Michelusi et al. [46] also consider a two-state harvesting process and determine a transmission policy such that energy harvesting and consumption are balanced. While two-state Markov models already exhibit some time correlation, more realistic models for the time correlation in harvesting processes are studied in [47] and [48]. These authors study traces of solar harvesting processes and statistically verify that a Markov modulated process can be used to model the solar energy harvesting process. Relaxing the assumption that the sensor node remains in its different operational modes for an exponential amount of time, a semi-Markov model for the battery dynamics is studied in [49].

While the former models account for energy storage, data buffering is not considered. Data buffering however is accounted for in [50, 51, 52, 53, 54]. In [53], Gelenbe considers a model with Poisson arrivals of data and energy. Assuming that the time to transmit a packet is far smaller than the time to harvest the energy for the transmission, there is either no data or no energy at the node, which simplifies the analysis considerably. In [52], a similar model is studied where the sensor nodes are also subject to ongoing energy loss through standby power consumption and leakage from batteries and capacitors. In addition, transmissions can be corrupted by noise and mutual interference. If transmissions can be neither considered to happen almost immediately nor postponed due to unavailability of the receiver, both the data and energy queue can be simultaneously non-empty. Therefore, Markov models with two queues (an energy and a data queue) are required. In [50, 51] such a Markov model is studied where energy and packet arrivals depend on an exogenous Markovian background process. This allows to include correlation in both harvesting, sensing and transmission processes. A similar Markov process is studied in [55] in the context of a "green" base station. Such a base station uses renewable energy sources for powering its operations. A somewhat different approach is proposed in [54]. In contrast to the models above, these authors do not adopt energy chunks but model the battery as a fluid queue. The model allows for correlated energy harvesting (a fluid Markov process with two states), packet queueing and re-transmissions, a sleep period and temporal death of the node. A temporal death state is reached when the node runs out of energy.

Various authors have also tackled control problems for EH-SNs by formulating the dynamics and control as a Markov decision process (MDP). The survey of Alsheikh et al. [56] reviews numerous applications of MDPs in EH-WSN and discusses and compares various algorithms and solution methods. We discuss some more recent contributions. In [57], Rao et al. use the framework of Markov decision processes to determine the optimal task scheduling for a sensor node. Tasks include sensing, reading and writing from flash storage, packet reception and transmission, as well as computation. The MDP formulation accounts for task priorities and deadlines. Although energy harvesting is making WSNs self-sustainable, Lei et al. [58] note that the uncertainty on harvesting leads to unreliability and instability which is becoming a major challenge in the design of networks. These authors formulate the problem as a constrained MDP and focus on scheduling algorithms that minimise data loss under delay constraints. Zordan et al. [59] investigate

energy-aware lossy data compression policies for SNs, and model the SN's transmission and energy dynamics as a constrained Markov decision problem. If a SN does not have sufficient energy to perform its tasks, a significant amount of energy can be saved by temporarily powering off. An MDP formulation for similar sleep and wake-up strategies is considered in [60].

2.2 Basic analytical model

For most real-world phenomena, it is far too complicated to model the phenomenon in its entirety. Hence, a first step is to identify the most important components of the system at hand that need to be included in the model, while components of lesser importance can be excluded. In this subsection, we start with a basic model, which already captures part of the dynamics of a SN. We will then add more complicated and realistic assumptions later on.

2.2.1 Mathematical model

We consider an energy harvesting sensor node operating in discrete time as depicted in Figure 2.1 . That is, time is divided into fixed length intervals or slots and all transmissions are synchronised with respect to slot boundaries. The sensor node is equipped with on-board memory to store the sensed information and a battery for storing harvested energy. For ease of analysis, we adopt the energy chunk paradigm. That is, we discretise the battery levels; the battery can store up to C discrete units (or chunks) of energy. We study the evolution of the value of information (VoI) of the sensed data and the energy levels at slot boundaries. During each slot, sensor data is collected and stored in on-board memory, and energy is collected and stored in the battery. Whenever the mobile sink passes by, the data is transferred to the mobile sink, provided the sensor node has sufficient energy to transmit. The specific assumptions on sensing, energy harvesting and data collection are introduced below.

Energy harvesting process

As we adopt the energy chunk paradigm, the amount of energy that is harvested during a slot is a discrete random variable. Let H_n denote the number of energy chunks that are harvested during slot n. H_n only includes the energy that is available for transmission. That is, accounting for any conversion loss and assuming that the node can constantly harvest sufficient energy for sensing, H_n is the excess energy that can be used for transmissions. The amount of energy provided by a single chunk corresponds to $1/N$th of the energy required to make a single transmission of the information. The choice of large N corresponds to more energy chunks (C is larger) which implies that the performance analysis is more computationally demanding (cfr. infra). The sequence $\{H_n, n \in \mathbb{N}\}$ constitutes a sequence of independent and identically distributed random variables, taking values in $\mathbb{N}$.

Notation	Definition
C	Maximum battery capacity
M	Number of energy chunks needed for sensing the data
N	Number of energy chunks needed for transmitting the data
α	Discounting factor for the value of information
c	Cost associated with data collection
B_n	Battery level at the beginning of slot n
V_n	Value of Information at the beginning of slot n
H_n	Number of energy chunks harvested during slot n
$\bar{H}_n$	Tail distribution of H_n
h_k	Probability that k energy chunks are harvested in the kth slot
S_n	The value of data sensed during slot n
s_0	Probability that there is nothing to sense
$\bar{S}$	Mean value of the data sensed in a slot
T_n	Binary random variable that indicates if there is a transmission during slot n or not
P_n	Binary random variable that indicates whether data is collected during the nth slot or not
A_n	Binary random variable that indicates if there is a data to transmit during slot n or not
E_n	State of the modulating process for energy harvesting
b_k	Stationary probability of having battery level k
$\widetilde{b}_k$	Stationary probability of having battery level k when there is no information at the sensor node
$\hat{b}_k$	Stationary probability of having battery level k when there is information at the sensor node
v_k	Mean value of information at the sensor node for battery level k
$\bar{V}_p$	Mean value of information after data collection

Table 2.1: List of notations used in this Chapter

Let h_k denote the probability that k energy chunks arrive in a slot. For further use, we always assume that the sensor node can harvest energy, that is, we assume $h_0 < 1$. Moreover, we introduce the following notation for the tail distribution function of H_n,

$$\bar{H}_k = \sum_{m=k}^{\infty} h_m = 1 - \sum_{m=0}^{k-1} h_m \,. \tag{2.1}$$

Sensor data arrival process

Assuming that sensing data does not require much storage, we do not track the size of the sensor data, but track the value (or the quality) of the information of the data instead. Note that in some specific cases, the size of the data can even be constant

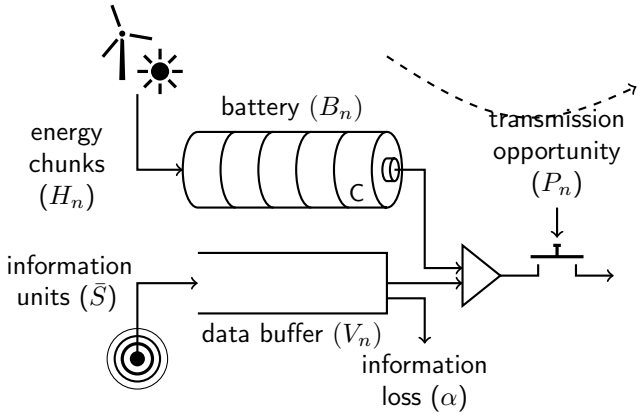

Figure 2.1: WSN Model

over time. This is e.g. the case if the data is a vector of environmental quantities that is regularly updated by the sensing process. The amount of information that is described by this vector however depends on the actual data values and can differ considerably over time.

Let S_n denote the value of the data sensed during the nth slot. We assume that the sequence S_n is stationary ergodic. For the sequence $\{S_n, n \in \mathbb{N}\}$ of the value of harvested information, no independence assumptions are required. We only assume that the mean value does not depend on time; let $\bar{S} = \mathsf{E}[S_0] < \infty$ and let $\sigma_m = \mathsf{E}[S_0 S_m] < \infty \; n \in \mathbb{N}$.

Assuming that older data is less relevant to decision making, the value of the information drops while it is not collected. To capture such loss, we assume that the value of information at the sensor node is discounted in each time slot with discount factor α. Moreover, we assume that the value of information is additive: the value of the data sensed during a time slot that cannot be transmitted is added to the (discounted) value already at the sensor.

Data collection process

Finally we assume that the time (in slots) between data collection constitutes a sequence of independent and identically geometrically distributed random variables with success probability p. Let P_n be the binary random variable that denotes whether data is collected at the nth slot boundary or not. Then, with the assumption above, the process $\{P_n\}$ constitutes a Bernoulli process with $\mathsf{P}[P_n = 1] = \mathsf{E}[P_n] = p$.

The data collection process models the availability of the sink at the location of the sensor node and therefore relates to the trajectory that is followed by the mobile sink. I.e., $P_n = 1$ if the sink is in the transmission range in slot n, while $P_n = 0$ if this is not the case. The probability p therefore corresponds to the fraction of time that the mobile sink is in range during the trajectory of the mobile sink.

2.2.2 Stochastic difference equations

We now study the evolution of the battery level and the VoI at slot boundaries. Let B_n denote the battery level at the beginning of time slot n and let V_n denote the VoI at the sensor node at the nth slot boundary. Assuming that the energy harvested in slot n cannot be used for sensing and transmitting data in slot n, and that any energy that cannot be stored in the battery is lost, we have,

$$B_{n+1} = \min(B_n - NT_n + H_n, C)\,. \tag{2.2}$$

Here T_n is the binary random variable that indicates if there is a transmission during slot n or not. We express T_n in terms of the battery level B_n, the value of information V_n, and the indicator of the mobile sink P_n below.

As the value of information is discounted with discount factor α and information is additive, we have,

$$V_{n+1} = \alpha V_n(1 - T_n) + S_n\,. \tag{2.3}$$

Here we assumed that all information is immediately transferred to the mobile sink when there is a transmission ($T_n = 1$), while any newly sensed data S_n is not yet available for transmission.

It now only remains to express T_n in terms of the sequence of transmission opportunities. We express T_n in terms of B_n and P_n as follows,

$$T_n = \begin{cases} 1 & \text{for } P_n = 1 \text{ and } B_n \geq N\,, \\ 0 & \text{otherwise.} \end{cases}$$

Alternatively, we can express T_n as,

$$T_n = 1_{\{B_n \geq N\}} P_n\,. \tag{2.4}$$

That is, there is a transmission provided there is energy to transmit ($B_n \geq N$), and an opportunity to transmit ($P_n = 1$). Here, $1_{\{\cdot\}}$ denotes the indicator function which equals 1 if its argument is true and zero if this is not the case.

2.2.3 Analysis

The set of recursions (2.2)–(2.4) now allows for determining the first two moments of the value of information collected by the IoT mobile sink. We first investigate the existence of a stationary solution (B^*, V^*) of these recursions.

Stability

The evolution of battery level does not depend on the value of information. Substituting (2.4) into (2.3) shows that for $h_0 < 1, h_1 > 0, 0 < p < 1$, the sequence B_n constitutes an ergodic unichain with finite state space $\{0, \ldots, C\}$. Hence, a stationary process $\{B_n^*, n \in \mathbb{Z}\}$ exists that adheres the recursion (2.3). Let $\bar{T}_n^* = 1 - P_n 1_{\{B_n^* \geq N\}}$ be the corresponding stationary indicator of having no transmission. We now define the stationary value of information process V_n^*.

Definition 2.1. *The stationary value of information process V_n^* is given by,*

$$V_n^* = \sum_{k=1}^{\infty} S_{n-k}\, \alpha^{k-1} \prod_{\ell=1}^{k-1} \bar{T}_{n-\ell}^*. \tag{2.5}$$

Provided that the sum on the right-hand side converges, the process V_n^* is stationary by the stationarity of the sequence $\{(S_n, B_n^*), n \in \mathbb{Z}\}$. Moreover, one can easily verify that (2.5) satisfies the recursion (2.3). Indeed, assume that V_n^* is given by (2.5), then we find that V_{n+1}^* can be expressed as,

$$\begin{aligned}
V_{n+1}^* &= \alpha V_n^* \bar{T}_n^* + S_n \\
&= \alpha \sum_{k=1}^{\infty} S_{n-k}\, \alpha^{k-1} \prod_{\ell=1}^{k-1} \bar{T}_{n-\ell}^* \bar{T}_n^* + S_n \\
&= \sum_{k=1}^{\infty} S_{n-k}\, \alpha^{k} \prod_{\ell=0}^{k-1} \bar{T}_{n-\ell}^* + S_n \\
&= \sum_{k=2}^{\infty} S_{n+1-k}\, \alpha^{k-1} \prod_{\ell=0}^{k-2} \bar{T}_{n-\ell}^* + S_n \\
&= \sum_{k=1}^{\infty} S_{n+1-k}\, \alpha^{k-1} \prod_{\ell=1}^{k-1} \bar{T}_{n+1-\ell}^*.
\end{aligned}$$

Before providing our results on the convergence of V_n^*, we recall some basic properties of martingales below.

Martingales Martingales play an important role in stochastic processes for which the conditional expectation of its future value, given the information accumulated up to now, equals its current value. Mathematically, a stochastic process $Z = \{Z_t\}_{t \geq 0}$ is called a martingale with respect to the filtration $\mathscr{F}_s$, if it satisfies:

1. $\mathsf{E}(|Z_t|) < \infty$ for all $t \geq 0$; and
2. $\mathsf{E}(Z_t | \mathscr{F}_s) = Z_s$ for all $t \geq s \geq 0$;.

The filtration $\mathscr{F}_s$ formalises the idea of "information" accumulated up to time s. A filtration is an increasing family of σ-fields. This is a vast topic in probability theory and we refer interested readers to [61] for more mathematical details.

Intuitively, the definition of a martingale means that the conditional expected value of the future value, given all its historical values, equals its current value. Note that this is not the same as conditioning on only the current value. For the stability proof, we rely on the following two theorems, which are stated without proof.

Theorem 2.1. ***Monotone convergence theorem***
Suppose that $\{X_n : n \geq 0\}$ is a sequence of non-negative random variables for which $X_n \leq X_{n+1}$ for $n \geq 0$, almost surely. Then,

$$X_\infty = \lim_{n \to \infty} X_n$$

exists and $\mathsf{E}[X_n] \nearrow \mathsf{E}[X_\infty]$ *as* $n \to \infty$.

Theorem 2.2. ***Martingale convergence theorem***
Let Z be a martingale bounded in $\mathscr{L}^1$*, i.e.,* $\sup_n \mathsf{E}[|Z_n|] < \infty$*, then the following statements are equivalent,*

1. $(Z_n)_{n\in\mathbb{N}}$ *are uniformly integrable;*
2. *There exist a random variable* Z_∞ *such that* $Z_n \to Z_\infty$ *almost surely and in* $\mathscr{L}^1$*;*
3. *There exist a random variable* Z_∞ *such that* $Z_n \to Z_\infty$ *in* $\mathscr{L}^1$*;*
4. *There exist a random variable* $Z_\infty \in \mathscr{L}^1$ *with* $Z_n = \mathsf{E}[Z_\infty|\mathscr{F}_n]\ \forall\, n \in \mathbb{N}$.

Stability theorems Having introduced martingales and their properties, we now rely on these theorems to show some properties of the stationary value of information process V_n^*. First we show that the stationary process V_n^* has finite mean.

Theorem 2.3. *The sum on the right hand side of eq.* (2.5)*, that is,* $\sum_{k=1}^{\infty} S_{n-k}\,\alpha^{k-1} \prod_{\ell=1}^{k-1} \bar{T}^*_{n-\ell}$*, converges to a random variable with finite mean.*

Proof. Consider the sequence, $\{Z_m, m \in \mathbb{N}\}$, with $Z_m = \phi_m - \sum_{k=1}^{m} \bar{S}\alpha^{k-1}$ and where ϕ_m is the partial sum,

$$\phi_m = \sum_{k=1}^{m} S_{n-k}\,\alpha^{k-1}\,.$$

Calculating the expected value of Z_m with respect to the filtration $\mathscr{F}_m = \sigma(S_{n-1}, S_n, \ldots, S_{n-m})$[1] yields,

$$\begin{aligned}\mathsf{E}[Z_{m+1}|\mathscr{F}_m] &= \mathsf{E}[Z_m + S_{n-m-1}\alpha^m - \bar{S}\alpha^m|\mathscr{F}_m] \\ &= Z_m + \alpha^m \mathsf{E}[S_{n-m-1} - \bar{S}|\mathscr{F}_m] \\ &= Z_m\,.\end{aligned}$$

Thus, the process $\{Z_m\}$ is a martingale. Moreover, it is bounded in $\mathscr{L}^1$ since $\sup_m \mathsf{E}[|Z_m|] = 0 < \infty$. From the martingale convergence theorem, the limit $\phi_\infty - \bar{S}/(1-\alpha)$ is finite, while $\mathsf{E}[\phi_\infty]$ is finite by the monotone convergence theorem. Finally, note that ϕ_∞ is an upper bound for the sum in right-hand side of eq. (2.5), which concludes the proof. □

Theorem 2.4. $|V_n - V_n^*| \to 0$ *for* $n \to \infty$ *for any initial value* V_0.

Proof. Consider again the process (B_n, V_n), starting at $n = 0$ with given (B_0, V_0). From eq. (2.3), we have,

$$V_n = \alpha^n V_0 \prod_{\ell=1}^{n} \bar{T}_{n-\ell} + \sum_{k=1}^{n} S_{n-k}\alpha^{k-1} \prod_{\ell=1}^{k-1} \bar{T}_{n-\ell} \tag{2.6}$$

[1] $\sigma(S_{n-1}, S_n, \ldots, S_{n-m})$ is the minimal σ-algebra generated by these random variables.

As B_n is an ergodic Markov process, we have $|B_n^* - B_n| \to 0$ for $n \to \infty$. Moreover, $|V_n^* - V_n| \to 0$ for $n \to \infty$. Indeed, substituting (2.5) and (2.6) into $|V_n^* - V_n|$ yields,

$$\begin{aligned}|V_n^* - V_n| &= \left| \sum_{k=1}^{\infty} S_{n-k}\, \alpha^{k-1} \prod_{\ell=1}^{k-1} \bar{T}_{n-\ell}^* - \alpha^n V_0 \prod_{\ell=1}^{n} \bar{T}_{n-\ell} - \sum_{k=1}^{n} S_{n-k} \alpha^{k-1} \prod_{\ell=1}^{k-1} \bar{T}_{n-\ell} \right| \\ &= \left| \sum_{k=1}^{n} S_{n-k} \alpha^{k-1} \prod_{\ell=1}^{k-1} \bar{T}_{n-\ell}^* + \sum_{k=n+1}^{\infty} S_{n-k}\, \alpha^{k-1} \prod_{\ell=1}^{k-1} \bar{T}_{n-\ell}^* \right. \\ &\quad \left. - \alpha^n V_0 \prod_{\ell=1}^{n} \bar{T}_{n-\ell} - \sum_{k=1}^{n} S_{n-k} \alpha^{k-1} \prod_{\ell=1}^{k-1} \bar{T}_{n-\ell} \right|\end{aligned}$$

By using the transformation $k = k - n$, we can write the second summation as $\alpha^n \sum_{k=1}^{\infty} S_{-k}\, \alpha^{k-1} \prod_{\ell=1}^{k-1} \bar{T}_{n-\ell}^*$. Since $\prod_{\ell=1}^{k-1} \bar{T}_{n-\ell}^* \leq 1$, we obtain following inequality,

$$|V_n^* - V_n| \leq \alpha^n \sum_{k=1}^{\infty} S_{-k}\, \alpha^{k-1} + \alpha^n V_0 + \sum_{k=1}^{n} S_{n-k} \alpha^{k-1} \left| \prod_{\ell=1}^{k-1} \bar{T}_{n-\ell}^* - \prod_{\ell=1}^{k-1} \bar{T}_{n-\ell} \right|$$

The sum in the first term is finite with probability 1, and as $\alpha < 1$, the first two terms converge to 0 almost surely for $n \to \infty$. For the third term, consider the random variable $\tau = \inf\{n; T_n = 1 \text{ and } B_m = B_m^* \text{ for } m \geq n\}$ which is finite almost surely. Then for $n > \tau$, the third term is 0. As $\lim n \to \infty P[\tau \geq n] = 0$, we conclude that the third term converges to 0 as well. □

Summarising, we have shown that a stationary ergodic process (B_n^*, V_n^*) exists with V_n^* given by (2.5), adhering the recursions (2.2) - (2.4). Moreover, whatever the initial conditions (B_0, V_0), $|B_n^* - B_n| \to 0$ and $|V_n^* - V_n| \to 0$, for $n \to \infty$.

Moments

We now turn our attention to calculating the first two moments of the stationary process V_n^*. The first moment tells us about the mean value of information at a particular battery level, while the variance is a measure for how the value of information is spread out from the average value for a particular battery level.

Mean VoI The set of recursions above allows for determining the value of the information collected by the mobile sink. To this end, let $v_k = \mathsf{E}[V_n^* 1\{B_n = k\}]$ be the mean value of the information at the sensor node for battery level k, and let $b_k = \mathsf{P}[B_n^* = k]$ be the stationary probability of having battery level k. By conditioning on the battery level and the availability of a transmission opportunity in the preceding slot, we find that the mean value of the information at battery level k adheres the following set of equations,

$$v_k = \alpha \sum_{\ell=0}^{C} v_\ell\, h_{k,\ell}\, (1 - p\, 1_{\{\ell > N\}}) + \bar{S} b_k \tag{2.7}$$

for $k = 0, 1, \ldots, C$, where we introduced,

$$h_{k,\ell} = 1_{\{k<C\}}\, h_{k-\ell} + 1_{\{k=C\}}\, \bar{H}_{C-\ell},$$

to simplify the notation. The first term in the equation above corresponds to the situation where the battery does not become saturated while the second term covers the opposite case.

Again by conditioning on the battery level and on the availability of a transmission opportunity in the preceding slot, the battery level probabilities adhere,

$$b_k = \sum_{\ell=0}^{C} b_\ell \left(h_{k,\ell} + p(h_{k,\ell-N} - h_{k,\ell})\, 1_{\{\ell>N\}}\right) \tag{2.8}$$

for $k = 0, 1, \ldots, C$.To simplify notation, we write the system of battery and VoI equations in terms of matrices. To this point, we introduce the column vector $\mathbf{v} = [v_k]_{k=0}^{C}$ and $\mathbf{b} = [b_k]_{k=0}^{C}$, as well as the following matrices,

$$\boldsymbol{\mathcal{A}} = [h_{k,\ell}\,(1 - p\, 1_{\{\ell>N\}})]_{k=0}^{C},$$

and,

$$\boldsymbol{\mathcal{B}} = [h_{k,\ell} + p(h_{k,\ell-N} - h_{k,\ell})\, 1_{\{\ell>N\}})]_{k,\ell=0}^{C}.$$

The set of eqs. (2.7) - (2.8) is then equivalent to $\mathbf{v} = \alpha\, \mathscr{A}\, \mathbf{v} + \bar{S}\mathbf{b}$ and $\mathbf{b} = \mathscr{B}\mathbf{b}$. Accounting for the normalisation condition $\mathbf{e}^T\, \mathbf{b} = 1$, we find,

$$\mathbf{b} = (\boldsymbol{\mathcal{B}} - \boldsymbol{\mathcal{I}} + \mathbf{e}\mathbf{e}^T)^{-1}\mathbf{e}, \text{ and } \mathbf{v} = \bar{S}(\boldsymbol{\mathcal{I}} - \alpha\, \boldsymbol{\mathcal{A}})^{-1}\mathbf{b}. \tag{2.9}$$

Here, $\mathbf{e}$ is a column vector of ones, the superscript T indicates the matrix transpose and $\boldsymbol{\mathcal{I}}$ denotes the identity matrix.

Finally, we can express the mean value of the sensed data per time slot that is actually collected in terms of v_k's as follows,

$$\bar{V} = \mathsf{E}[V_n\, 1_{\{P_n=1, B_n\geq N\}}] = p \sum_{k=N}^{C} v_k\,. \tag{2.10}$$

Indeed, there are only transmissions if the battery level exceeds the threshold and there is a transmission opportunity.

Variance of the VoI The calculation of the second moment is considerably more tedious. From the system of eqs. (2.4)–(2.5), we have,

$$\begin{aligned} v_k^{(2)} &= \mathsf{E}[(V_{n+1}^*)^2\, 1_{\{B_{n+1}=k\}}] \\ &= \alpha^2 \sum_{\ell=0}^{C} (1 - p\, 1_{\{\ell>N\}})\, h_{k,\ell}\, v_\ell^{(2)} + 2\alpha \sum_{\ell=0}^{C} (1 - p\, 1_{\{\ell>N\}})\, h_{k,\ell}\, \xi_\ell^{(0)} + \sigma_0\, b_k \end{aligned}$$

for $k = 0, 1, \ldots, C$, with $\xi_\ell^{(0)} \doteq \mathsf{E}[V_n^* S_n 1_{\{B_n^*=\ell\}}]$. This set of equations then corresponds to the following matrix equation,

$$\mathbf{v}^{(2)} = \alpha^2 \mathcal{A}\mathbf{v}^{(2)} + 2\,\alpha\mathcal{A}\xi^{(0)} + \sigma_0 \mathbf{b}\,,$$

with $\mathbf{v}^{(2)} = [v^{(2)}]_{k=0}^{C}$ and $\xi^{(0)} = [\xi_k^{(0)}]_{k=0}^{C}$. To determine the remaining unknown vector $\xi^{(0)}$, let $\xi_k^{(m)} \doteq \mathsf{E}[V_{n-m}^* S_n 1_{\{B_{n-m}^*=k\}}]$, such that in view of the system equations (2.5)–(2.4) we have,

$$\xi_k^{(m)} = \alpha \sum_{\ell=0}^{C} (1 - p1_{\{\ell \geq N\}}) h_{k-\ell} \xi_\ell^{(m+1)} + \sigma_{m+1} b_k\,.$$

The former equation allows for calculating $\xi_k^{(m)}$ recursively. Indeed, defining the vector $\xi^{(m)} = [\xi_k^{(m)}]_{k=0}^{C}$, we have,

$$\xi^{(m)} = \alpha\mathcal{A}\xi^{(m+1)} + \sigma_{m+1}\mathbf{b}\,.$$

Recursively substituting this equation into itself then yields,

$$\xi^{(0)} = \sum_{\ell=0}^{m-1} \sigma_{\ell+1}\alpha^\ell \mathcal{A}^\ell \mathbf{b} + \alpha^m \mathcal{A}^m \xi^{(m)} = \sum_{\ell=0}^{\infty} \sigma_{\ell+1}\alpha^\ell \mathcal{A}^\ell \mathbf{b}\,.$$

where we used the fact that $\alpha^m \mathcal{A}^m \to 0$ for $m \to \infty$ as its largest eigenvalue is less than one.

Summarising, the second order moment vector $\mathbf{v}^{(2)}$ can be written as,

$$\mathbf{v}^{(2)} = (\mathcal{I} - \alpha^2\mathcal{A})^{-1} \left(2 \sum_{\ell=0}^{\infty} \sigma_\ell \alpha^\ell \mathcal{A}^\ell \mathbf{b} - \sigma_0 \mathbf{b} \right)$$

The variance of the value of information collected in a slot is then,

$$\mathsf{var}[V] = \mathsf{E}[(V_n^*)^2 1_{\{P_n=1, B_n^* \geq N\}}] - \bar{V}^2 = p \sum_{k=N}^{C} v_k^{(2)} - \bar{V}^2. \tag{2.11}$$

2.2.4 Extension to Markov modulated energy arrivals

The assumption that the number of energy chunks that arrive in a slot constitutes a sequence of independent random variables is not essential for the calculations. We here extend the method to allow for correlated arrivals. We discuss correlated arrivals in detail later in the chapter. For the moment, we limit the discussion to the calculation of the mean value of the sensed data per time slot.

Let $\{E_n, n \in \mathbb{Z}\}$ be an ergodic Markov process with finite state space $\mathscr{J} = \{1, \cdots, J\}$, and let θ_{ij} denote the transition probability from state i to state j, for $i, j \in \mathscr{J}$. E_n is the environment process that modulates the energy arrival process. That is, we assume that the number of energy chunks H_n that arrive in slot n,

depends on E_n. Such energy arrival processes have been proposed a.o. for energy harvesting body sensor networks in [45] and for solar harvesting [62].

Let $h_k^{(i)} = \mathsf{P}[H_n = k | E_n = i]$ be the probability that k chunks arrive when the environment is in state i. Further let $\bar{H}_k^{(i)} = \sum_{\ell \geq k} h_k^{(i)}$ and $h_{k,\ell}^{(i)} = 1_{\{k<C\}} h_{k-\ell}^{(i)} + 1_{\{k=C\}} \bar{H}_{C-\ell}^{(i)}$. We now calculate the joint probability of the environment state and the battery level. Let $b_k^{(j)} = \mathsf{P}[B_n = k, E_n = j]$. By conditioning on the battery level, the environment state and the availability of a transmission opportunity in the preceding slot, these probabilities adhere,

$$b_k^{(j)} = \sum_{i=1}^{J} \theta_{ij} \sum_{\ell=0}^{C} b_\ell^{(i)} \left(h_{k,\ell}^{(i)} + p(h_{k,\ell-N}^{(i)} - h_{k,\ell}^{(i)}) 1_{\{\ell>N\}} \right), \tag{2.12}$$

for $k = 0, 1, \ldots, C$. The set of equations above, complemented by the normalisation condition $\sum_{k=0}^{C} \sum_{j=1}^{J} b_k^{(j)} = 1$, allows for determining the probabilities $b_k^{(j)}$.

Let $v_k^{(j)} = \mathsf{E}[V_n 1_{\{B_n=k, E_n=j\}}]$ be the mean value of information at the sensor node for battery level k and the environment state j. By conditioning on the battery level, the environment state and the availability of the transmission opportunity in the preceding slot, we find the mean value of information at battery level k $k = 0, 1, \ldots, C$ and the environment state j adheres,

$$v_k^{(j)} = \alpha \sum_{i=1}^{J} \theta_{ij} \sum_{\ell=0}^{C} v_\ell^{(i)} h_{k,\ell}^{(i)} (1 - p 1_{\{\ell>N\}}) + \bar{S} b_k^{(j)}. \tag{2.13}$$

The system of equations (2.12) - (2.13) are again linear, though there are now J equations for every battery state. The mean value of the sensed data per time slot that is actually collected then finally equals,

$$\bar{V} = p \sum_{i=1}^{J} \sum_{k=N}^{C} v_k^{(i)}. \tag{2.14}$$

2.2.5 Numerical evaluation and discussion

We now numerically investigate the optimal data collection policy for the sensor node at hand. We assume that there is a cost c associated to data collection, so that the average value after collection equals

$$\bar{V}_p = -cp + \bar{V}.$$

Figures 2.2(a) and 2.2(b) depict the value of information $\bar{V}_p$ in terms of the data collection probability p. We assume that the mean value of information sensed in a slot $\bar{S}$ equals twice the cost of collecting it: $c = 1$ and $\bar{S} = 2$. Moreover, $N = 4$ energy chunks are required for transmission and the number of harvested energy chunks is Poisson distributed with mean λ. Figure 2.2(a) fixes the discount factor to $\alpha = 0.9$ and shows $\bar{V}_p$ for various battery capacities $C \in \{4, 8, 32\}$ and

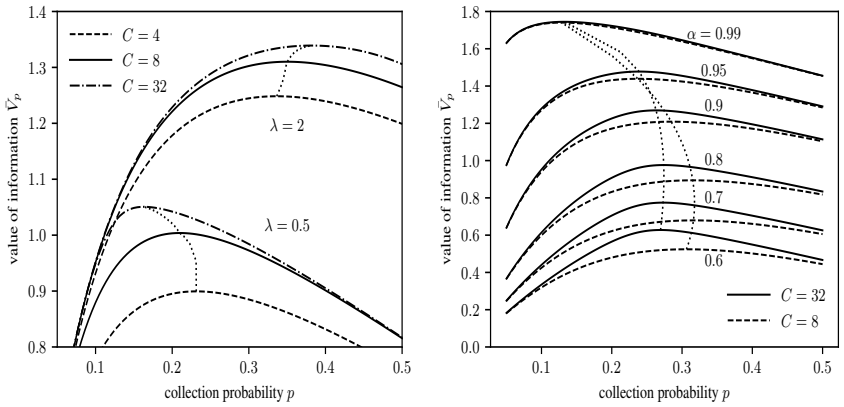

(a) Varying C (b) Varying α

Figure 2.2: Value of the information $\bar{V}_p$ versus p for different (a) C as indicated; and (b) α as indicated.

$\lambda \in \{0.5, 2\}$ as indicated. In contrast, Figure 2.2(b) fixes the energy arrival rate to $\lambda = 1$, and shows the value of information $\bar{V}_p$ for various discount factors $\alpha \in \{0.6, 0.7, 0.8, 0.9, 0.95, 0.99\}$ and battery capacities $C \in \{8, 32\}$ as indicated.

If no data is collected, there is neither cost nor data so that the value is zero for $p = 0$. As the cost of data collection is limited in the figures, the value of information first increases for increasing p and then decreases again. For high p, the chance of insufficient energy increases so that the gain of more frequent data collection cannot compensate the collection cost. Figure 2.2(a) and 2.2(b) further reveal that increasing the battery size is beneficial, as a larger battery can better compensate periods with little energy harvesting. The marginal gain of increasing the battery capacity however drops quickly. In addition, Figures 2.2(a) and 2.2(b) show that increasing λ and α is beneficial as well. This is also expected as there can be more transmissions if λ increases (there is more energy) and there will be more information if α increases.

The dotted lines in Figures 2.2(a) and 2.2(b) connect the values of the different curves at the optimal collection probability (for fixed λ and variable C in Figure 2.2(a) and for fixed C and variable α in Figure 2.2(b)). Figure 2.2(a) shows that the optimal collection probability can either increase or decrease for increasing C, depending on λ. For larger λ, the optimal collection probability increases for increasing C. This is what one expects as the chance to have energy for transmission increases when C increases (there is less energy loss). For small λ, the optimal collection probability decreases for increasing C. This can be explained by noting that energy is scarce for small λ. If C is small as well, even more energy is lost if the information is not frequently collected. When C increases, the energy loss drops and the collection probability can drop as well. For increasing α, Figure

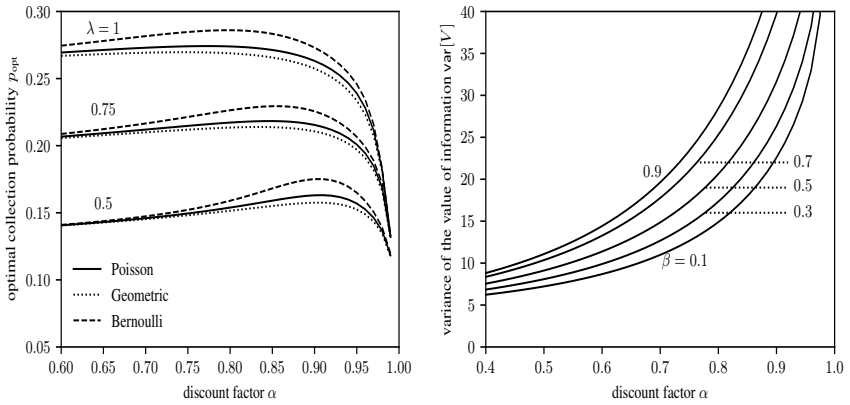

(a) Varying distribution (b) Varying β

Figure 2.3: (a) Optimal polling probability p versus the discount factor α for different harvesting distributions and (b) Variance of the value of the information $\mathsf{var}[V]$ versus the discount factor α for different β as indicated.

2.2(b) shows a slight increase followed by a quick decrease of the optimal collection probability. For α large, a drop in α means that the value of information is discounted faster such that we need to collect more. For α small, the cost of collection is high compared to the value at the sensor node. If α increases, this value increases so that we can collect more.

The latter observations are also confirmed by Figure 2.3(a) that depicts the optimal collection probability versus α for different energy arrival distributions and different values of the mean number of energy chunks λ arriving in a slot as indicated. The collection cost is $c = 2$, the battery can store $C = 32$ energy chunks and the mean value of the sensed data is $\bar{S} = 2$. The optimal collection probability is higher for higher λ as an increase in λ implies that it is less likely that a lack of energy prevents transmissions. Moreover, as an increase in the variance of the energy chunk distribution (the variance of the geometric distribution is higher than that of the Poisson distribution, which in turn is higher than that of the Bernoulli distribution) implies that it is more likely to run out of energy, p_{opt} decreases with the variance. Finally, we note that the optimal collection probability is not sensitive to changes in α for low α, while it is very sensitive for high α, irrespective of the energy chunk distribution.

Figure 2.3(b) illustrates the influence of the correlation in the information process S_n on the variance of the value of information. We assumed that the autocovariance function of the information process decays exponentially with rate β: $\sigma_n = \beta^n \mathsf{var}[S_0] + \bar{S}^2$. Such a decay can e.g. be found when the information process constitutes an auto-regressive process of order 1. Figure 2.3(b) shows the variance of the value of the information at the optimal collection probability versus the dis-

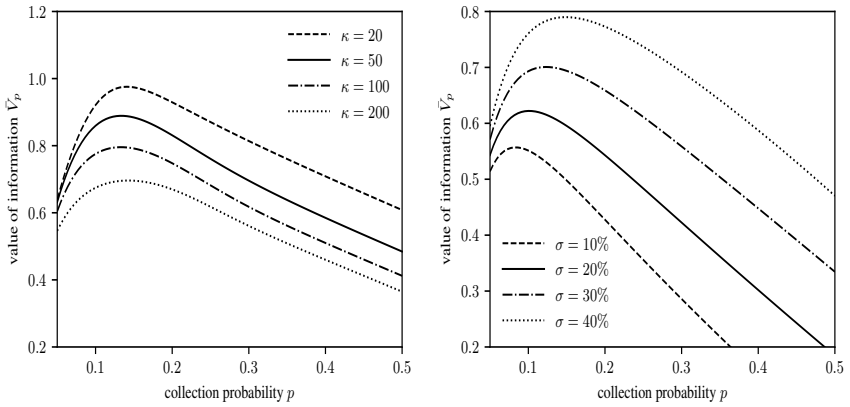

(a) Varying κ (b) Varying σ

Figure 2.4: (a) Value of the information $\bar{V}_p$ versus the polling probability p (a) for different κ and (b) for different σ as indicated.

count factor α for β as indicated and for $\mathsf{var}[S_0] = 16$ and $\bar{S} = 2$. The collection cost is $c = 2$, the battery can store $C = 32$ chunks and the energy arrival distribution is a Poisson distribution with mean $\lambda = 1$. The figure shows that for higher α as well as for higher positive correlation in the sensing process, the variance of the value of information increases considerably. While correlation does not affect the mean value of information, it does affect the corresponding variance meaning that the collected value of information is more likely to deviate considerably from its average value.

Finally, we investigate the effect of correlation in the harvesting process. Using the results of Section 2.2.4, Figures 2.4(a) and 2.4(b) show the value of the information $\bar{V}_p$ versus the collection probability p when the harvesting process is an interrupted Poisson process. The harvesting process is either active or inactive, the mean time to remain active and inactive being denoted by κ_a and κ_i, respectively. Let $\kappa = \kappa_a + \kappa_i$ denote the mean length of an active-inactive cycle and let $\sigma = \kappa_a/\kappa$ denote the fraction of active slots. While active, the number of energy chunks is Poisson distributed with mean λ, and there is no harvesting during inactive slots. In both Figures, the collection cost is $c = 1$, the battery can store $C = 32$ energy chunks, the discount factor is $\alpha = 0.9$, the mean value of the sensed data is $\bar{S} = 2$, and $N = 4$ chunks are required per transmission. In Figure 2.4(a), we fix $\sigma = 50\%$ and $\lambda = 1$ and consider different κ as indicated. Large κ means that there are long periods with harvesting followed by long periods without harvesting, which clearly affects performance. Moreover, the optimal collection probability decreases for larger κ as well, as it is likely that there is no energy during long periods without harvesting. In Figure 2.4(b), we fix $\kappa = 100$ and choose different σ as indicated, while we keep the mean number of energy chunks per slot

constant, $\sigma\lambda = 1$. Small σ means that harvesting is concentrated in a few slots, again followed by many slots without harvesting, and therefore negatively affects performance. For increasing σ, the optimal collection probability increases as the lengths of the periods without harvesting decrease.

2.3 Energy consumption for sensing

In the basic model, we assumed that there is always sufficient energy for sensing the information from the environment. That is, we did not explicitly account for any energy expenditure related to sensing. However, in many real situations, sensors dissipate energy while sensing and it is reasonable to assume that they may not have sufficient energy to sense the information in some time slots. In this section, we incorporate this complication.

We again introduce a discrete-time stochastic model for studying the optimal data collection probability in energy-harvesting hybrid WSNs and aim at controlling the collection frequency of the mobile sink. The concept of value or quality of information is again key to our study. We first assume that the nodes are completely unaware of the value of their information. We then refine the model: while the sensor node is still unaware of the value of the information it carries, it is aware whether or not there is any value.

2.3.1 Mathematical model

We consider a stochastic performance model of an energy harvesting sensor node in isolation. As in the preceding subsection, the performance of the sensor node depends on three exogenous processes: (i) the sensing process, which describes the value of the information that is sensed; (ii) the energy harvesting process; and (iii) the data collection process, which models the presence of the mobile sink such that the SN can offload its information.

We retain the assumptions and notation of the harvesting process, the data collection process, the visits of the sink and the battery capacity. Recall that the number of harvested energy chunks is independent from slot to slot, while the value of the sensed information constitutes a stationary ergodic sequence. For the energy expenditure, we now however account for the energy that is consumed by sensing. More precisely, we assume that transmitting and sensing data requires $N > 0$ and $M > 0$ energy chunks, respectively, sensing having priority over transmissions if there is insufficient energy for both. Let T_n be the indicator that there is a transmission during slot n. As the sensor node harvests H_n chunks during slot n, the evolution of battery level at slot boundary now becomes,

$$B_{n+1} = \min(B_n - M1_{\{B_n \geq M\}} - NT_n + H_n, C)\,. \tag{2.15}$$

This recursion accounts for the fact that the node only senses if there is a sufficient energy to sense (this is for $B_n \geq M$). Similarly, T_n takes care of the energy utilisation when there is a transmission during a slot n.

Let V_n denote the value of the sensed data in the sensor node at the beginning of the n^{th} slot. We retain the assumption that the value of the sensed data is additive and discounted over time. Let $0 \leq \alpha \leq 1$ denote the discount factor. The values of the data at two consecutive slot boundaries then relate as,

$$V_{n+1} = \alpha V_n(1-T_n) + S_n 1_{\{B_n \geq M\}}\,. \tag{2.16}$$

The recursion above implies that any data sensed during slot n cannot be transmitted during slot n. In addition, any chunks of energy harvested during slot n cannot be used to sense and/or transmit data in slot n.

It now remains to express the indicator T_n that there is a transmission in terms of B_n. We assume that the sensor node cannot evaluate the value of its information, and therefore transmits if sufficient energy is available. We therefore have,

$$T_n = \begin{cases} 1 & \text{for } P_n = 1 \text{ and } B_n \geq M+N\,, \\ 0 & \text{otherwise.} \end{cases}$$

The set of recursions above now allows for determining the value of the information collected by the mobile sink. To this end, let $v_k = \mathsf{E}[V_n 1\{B_n = k\}]$ be the mean value of the information at the sensor node for battery level k, and let $b_k = \mathsf{P}[B_n = k]$ be the probability of having battery level k. In view of the equations for V_n, B_n and T_n and by conditioning on the battery level and the availability of a transmission opportunity in the preceding slot, we find that the mean value of the information at battery level k adheres to the following set of equations,

$$v_k = \alpha \sum_{\ell=0}^{M-1} v_\ell h_{k-\ell} + \alpha \sum_{\ell=M}^{C} v_\ell h_{k-\ell+M} - \alpha p \sum_{\ell=M+N}^{C} v_\ell h_{k-\ell+M} + \bar{S}(b_k - \sum_{\ell=0}^{M-1} b_\ell h_{k-\ell})\,, \tag{2.17}$$

for $k = 0, 1, \ldots, C-1$. whereas for $k = C$ we have,

$$v_C = \alpha \sum_{\ell=0}^{M-1} v_\ell \bar{H}_{C-\ell} + \alpha \sum_{\ell=M}^{C} v_\ell \bar{H}_{C-\ell+M} - \alpha p \sum_{\ell=M+N}^{C} v_\ell \bar{H}_{C-\ell+M} + \bar{S}(b_C - \sum_{\ell=0}^{M-1} b_\ell \bar{H}_{C-\ell})\,. \tag{2.18}$$

To find the battery level probabilities, we again condition on the battery level and the availability of a transmission opportunity in the preceding slot. We have the following equations for the battery level probabilities,

$$b_k = \sum_{\ell=0}^{M-1} b_\ell h_{k-\ell} + \sum_{l=M}^{C} b_\ell h_{k-\ell+M} + p \sum_{l=M+N}^{C} b_\ell (h_{k-\ell+M+N} - h_{k-\ell+M})\,, \tag{2.19}$$

for $k = 0, 1, \ldots, C-1$. The system of equations (2.19) along with the normalisation condition

$$\sum_{k=0}^{C} b_k = 1\,,$$

allows for solving for the probabilities b_k. We can then solve the system of equations (2.17) and (2.18) for the conditional mean values v_k.

Finally, we express the mean value of the sensed data per time slot that is actually collected in terms of the v_k's as follows,

$$\bar{V} = p \sum_{k=M+N}^{C} v_k\,,$$

as there are only transmissions if the battery level exceeds the threshold and there is a transmission opportunity.

Remark 2.1. *If C is small, both systems of equations (for b_k and v_k) are easily solved. For larger C, we can exploit structural properties of the systems of equations. As $h_k = 0$ for $k < 0$, we see that equation* (2.19) *expresses b_k in terms of the probabilities b_ℓ for $\ell \leq k+M+N$. This implies that the Markov chain B_k is a $G/M/1$-type Markov chain. Hence, solution methods for a $G/M/1$-type Markov chain (e.g. [63]) can be applied to solve the system of equations of the b_k's. Analogously, we see that equation* (2.17) *expresses v_k in terms of v_ℓ, for $\ell < k+M$.*

Remark 2.2. *The assumption $h_0 > 0$ and equation* (2.17) *imply that $\lim_{p\to 0} v_k < \infty$ for $k < C$ and any value of α, as well as for $k = C$ and $\alpha < 1$. For $\alpha = 1$, we have $0 < \lim_{p\to 0} pv_C < \infty$. This shows that for $\alpha < 1$ we have $\lim_{p\to 0} \bar{V} = 0$, whereas for $\alpha = 1$ we have $\lim_{p\to 0} \bar{V} = \lim_{p\to 0} pv_{C_B} > 0$.*

Remark 2.3. *We assumed that the battery can be modelled by a queueing-like system with "arrivals" and "departures" of chunks of energy. Such battery models were considered several times in literature, see e.g. [64,65]. While being modelled as a queueing system, one prefers that the battery/queue is full in contrast to most other queueing systems. That is, the preferred operation differs significantly.*

2.3.2 A refinement

While it is reasonable to assume that the sensor node cannot value its data, it is not always reasonable to assume that the sensor node is unaware of the presence of data. We therefore now refine the model so that the sensor node does not transmit when there is no data to transmit. To this end, we introduce the indicator A_n, which is 1 if the node has data to transmit and 0 otherwise. Of course we have $A_n = 1_{\{V_n>0\}}$, but it is more convenient to track A_n separately, see below. In addition, we assume that the sequence $\{S_n, n \in \mathbb{N}\}$ exhibits the following independence assumption. The indicators, $1_{\{S_n=0\}}$, that there is nothing to sense constitutes a sequence of independent and identically distributed random variables. Note that this assumption does not exclude the presence of correlation in the sensing process. As

in the preceding section, $\bar{S} = \mathsf{E}[S_n]$ denotes the mean value of the sensed information. Moreover, let $s_0 = \mathsf{P}[S_n = 0]$ denote the probability that there is nothing to sense.

Following similar arguments as in the preceding section, we find that the system variables V_n, A_n and B_n adhere the following set of recursive equations,

$$\begin{aligned} V_{n+1} &= \alpha V_n(1-T_n) + S_n 1_{\{B_n \geq M\}}\,, \\ A_{n+1} &= 1_{\{S_n>0\}} 1_{\{B_n \geq M\}} + (1 - 1_{\{S_n>0\}} 1_{\{B_n \geq M\}}) A_n (1-T_n)\,, \\ B_{n+1} &= \min(B_n - M 1_{\{B_n \geq M\}} - NT_n + H_n, C)\,, \end{aligned}$$

where T_n denotes the indicator that there is a transmission,

$$T_n = 1_{\{B_n \geq M+N\}} A_n P_n\,.$$

That is, there is a transmission when (i) there is sufficient energy ($B_n \geq M+N$), (ii) there is something to send ($A_n = 1$) and (iii) there is a transmission opportunity ($P_n = 1$).

In contrast to the preceding section, the sequence $\{B_n, n \in \mathbb{N}\}$ is not a Markov chain as the evolution of B_n depends on the presence or absence of information. Therefore we focus on the sequence $\{(A_n, B_n), n \in \mathbb{N}\}$, which is a Markov chain (from (1.4)). Let $\widetilde{b}_k = \mathsf{P}[B_n = k, A_n = 0]$ be the probability that there are k chunks of energy in the battery at slot boundaries and there is no information at the sensor node. By conditioning on the values of P_n, H_n and A_n, we find,

$$\widetilde{b}_k = \sum_{\ell=0}^{M-1} \widetilde{b}_\ell h_{k-\ell} + s_0 \sum_{\ell=M}^{C} \widetilde{b}_\ell h_{k-\ell+M} + p\, s_0 \sum_{\ell=M+N}^{C} \widehat{b}_\ell h_{k-\ell+M+N}\,, \tag{2.20}$$

for $k = 0, 1, \ldots, C-1$, and,

$$\widetilde{b}_C \quad = \quad \sum_{\ell=0}^{M-1} \widetilde{b}_\ell \bar{H}_{C-\ell} \quad + \quad s_0 \sum_{\ell=M}^{C} \widetilde{b}_\ell \bar{H}_{C_B-\ell+M} \quad + \quad p\, s_0 \sum_{\ell=M+N}^{C} \widehat{b}_\ell \bar{H}_{C-\ell+M+N}\,.$$

Here, $\widehat{b}_k = \mathsf{P}[B_n = k, A_n = 1]$ is the probability to have k chunks and information at a slot boundary. Again, by conditioning on the values of P_n, H_n and A_n, we have,

$$\begin{aligned} \widehat{b}_k = \sum_{\ell=0}^{M-1} \widehat{b}_\ell h_{k-\ell} + \sum_{\ell=M}^{C} (\widehat{b}_\ell + \widetilde{b}_\ell (1-s_0)) h_{k-\ell+M} \\ + p \sum_{\ell=M+N}^{C} \widehat{b}_\ell ((1-s_0) h_{k-\ell+M+N} - h_{k-\ell+M})\,, \end{aligned} \tag{2.21}$$

for $n = 0, 1, \ldots, C-1$. Complementing the set of equations above with the normalisation condition,

$$\sum_{n=0}^{C} (\widehat{b}_n + \widetilde{b}_n) = 1\,,$$

allows for determining the probabilities $\widetilde{b}_n$ and $\widehat{b}_n$. For further use, we also define the probability b_n to have n chunks of energy at the node, irrespective of whether there is information at the node,

$$b_n = \widetilde{b}_n + \widehat{b}_n \,.$$

We now focus on the mean value of the information at the sensor node. Let $v_n = \mathsf{E}[V_k 1_{\{B_k=n\}}]$ be the mean value of information when there are n chunks of energy available. Notice that by the definition of A_k we have that $A_k = 0$ implies $V_k = 0$. Hence, there is no need to focus on the expectation of V_k for $A_k = 0$ and $A_k = 1$ as $v_n = \mathsf{E}[V_k 1_{\{B_k=n\}}] = \mathsf{E}[V_k 1_{\{B_k=n,A_k=1\}}]$ and $\mathsf{E}[V_k 1_{\{B_k=n,A_k=0\}}] = 0$. By conditioning on the presence of transmission opportunities, the availability of data and the amount of harvested energy, we find,

$$v_k = \sum_{\ell=0}^{M-1} v_\ell \alpha h_{k-\ell} + \sum_{\ell=M+N}^{C} \widehat{b}_\ell p \bar{S} h_{k-\ell+M+N} + \sum_{\ell=M}^{C} (\alpha v_\ell + \bar{S} b_\ell) h_{k-\ell+M} - \sum_{\ell=M+N}^{C} (\alpha v_\ell + \bar{S}\widehat{b}_\ell) p h_{k-\ell+M} \,,$$

for $k = 0, \ldots, C-1$, while for $k = C$ we have,

$$v_C = \sum_{\ell=0}^{M-1} v_\ell \alpha \bar{H}_{C-\ell} + \sum_{\ell=M+N}^{C} \widehat{b}_\ell p \bar{S} \bar{H}_{C-\ell+M+N} + \sum_{\ell=M}^{C} (\alpha v_\ell + \bar{S} b_\ell) \bar{H}_{C-\ell+M} - \sum_{\ell=M+N}^{C} (\alpha v_\ell + \bar{S}\widehat{b}_\ell) p \bar{H}_{C-\ell+M} \,.$$

Finally, as we collect information when there is energy and information at the sensor at a transmission opportunity, the mean value of the information collected at a slot boundary equals,

$$\bar{V} = p \sum_{\ell=M+N}^{C} v_\ell \,.$$

Remark 2.4. *We note that the model of this section does not reduce to the model of Section 2.3 when the sensor always picks up information, that is, for $s_0 = 0$. Even for $s_0 = 0$, it is still possible that there is no new value of information during a time slot as there may be no sensing due to a lack of energy. If we additionally assume that sensing does not take energy ($M = 0$), both models do correspond. Indeed, equation* (2.20) *then implies $\widetilde{b}_k = 0$, whereas the sets of equations* (2.19) *and* (2.21) *are the same.*

2.3.3 Optimal data collection and numerical results

We now investigate the optimal data collection policy for the sensor node at hand. We assume that there is a cost c associated to data collection so that the average

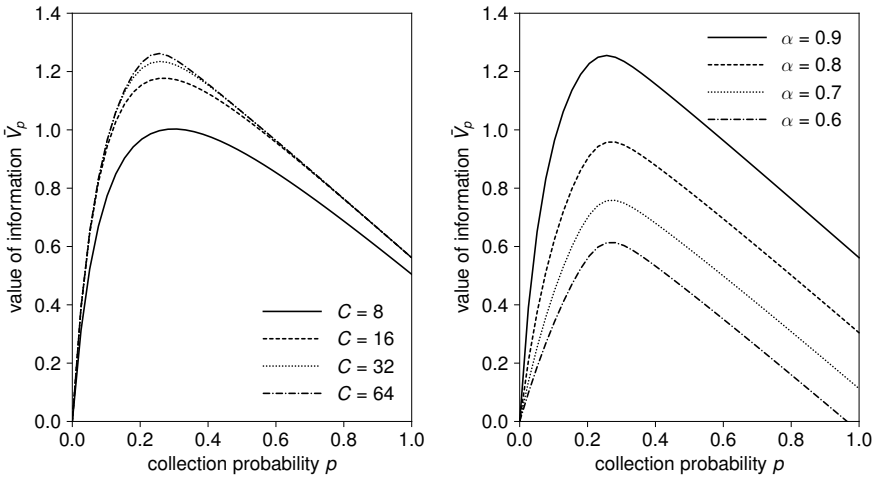

(a) Varying C (b) Varying α

Figure 2.5: The mean value of the information $\bar{V}_p$ versus the polling probability p for (a) different values of the battery capacity C and (b) different values of the decay rate α as indicated.

value after collection equals,

$$\bar{V}_p = -cp + \bar{V}\,.$$

We first illustrate the analysis of the initial model, introduced in Section 2.3.1 by some numerical examples. We then complement these with some numerical results for the refinements which were discussed in Section 2.3.2 In either case, we particularly focus on the optimal collection probability p.

Information-agnostic transmissions

We first investigate how the battery capacity and discount factor affect the mean value of information. To this end, we consider the initial model assuming Poisson energy harvesting — the energy harvesting distribution is Poisson with mean λ — and energy discretisation so that $M = 1$ and $N = 4$ chunks of energy are required for sensing and transmitting, respectively.

Figures 2.5(a) and 2.5(b) depict the value of information $\bar{V}_p$ in terms of the data collection rate p. We assume that the cost of collection is half the mean value of information collected in a slot: $c = 1$ and $\bar{S} = 2$. Figure 2.5(a) fixes the discount factor to $\alpha = 0.9$ and shows $\bar{V}_p$ for various values of the battery capacity C as indicated. In contrast, Figure 2.5(b) fixes the battery capacity to $C = 32$ and shows $\bar{V}_p$ for various values of the discount factor. For both figures, the mean number of chunks of harvested energy equals $\lambda = 2$.

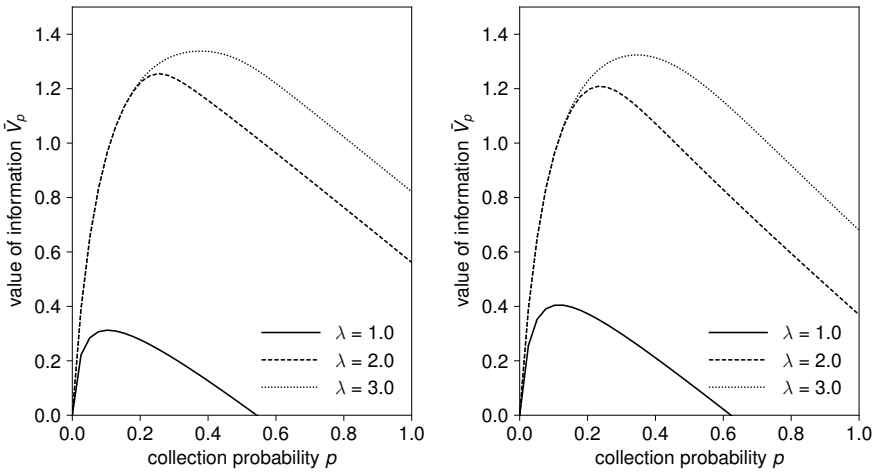

(a) Poisson (b) Geometric

Figure 2.6: The mean value of the information $\bar{V}_p$ versus the polling probability p for a Poisson (a) and geometric (b) energy harvesting distribution, for different values of the mean amount of harvested energy λ as indicated.

It can be seen from both figures that the value of information $\bar{V}_p$ first increases for increasing values of the collection probability and then decreases again. This observation can be explained by noting that for higher values of p the chance of having insufficient energy increases as more energy is consumed for transmissions. For high p, it is quite likely that there is insufficient energy to transmit so that the possible gain of frequent data collection cannot compensate the collection cost. Further, Figure 2.5(a) shows that it is beneficial to increase the battery size. Having a battery with more capacity facilitates compensating periods with little energy harvesting. However, the marginal gain obtained by increasing the battery capacity quickly disappears. Increasing the discounting factor is equally beneficial as can be seen from Figure 2.5(b). A higher discounting factor implies that the value of information decays more slowly so that more information is available during collection.

We now focus on the effect of the distribution of the harvested energy. To this end, figures 2.6(a) and 2.6(b) depict the mean value of information versus the collection probability p for Poisson distributed (Figure 2.6(a)) and geometrically distributed (Figure 2.6(b)) energy harvesting. Different values for the mean number λ of harvested chunks in a slot are assumed as indicated. As for the preceding figures, $M = 1$ and $N = 4$ chunks of energy are required for sensing and transmitting, respectively. Moreover, the discounting factor is equal to $\alpha = 0.9$, the mean value of sensed information $\bar{S} = 2$ is twice the collection cost $c = 1$, and the battery can store up to $C = 32$ chunks of energy.

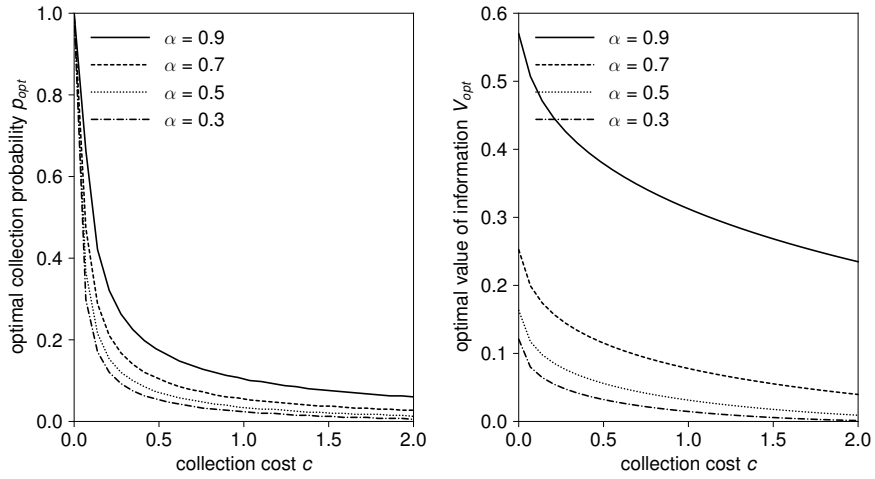

(a) optimal probability (b) optimal value

Figure 2.7: The optimal collection probability p_{opt} (a) and the corresponding value of information V_{opt} (b) for different values of α as indicated.

Comparing Figures 2.6(a) and 2.6(b) reveals that the distribution of the harvested energy can affect the value of information $\bar{V}_p$ as well as the optimal collection probability p. Increasing the harvesting capability of the sensor node (increasing λ) is initially beneficial, but the marginal gain from a further increase quickly disappears. Indeed, if there is already sufficient energy, one cannot expect that a further increase of the harvesting capability considerably improves the performance of the sensor node.

Finally, we consider the effect of the collection cost on the optimal collection probability and the associated optimal value of information. Figure 2.7(a) shows the optimal collection probability p versus the collection cost c for different values of the discount factor α as depicted. Figure 2.7(b) depicts the value of information corresponding to this optimal probability versus the collection cost c. Apart from the discount factor and the collection cost, the parameters are chosen as in Figures 2.5(a) and 2.5(b): the mean value of sensed information equals $\bar{S} = 2$, the energy harvesting distribution is a Poisson distribution with mean 1, $M = 1$ and $N = 4$ chunks of energy are required for sensing and transmissions and the battery can store up to $C = 32$ of these chunks.

The optimal collection probability quickly decreases for increasing collection costs. As the collection cost increases, any gain of collecting quickly drops due to the cost of collecting. Further, if α is higher, it is more beneficial to collect (see Figure 2.5(b)) so that the optimal collection probability is higher as well. In addition, the value of information $\bar{V}_p$ at the optimal collection probability is higher for increasing values of α so that it is not only beneficial to collect more, but the

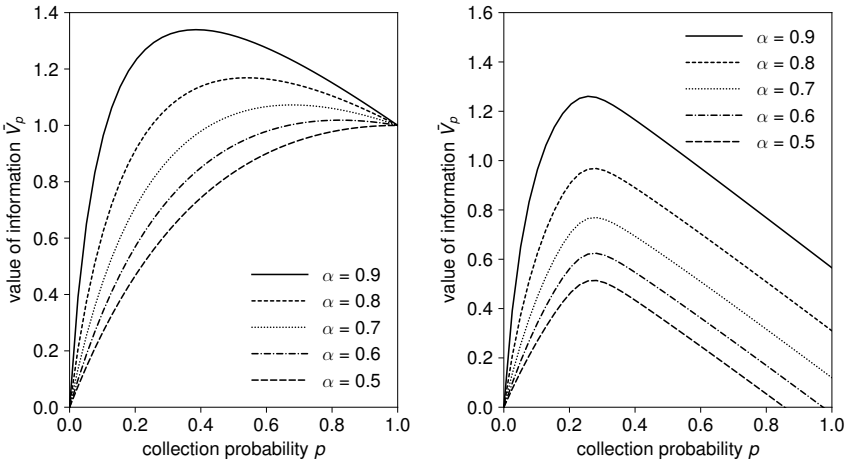

(a) $s_0 = 0.9$ (b) $s_0 = 0.1$

Figure 2.8: The mean value of information versus the collection probability for (a) $s_0 = 0.9$ and (b) $s_0 = 0.1$ and different values of α as indicated.

net gain of collecting more is higher as well.

Information-aware transmissions

To evaluate the use of the refined model, we now focus on how the absence of information probability s_0 affects the value of information.To make its influence clear, figures 2.8(a) and 2.8(b) depict the value of information versus the collection probability, for high and low s_0 respectively, and for various values of the discount factor α as depicted. To allow for a comparison with the model of Section 2 and the results of Section 4.1, we largely adopt the parameters of the latter: the mean value of sensed information equals $\bar{S} = 2$, which is twice the cost $c = 1$ of collecting. The energy harvesting distribution is a Poisson distribution with mean λ =2. In addition, $M = 1$ and $N = 4$ chunks of energy are required for sensing and transmissions and the battery can store up to $C = 32$ of these chunks.

As $\bar{S}$ is fixed, a high s_0 not only means that most slots there is no information, but also means that there is considerable information in the slots with information. That is, the sensing is a bursty process. In contrast, small s_0 means that many slots carry a small amount of information. It is not surprising that these considerable differences in information arrival patterns translate into different collected values of information. This is indeed confirmed by comparing Figures 2.8(a) and 2.8(b). The figures show that burstiness is beneficial. This can be explained by noting that no energy is lost on sending a limited amount of information. Indeed, for $s_0 = 0.9$ the chance that there is no information is considerable, whereas the value of the information is considerable whenever there is something to send. Further compar-

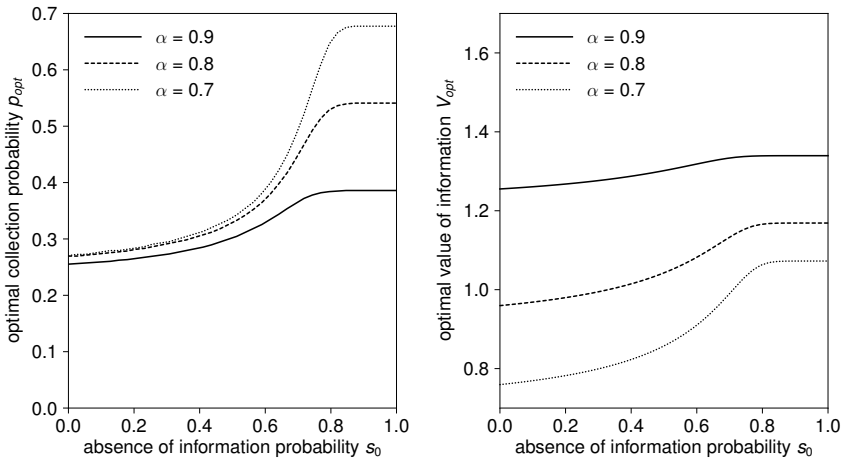

(a) optimal collection probability

(b) optimal value of information

Figure 2.9: The optimal collection probability p_{opt} (a) and the value of information V_{opt} (b) versus absence of information probability s_0 for different values of α as indicated.

ison reveals that the value of information is considerably larger for bursty sensing compared to non-bursty sensing. Moreover, the optimal collection probability is only sensitive to changes in the discount factor for bursty sensing.

This observation is also confirmed by Figures 2.9(a) and 2.9(b) which depict the optimal collection probability and the corresponding value of information versus the probability s_0, respectively. Different values of the discount factor are assumed as depicted. The same parameters are assumed as in Figures 2.8(a) and 2.8(b), with the exception of s_0, which now varies. We see that the optimal collection probability and the corresponding value of information increases for increasing s_0 as explained before. Moreover, the difference between the optimal collection probabilities for different α is largest for high s_0. Somewhat surprising and opposite to the collection probabilities, the difference between the corresponding values of information is largest for small s_0.

2.4 Correlated energy harvesting

Due to the vast increase in the number of battery powered wireless devices over the past couple of decades, energy harvesting from natural resources is becoming more crucial than ever to prolong the lifetime of such devices. The various sources for energy harvesting (EH) are wind turbines, photovoltaic cells, electrostatic and piezoelectric devices and electromagnetic devices [66]. However, due to the random nature of harvesting sources, the design and modelling of the system require careful analysis. In particular, depending on the spatial distribution of EH devices,

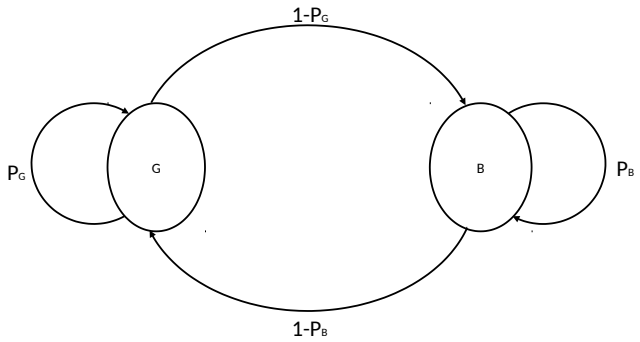

Figure 2.10: Markov chain model of energy harvesting

the amount of energy harvested by different devices can be highly correlated. For example, consider EH devices harvesting energy from tidal motion. The device located at the tidal crest can generate energy faster than the device located at the tidal trough. In this case, the time delay in the generation of energy between such devices is equal to the speed of one wavelength [67].

Similarly, the amount that can be harvested exhibits temporal correlation as well. For example, if a cloud passes by a sensor's solar panel, the panel temporarily outputs less energy. In a typical scenario, the cloud passes by slowly. It is then the case that if there is a cloud at time k (and the corresponding energy output reduction), it is more likely that the cloud is still there at time $k+1$. One simple way to model the temporal correlation in the energy harvesting process is to model it by a two state Markov chain as depicted in Figure 2.10. The state space of the Markov chain is $\{G,B\}$, where G and B denote the *GOOD* and *BAD* harvesting states, respectively. Let E_k be the underlying harvesting process and if $E_k = G$, then we can assume that energy is harvested with a good rate, for example the amount is Poisson distributed with a high mean. If $E_k = B$, then there is no energy harvesting. Such correlation was already accounted for in Section 2.2.4 in the simplified setting where energy consumption for sensing was not accounted for.

We now introduce time correlation in the energy harvesting process in the more general framework of Section 2.3. We again show that the model allows for studying the trade-off between the cost of frequent data collection — data collection is not only costly but also induces increased energy consumption at the SNs — and timely data delivery. Recall that the modelling assumptions allow for time correlation in the data sensing process, so that now both the sensing and energy harvesting processes exhibit time correlation. At the end of the section, we present various numerical examples that investigate the SN performance in terms of various system parameters including the polling probability of the mobile sink, the

battery capacity, the parameters of the harvesting process, etc. In particular, the numerical section discusses how correlation in the harvesting process affects the performance of the network.

2.4.1 Mathematical model

We now model the sensor node with the additional complication of time correlation in the energy harvesting process. The basic operation of the node is the same as in the preceding sections, i.e., sensor data is collected and stored in on-board memory, and energy chunks are collected and stored in the battery. Whenever the mobile sink passes by, the data (if any) is transferred to the mobile sink, provided the sensor node has sufficient energy to transmit the data and there is any data to transmit. Hence, three interacting random processes — the energy harvesting process, the sensor data arrival process and the data collection process — determine the evolution of the state of the sensor node over time. Since the sensor data arrival and the data collection process are the same as in preceding section, we only describe the energy harvesting process below.

Energy harvesting process

We introduce a Markov-modulated energy harvesting process, where the modulating process takes values in the set $\mathscr{J} = \{1,\ldots,J\}$. Let $E_n \in \mathscr{J}$ denote the state of the modulating process during slot n, and let H_n denote the number of chunks of energy that are harvested in this slot. The energy harvesting process is then characterised by the following marked state transition probabilities,

$$\theta_{ij}(m) = \mathsf{P}[H_n = m, E_{n+1} = j | E_n = i] .$$

That is, $\theta_{ij}(m)$ is the transition probability to go from state i to state j while harvesting m chunks of energy. For further use, we also define the transition probabilities $\bar{\theta}_{ij}^{(m)}$ from state i to state j while harvesting at least m chunks,

$$\bar{\theta}_{ij}(m) = \mathsf{P}[H_n \geq m, E_{n+1} = j | E_n = i] = \sum_{\ell=m}^{\infty} \theta_{ij}(\ell) .$$

The other battery parameters are the same; the battery can store at most C energy chunks with M chunks required for sensing and N for the transmission. Sensing has priority over transmissions, meaning that the node senses when there are M chunks present and transmits when there are $M+N$ energy chunks present, there is information to send and the mobile sink is in range.

2.4.2 Performance analysis

We subsequently study the evolution of the battery level and the value of information. Compared to Section 2.3, there is only a change in the assumptions on the

energy harvesting process. Therefore, the recursions that describe how the battery levels, and the value of information changes over time still apply. Recall that the battery level B_k, the value of information V_k and the indicator A_k adhere the following recursions,

$$\begin{aligned}
B_{n+1} &= \min(B_n - M1_{\{B_n \geq M\}} - NT_n + H_n, C)\,, \\
V_{n+1} &= \alpha V_n(1-T_n) + S_n 1_{\{B_n \geq M\}}\,, \\
A_{n+1} &= 1_{\{S_n>0\}} 1_{\{B_n \geq M\}} + (1 - 1_{\{S_n>0\}} 1_{\{B_n \geq M\}}) A_n (1-T_n)\,.
\end{aligned}$$

The first and second term of A_{n+1} correspond to the case that information was and was not sensed during the preceding slot, respectively. In the latter case, there is only information at the sensor node if there was already information at the preceding slot boundary that was not transmitted. Notice that the evolution of A_n only depends on the indicator that there is information $1_{\{S_n>0\}}$, and not on the actual value of S_n. Finally, we again express T_n in terms of A_n, B_n and P_n as follows,

$$T_n = A_n\, 1_{\{B_n \geq M+N\}}\, P_n\,.$$

Battery level probabilities

We first focus on expressions for the battery level probabilities. To this end, we note that the process $\{(B_n, A_n, E_n), n \in \mathbb{N}\}$ is a Markov process, and we study its stationary distribution. Let

$$\widetilde{b}_j(k) = \lim_{n\to\infty} \mathsf{P}[B_n = k, A_n = 0, E_n = j]$$

be the stationary probability that there are k chunks of energy in the battery, while there is no information at the sensor node ($A_n = 0$), and the energy harvesting process is in state $E_n = j$, $j \in \mathscr{J}$. The stationary battery level probabilities $\widehat{b}_j(k)$ when there is information at the sensor node are defined likewise,

$$\widehat{b}_j(k) = \lim_{n\to\infty} \mathsf{P}[B_n = k, A_n = 1, E_n = j]\,.$$

Note that we account for the availability of information as the decision to transmit depends on the availability of information, which in turn affects the battery level.

Expressing the state probabilities at slot $n+1$ in terms of those at slot n by conditioning on the values of A_n, P_n, E_n and H_n, and then sending n to ∞ yields the following set of balance equations,

$$\begin{aligned}
\widetilde{b}_j(k) = \sum_{i=1}^{J}\sum_{\ell=0}^{M-1} \tilde{b}_i(\ell)\theta_{ij}(k,\ell) + s_0 \sum_{i=1}^{J}\sum_{\ell=M}^{C} \tilde{b}_i(\ell)\theta_{ij}(k,\ell-M) \\
+ p s_0 \sum_{i=1}^{J}\sum_{\ell=M+N}^{C} \widehat{b}_i(\ell)\theta_{ij}(k,\ell-M-N)\,, \quad (2.22)
\end{aligned}$$

and,

$$\widehat{b}_j(k) = \sum_{i=1}^{J}\sum_{\ell=0}^{M-1} \widehat{b}_i(\ell)\theta_{ij}(k,\ell) + \sum_{i=1}^{J}\sum_{\ell=M}^{C} \left(\widehat{b}_i(\ell) + (1-s_0)\widetilde{b}_i(\ell)\right)\theta_{ij}(k,\ell-M) + p\sum_{i=1}^{J}\sum_{\ell=M+N}^{C} \widehat{b}_i(\ell)\left((1-s_0)\theta_{ij}(k,\ell-M-N) - \theta_{ij}(k,\ell-M)\right), \quad (2.23)$$

for $k = 0,1,\ldots,C$ with $j \in \mathscr{J}$. Here, with a slight abuse of notation, we introduced the following shorthand notation for $i, j \in \mathscr{J}$ and $\ell \leq k$,

$$\theta_{ij}(k,\ell) = \begin{cases} \bar{\theta}_{ij}(k-\ell) & \text{for } k = C, \\ \theta_{ij}(k-\ell) & \text{otherwise.} \end{cases}$$

We collect the probabilities $\widetilde{b}_j(k)$ and $\widehat{b}_j(k)$ in the row vectors $\widetilde{\mathbf{b}}(k) = [\widetilde{b}_j(k)]_{j=1}^{J}$ and $\widehat{\mathbf{b}}(k) = [\widehat{b}_j(k)]_{j=1}^{J}$ for each k, and introduce the row vector $\mathbf{b}(k) = [\widetilde{\mathbf{b}}(k), \widehat{\mathbf{b}}(k)]$. The equations above can then be summarised in the following matrix equation,

$$\mathbf{b}(k) = \sum_{\ell=0}^{C} \mathbf{b}(\ell)\boldsymbol{\mathcal{B}}(\ell,k), \quad (2.24)$$

where $\boldsymbol{\mathcal{B}}(\ell,k) = [\boldsymbol{\mathcal{B}}_{ij}(\ell,k)]_{i,j=1}^{2}$ with,

$$\begin{aligned}
\boldsymbol{\mathcal{B}}_{11}(\ell,k) &= 1_{\{\ell<M\}}\boldsymbol{\mathcal{A}}(k,\ell) + s_0 1_{\{\ell\geq M\}}\boldsymbol{\mathcal{A}}(k,\ell-M), \\
\boldsymbol{\mathcal{B}}_{21}(\ell,k) &= p s_0 1_{\{\ell\geq M+N\}}\boldsymbol{\mathcal{A}}(k,\ell-M-N), \\
\boldsymbol{\mathcal{B}}_{12}(\ell,k) &= 1_{\{\ell\geq M\}}(1-s_0)\boldsymbol{\mathcal{A}}(k,\ell-M), \\
\boldsymbol{\mathcal{B}}_{22}(\ell,k) &= 1_{\{\ell<M\}}\boldsymbol{\mathcal{A}}(k,\ell) + 1_{\{\ell\geq M\}}\boldsymbol{\mathcal{A}}(k,\ell-M) \\
&\quad + p 1_{\{\ell\geq M+N\}}\left((1-s_0)\boldsymbol{\mathcal{A}}(k,\ell-M-N) - \boldsymbol{\mathcal{A}}(k,\ell-M)\right).
\end{aligned}$$

In the former expressions, $\boldsymbol{\mathcal{A}}(k,\ell)$ is the $J \times J$ matrix with elements $\theta_{ij}(k,\ell)$, $i, j \in \mathscr{J}$. Finally, let $\mathbf{b} = [\mathbf{b}(k)]_{k=0}^{C}$ and $\boldsymbol{\mathcal{B}} = [\boldsymbol{\mathcal{B}}(\ell,k)]_{\ell,k=0}^{C}$ so that (2.24) immediately yields $\mathbf{b} = \mathbf{b}\boldsymbol{\mathcal{B}}$. The stationary probability vector $\mathbf{b}$ is the normalised solution of this matrix equation.

It is easy to check that $\boldsymbol{\mathcal{B}}(\ell,k)$ is a zero matrix for $k < l - M - N$. Indeed, the battery level drops for at most $M+N$ levels during a slot. Hence, $\mathscr{B}$ has an upper-Hessenberg block structure with blocks of size $(2J(M+N)) \times (2J(M+N))$. This block structure can then be exploited to calculate the stationary probability vector $\mathbf{b}$, for example by using linear level reduction (see e.g. [68]).

Mean value of information

We now study the mean value of information at the sensor node. Noting that $A_n = 0$ implies $V_n = 0$, we obviously have,

$$\mathsf{E}[V_n 1_{\{B_n=k, A_n=0, E_n=j\}}] = 0,$$

for $k = 0, 1, \ldots, C$ and $j \in \mathscr{J}$. Let

$$v_j(k) \doteq \lim_{n\to\infty} \mathsf{E}[V_n 1_{\{B_n=k, A_n=1, E_n=j\}}]$$

be the mean value information when there is information, when there are k chunks of energy and the harvesting process is in state j, $k = 0, 1, \ldots, C$ and $j \in \mathscr{J}$. Furthermore, let $v(k) = \sum_{j=1}^{J} v_j(k)$ be the mean value information when there is information and there are k chunks of energy.

As for the battery level probabilities, we again condition on the values of B_n, A_n and P_n, to express the mean $\mathsf{E}[V_{n+1} 1_{\{B_{n+1}=k, A_{n+1}=1, E_{n+1}=j\}}]$ in terms of the mean $\mathsf{E}[V_n 1_{\{B_n=k, A_n=1, E_n=j\}}]$ and the battery level probabilities. After taking the limit $n \to \infty$, we find

$$\begin{aligned} v_j(k) = &\sum_{i=1}^{J} \sum_{\ell=M}^{C} (\alpha v_i(\ell) + \bar{S}(\widehat{b}_i(\ell) + \widetilde{b}_i(\ell)))\theta_{ij}(k, \ell - M) \\ &+ \alpha \sum_{i=1}^{J} \sum_{\ell=0}^{M-1} v_i(\ell)\theta_{ij}(k,\ell) + p\bar{S} \sum_{i=1}^{J} \sum_{\ell=M+N}^{C} \widehat{b}_i(\ell)\theta_{ij}(k, \ell - M - N) \\ &- p \sum_{i=1}^{J} \sum_{\ell=M+N}^{C} (\alpha v_i(\ell) + \bar{S}\widehat{b}_i(\ell))\theta_{ij}(k, \ell - M), \end{aligned} \tag{2.25}$$

for $k \in \{0, 1, \ldots, C\}$. Collecting the $v_j(k)$ for $j \in \mathscr{J}$ in the row vector $\mathbf{v}(k) = [v_j(k)]_{j=1}^{J}$, we obtain the system of vector equations,

$$\mathbf{v}(k) = \alpha \sum_{\ell=0}^{C} \mathbf{v}(\ell)\boldsymbol{\mathcal{V}}(\ell, k) + \bar{S}\mathbf{w}(k), \tag{2.26}$$

for $k \in \{0, 1, \ldots, C\}$ with

$$\boldsymbol{\mathcal{V}}(\ell, k) = 1_{\{\ell<M\}}\boldsymbol{\mathcal{A}}(k,\ell) + 1_{\{\ell\geq M\}}\boldsymbol{\mathcal{A}}(k, \ell - M) - p1_{\{\ell\geq M+N\}}\boldsymbol{\mathcal{A}}(k, \ell - M),$$

and

$$\begin{aligned} \mathbf{w}(k) = &\sum_{\ell=M}^{C} \left(\widehat{\mathbf{b}}(\ell) + \widetilde{\mathbf{b}}(\ell)\right) \boldsymbol{\mathcal{A}}(k, \ell - M) \\ &+ p \sum_{\ell=M+N}^{C} \widehat{\mathbf{b}}(\ell) \left(\boldsymbol{\mathcal{A}}(k, \ell - M - N) - \boldsymbol{\mathcal{A}}(k, \ell - M)\right). \end{aligned}$$

As for the battery probabilities, the equations for the mean value of information is a set of $J(C+1)$ equations with as many unknowns and is easily solved provided C is not prohibitively large. For larger C, one can again exploit the upper-Hessenberg block structure of the set of equations, the blocks now being $J(M+N) \times J(M+N)$ matrices.

2.4.3 Cost and profit of collection

Once the mean value of information at the sensor node for the different battery levels is determined by numerically solving the systems of equations in the preceding subsections, we can determine the cost or profit of data collection. Noting that data is only collected if there is sufficient energy and the mobile sink passes by, we find that the profit of the data collection, i.e. the mean value of information of the sensor data that is actually collected (per time slot), can be expressed in terms of the v_k's as follows,

$$\bar{V} = p \sum_{k=M+N}^{C} \sum_{j=1}^{J} v_j(k) \,.$$

Assuming that there is a fixed cost for every time the mobile sink collects data from the sensor, the mean cost of collection is linear in p

$$\bar{C} = c\, p$$

where c is a constant cost, expressed in terms of the value of information. The cost c can be anything related to the latency or loss of information while sending the data. Subtracting the cost of collection from the mean value of information that is collected, we find that profit or the mean value of the data collection equals

$$\bar{V}_p = -c\, p + \bar{V} \,.$$

Remark 2.5. *Recall that the collection cost relates to the trajectory that is taken by the mobile sink: p is the probability that the sink is available, or the fraction of time that the sink is in range. If the mobile sink moves continuously, a higher p means that the mobile sink will visit the sensor node more often, while if the mobile sink is not constantly moving, increasing p means that the mobile sink remains idle for less time. In either case there is a cost increase, which we assume to be proportional to p.*

Remark 2.6. *While we mainly focus on a single node, it is worth pointing out that the results for the single sensor node can also be used to find the optimal trajectory of the mobile sink. By carefully analysing a given trajectory of a mobile sink that covers a set of sensor nodes, one can find the fraction of time the mobile sink is in range for every sensor node. Say p_k is this fraction for the kth sensor node. Given p_k, the calculations above allow for finding the value of information at the kth sensor node. It then remains to find the trajectory of the mobile sink which maximises the sum of the values of information.*

2.4.4 Numerical results and discussion

Having established a numerical procedure to calculate the mean value of the data collection in Section 2.4.2 and of the cost in Section 2.4.3, we now illustrate our approach by some numerical examples. In particular, we study the mean value of the data collection $\bar{V}_p$ in terms of the collection probability p, as well as the

optimal collection probability in terms of various system parameters, including the effect of time correlation in the energy harvesting process. Note that the optimal collection probability below is only locally optimal. That is, it is the collection probability that optimises the value of information of the single sensor node under consideration, while accounting for some collection cost.

For the numerical examples, we assume that the harvesting process is modulated by a Markov process with two states, $\mathscr{J} = \{1,2\}$. The harvesting process is inactive in State 1 while the number of energy chunks constitutes a sequence of independent Poisson distributed random variables with mean λ when the modulating process is in State 2 with $h_m = \exp(-\lambda)\lambda^m/m!$. As there are only two states, it suffices to specify the transition probability from the active to the inactive state θ_{21} and the transition probability from the inactive to the active state θ_{12}.

The following alternative characterisation of the harvesting process will be used in the remainder. Let σ be the fraction of time the harvesting process is in the active state and let κ be the average duration of an active and an inactive period. The latter is a measure for the time-scale of the energy harvesting process, larger κ meaning that the harvesting process alternates more slowly between states. Simple calculations yield,

$$\sigma = \frac{\theta_{21}}{\theta_{12}+\theta_{21}}, \qquad \kappa = \frac{1}{\theta_{12}} + \frac{1}{\theta_{21}}, \qquad \lambda^* = \lambda\,\sigma = \frac{\lambda\,\theta_{21}}{\theta_{12}+\theta_{21}}$$

For a fixed σ, any choice $\kappa \geq \max(\sigma^{-1},(1-\sigma)^{-1})$ uniquely defines θ_{12} and θ_{21}. In particular, for $\kappa = \sigma^{-1}+(1-\sigma)^{-1}$ we have no time correlation as $\theta_{12} = 1-\theta_{21}$ so that the next state is active or inactive, independently from the current state.

We now define the parameter values used throughout this section. On average $\lambda = 5$ energy chunks are harvested in active slots, unless indicated otherwise. It takes $M = 1$ energy chunk to sense the data and $N = 4$ energy chunks for transmitting the information. The average value of the sensing data is $\bar{S} = 2$, while we assume that during most time slots there is no data: $s_0 = 0.9$. Moreover, we set the information decay rate equal to $\alpha = 0.9$ and the maximum capacity of the battery to $C = 16$, unless otherwise specified. Finally, the cost to collect the data is $c = 1$ for all plots.

Figure 2.11 depicts the mean value of information $\bar{V}_p$ in terms of the collection probability p. Energy harvesting is slightly bursty: we assume $\sigma = 0.4$ and $\kappa = 16$. Figure 2.11(a) shows the mean value of information for different battery capacities C as indicated, while the decay rate is fixed to $\alpha = 0.9$. On the other hand, Figure 2.11(b) fixes the battery capacity to $C = 16$ and shows $\bar{V}_p$ for different decay rates as indicated. From both figures, we see that $\bar{V}_p = \bar{V} - \bar{C}$ is a concave function of p. This observation can be explained by noting that an increase of p is beneficial for small p, as the data is collected more often (the increase of $\bar{V}$ compensates the additional collection cost $\bar{C}$). For high p, it is however quite likely that there is insufficient energy to transmit. Therefore, the possible gain of frequent data collection cannot compensate the collection cost (the increase of $\bar{V}$ no longer compensates the additional collection cost $\bar{C}$). Further, Figure 2.11(a)

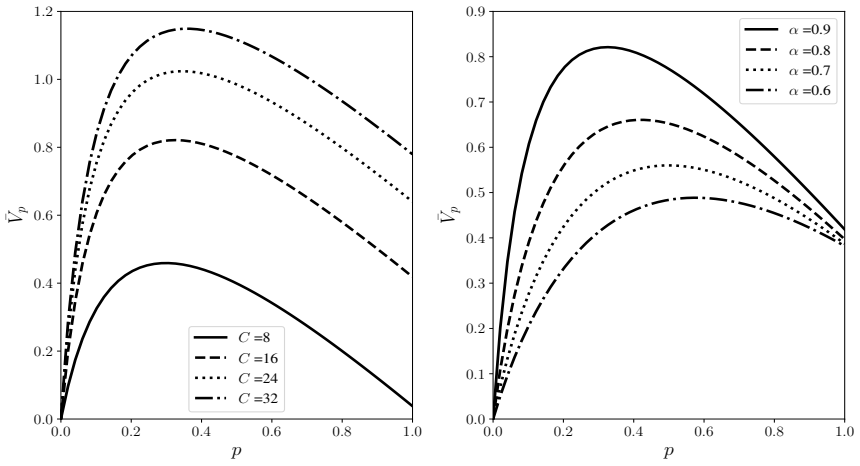

(a) Curves for different C

(b) Curves for different α

Figure 2.11: The mean value of the data collection $\bar{V}_p$ versus the polling probability p for (a) different values of the battery capacity C and (b) different values of the decay rate α as indicated.

shows that it is beneficial to increase the battery size. Having a battery with more capacity facilitates compensating periods with limited energy. Similarly, Figure 2.11(b) indicates that increasing the discounting factor also leads to better performance. A higher discounting factor implies that the value of information decays more slowly so that more information is available for collection. Of course, the discounting factor models the timeliness of the information and cannot be modified freely in practice. One may expect that for $p = 1$, $\bar{V}_p$ does not depend on the discounting factor as data is constantly collected. This is however not the case, as a lack of energy prevents constant transmissions. Summarising, in selecting the collection probability p, there is a clear trade-off between the cost of frequent collection $\bar{C}$, and the collected information $\bar{V}$, while more battery capacity and higher discounting factors both lead to a higher mean value of information $\bar{V}_p$.

We now focus on the effect of varying the length of the active and inactive harvesting periods. Figure 2.12(a) depicts $\bar{V}_p$ versus the polling probability p for different κ as indicated. Here, we fix the fraction of time the system is active: $\sigma = 0.4$. It is observed that increasing the length of the active and inactive periods affects $\bar{V}_p$ adversely. For high values of κ, the system has longer active periods followed by longer inactive periods. During long inactive periods, the battery drains completely as there is no energy harvesting while excess energy during active periods is lost as the battery capacity is limited. As a result, there will be less value of information to be collected by the mobile sink. Figure 2.12(b)

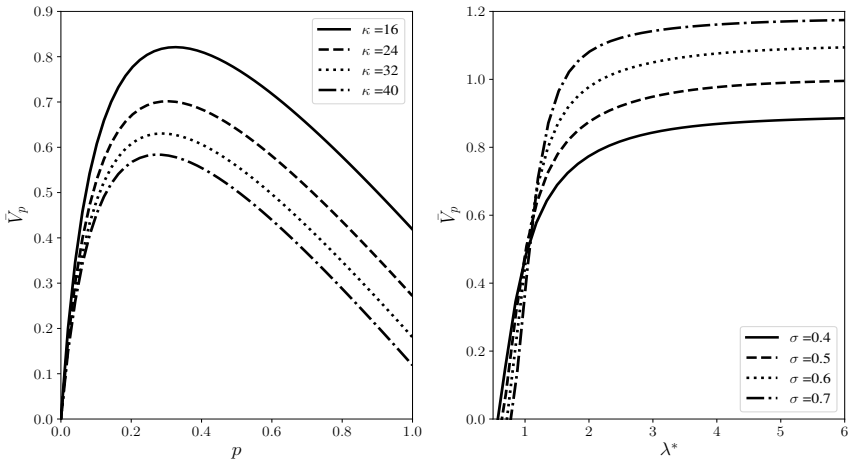

(a) Curves for different κ (b) Curves for different σ

Figure 2.12: The mean value of the data collection $\bar{V}_p$ versus the polling probability for different energy harvesting process (a) and mean value of the data collection $\bar{V}_p$ versus energy harvesting rate λ for different fractions of active time σ as indicated (b).

shows the mean value of the data collection versus the energy harvesting rate for different values of σ. We fix the data collection probability to $p = 0.2$ and the time-scale parameter to $\kappa = 16$. It can be clearly seen from the figure that the increase in harvesting capability improves the system performance. As κ is fixed, increasing σ means the system has longer active periods during which the battery level increases on average, and shorter inactive period for which the battery level decreases on average. Therefore, the chance of having sufficient energy for data transmissions increases, and therefore also the mean value of information collected by the mobile sink. However, if there is already sufficient energy for data sensing and transmissions, no further improvement is seen. In this case, the fixed battery capacity plays an important role. There is no additional benefit from longer active periods for high λ, since the battery reaches its maximum capacity quickly and excess energy chunks are lost. Note that the order of the curves is reversed for very low energy harvesting rates. This may be explained by the fact that during longer active periods with less harvesting (large σ) there is energy for sensing but not enough energy for transmissions when an opportunity arises. For larger λ, smaller σ imply that the harvesting is more concentrated. However not all energy can be stored as the battery capacity is finite.

To better understand the influence of the time-scale parameter κ, Figure 2.13 shows $\bar{V}_p$ versus κ, for fixed $\sigma = 0.4$ and various λ as indicated (Figure 2.13(a)) and for fixed $\lambda = 5$ and various σ as indicated (Figure 2.13(b)). As in the preced-

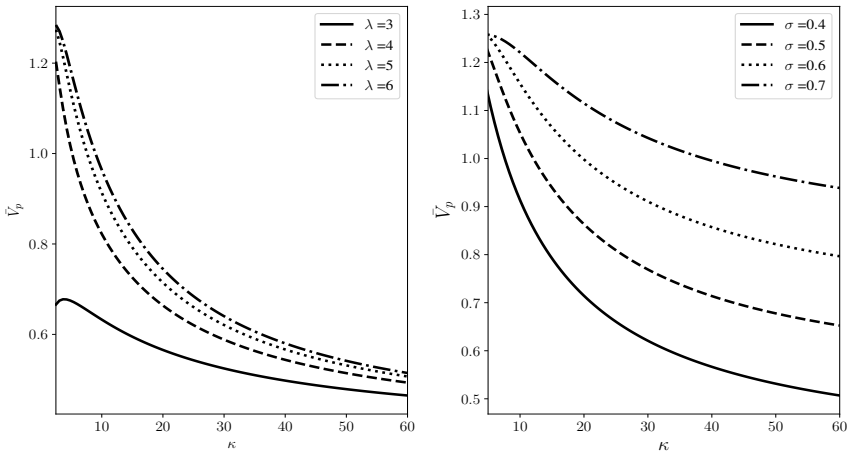

(a) Curves for different λ

(b) Curves for different σ

Figure 2.13: The mean value of data collection $\bar{V}_p$ versus average duration of active and inactive process κ for (a) different values of the energy harvesting rate λ and (b) different fractions of active time σ as indicated.

ing plot, the collection probability is fixed to $p = 0.2$. Figure 2.13 confirms the observation that an increase of κ leads to a decrease of $\bar{V}_p$. Even when the harvesting capability is considerable, a performance degradation is unavoidable when harvesting is interrupted for a long time. This effect is mitigated if one increases the battery capacity, as a fully charged battery with higher capacity can sustain the operation of the SN for longer times without harvesting.

The time-scale parameter κ also affects the value of the optimal collection probability p_{opt}. Figure 2.14 depicts the value of the optimal collection probability p_{opt} (Figure 2.14(a)) and the corresponding mean value of information $\bar{V}_{opt}$ (Figure 2.14(b)) versus κ for different values of the discounting factor α as indicated. We set $\sigma = 0.2$ and $\lambda = 5$. For increasing κ, it is optimal to collect more if κ is small. In contrast, for higher κ-values, it is optimal to collect less if κ further increases. While this is not intuitively clear, simple arguments show that the optimal collection probability increases as long as the average information at the sensor node exceeds the collection cost. As the average information at the sensor decreases for increasing κ, the optimal collection probability first increases and then decreases. Similar arguments explain the difference in decay rate of the optimal collection probability for different discount factors α. The resulting optimal mean value is easier explained: discounting less means that the information is longer available at the sensor node, and that more information is collected.

We now investigate how the absence of information probability s_0 affects the

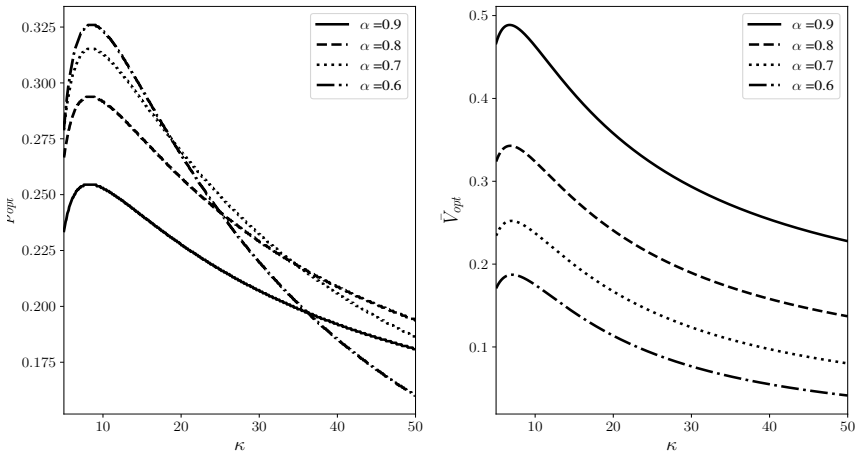

(a) optimal collection probability (p_{opt}) (b) optimal value of information ($\bar{V}_{opt}$)

Figure 2.14: The optimal collection probability p_{opt} (a) and the corresponding mean value of the collected information $\bar{V}_{opt}$ (b) vs. the time-scale parameter κ for different α as indicated.

optimal data collection probability and the corresponding value of information. In Figure 2.15, we vary s_0 while $\bar{S}$ is fixed. Higher s_0 means there is less chance that information arrives in a slot. However, if there is data, the information it carries is more significant. In other words, the process S_n is more bursty. We again plot the optimal collection probability p_{opt} (Figure 2.15(a)) and the corresponding value of information $\bar{V}_{opt}$ (Figure 2.15(b)). The harvesting process is characterised by $\sigma = 0.2$ and $\kappa = 16$. It is observed from Figure 2.15(a) that the optimal collection probability increases as the information process becomes bursty. Indeed, for increasing s_0, the data should be collected more frequently as one does not want to miss out on the rare occasions that there is information.

Finally, we analyse the effect of changing M and N on the mean value of data collection in Figure 2.16. We increase the battery capacity to $C = 64$ and keep high energy harvesting rate, $\lambda = 16$. This is done to ensure that the node has enough energy to sense or transmit the information when M and N are high. The values of the other parameters are $\sigma = 0.6$, $\kappa = 8$ and $p = 0.3$. Figure 2.16(a) shows the mean value of information $\bar{V}_p$ versus the number of energy chunks required to sense the data for different N as indicated. It can be easily seen from the figure that increasing M affects $\bar{V}_p$ adversely. Larger M means that the node requires more energy to sense new information from the environment. Thus, there will be less information present at the node as M increases, resulting in less data collection at the sink. It is also observed from the figure that performance of the system is

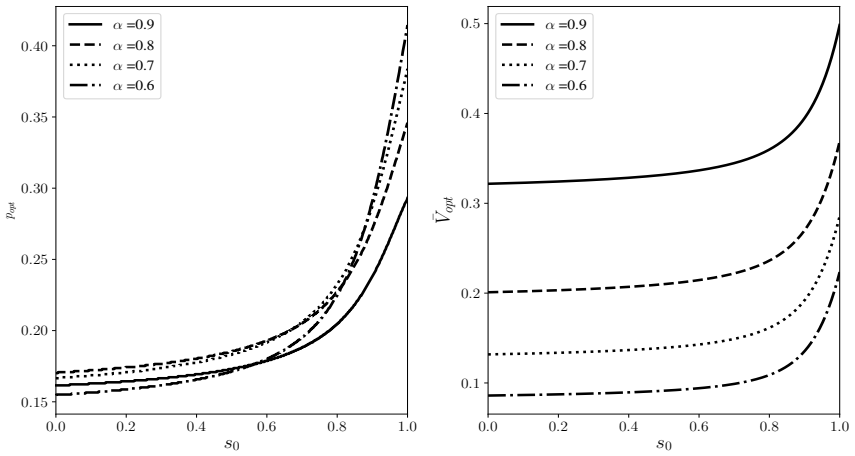

(a) optimal collection probability (p_{opt}) (b) optimal value of data collection ($\bar{V}_{opt}$)

Figure 2.15: The optimal collection probability p_{opt} (a) and the corresponding mean value of the collected information $\bar{V}_{opt}$ (b) vs. the absence of information probability s_0 for different α as indicated.

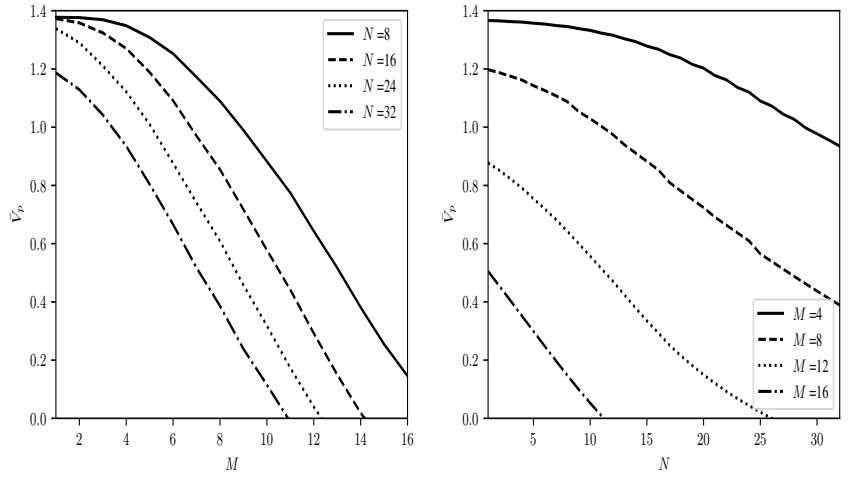

(a) Curves for different N (b) Curves for different M

Figure 2.16: The mean value of data collection $\bar{V}_p$ versus (a) number of energy chunks for sensing M and (b) number of energy chunks for transmission N as indicated.

better for small N as expected. This is also confirmed by Figure 2.16(b) where we observe $\bar{V}_p$ decreasing with N. Note that the curves are not entirely smooth. Close inspection shows that the M values of $\bar{V}_p$, which cause the irregularity are those values for which the battery capacity C can be expressed as the sum of an integer multiple of M and an integer multiple of $M+N$. For these values, a full battery provides just enough energy for a number of sensing operations and transmissions. A further increase of N then implies that a full battery no longer provides enough energy for these operations.

2.5 Summary

In this chapter, we investigated the value of information in hybrid wireless sensor networks that harvest energy from their environment. We first proposed a basic analytical model and provided the stability analysis of the value of information process, only assuming that the value of the sensed information is a stationary ergodic process. We also calculated the first two moments theoretically under these assumptions, before numerically illustrating the impact of different parameters on VoI.

We then investigated various extensions of the basic model. A first extension comprised the inclusion of energy expenditure for the sensing operation. We studied this extension in two settings. Initially, we assumed that the sensor nodes were unable to assess neither the presence nor the value of the information. A refined model then assumed that sensor nodes were able to assess the presence of information but not the value of information. For both models, numerical examples revealed the complex interplay between battery dynamics and the value of information. For the refined model, we however needed to impose an additional assumption on the sensing process: while we still allow for stationary sensing, we do assume that the indicator that there is no information constitutes a sequence of independent random variables.

Since energy harvesting is expected to be bursty, we then extended our model to allow for burstiness in the harvesting process. More precisely, we introduced a Markovian environment process which modulates the energy harvesting process. As the basic model and its refinements already accounted for temporal correlation in the sensing process, we could now model correlation in both the harvesting and sensing processes. As expected, we observed that battery dynamics have an even more profound impact on the value of information.

3

A stochastic recursion model

Every day we make many decisions that have immediate and long-term consequences. So to make the optimal decision, one not only needs to account for their present impact, but also for their impact on future outcomes. In this chapter, we describe a sequential decision-making model for an energy-harvesting sensor node. At specified points in time, the sensor node observes its battery and value of information state and chooses an action accounting for its environment. The environment can include a single or a combination of many surrounding objects such as the node's location coordinate, the available energy in the battery and the value of information. The action choice produces two results: the node receives an immediate reward (or incurs an immediate cost), and the system evolves to a new state at a subsequent point in time according to a probability distribution that depends on the action taken. At this subsequent point in time, the node faces a similar problem, but the state of the system is (possibly) different. The actions that a sensor node can take, can be simple decision rules like sleep-wake strategies for transmission to conserve energy or complex commands like a change of transmission power to achieve error-free communications, or to optimise the amount of information that can be sent. Such complex system dynamics can be modelled using Markov decision processes (MDPs) in order to achieve the desired objective. The goal of a node is then to choose the sequence of actions that leads to the optimal performance with respect to a predefined performance criterion. A Markov decision process adds actions to the Markovian description of the model, while retaining the Markov property: the state of the system is such that the future evolution depends only on the present and not on the past [29].

We particularly aim at designing an optimal transmission policy (which is essentially a set of decision rules describing the action to be taken in each state of the system) of a sensor node in an EH-WSN. We allow for the temporal non-availability of the sink by introducing so-called transmission opportunities, which is a natural assumption when the sink in question is wirelessly connected or even mobile. From time to time, the sensor nodes gather information to which we assign

a value. This value degrades over time as the information is waiting for transmission in the memory of the sensor node. At each transmission opportunity, the sensor node decides whether to transmit data or not, depending on the amount of available energy and the value of information (VoI), both of which are assumed to be discrete values. We investigate the structure of the optimal policy and the resulting optimal mean value of information transmitted from the sensor node. If the sensor node decides to transmit, it deletes the information from its memory and hence the value of information present in the node resets to zero. From a queueing-theoretical point of view, such behaviour is also found in queues with disasters, which have been used amongst others for modelling satellite communication and internet applications [69]. We adopt the policy iteration algorithm to solve such a large network to obtain the optimal transmission policy.

In many applications, updating the information is very crucial. For example, temperature and humidity updates from a forest can be very useful to predict the forest fire which can further help to take necessary measures to control it in reasonable time. In such cases, the source generates the information with a time-stamp that is passed through a network to the sink. These time stamps can be used to measure the freshness of the information. This is a very popular concept in the wireless sensor networking context and sometimes referred to as *age of information*. We incorporate this structure by introducing the non-additive nature of VoI i.e., newly sensed information replaces the current information if it has a higher value. Thus, the node keeps the most updated information and transmits it whenever there is an opportunity. With numerical experiments, we analyse the impact of this structure on the optimal transmission policy. We observe that the optimal policy is of the threshold type and this threshold is sensitive to different system parameters. f

The remainder of the chapter is organised as follows. In the next section, we discuss related literature on Markov decision processes for energy harvesting sensor nodes. We then introduce the Markov decision process for age- and energy-dependent transmissions in sensor networks in Section 3.2 and discuss some structural properties of the value function in Section 3.3. Finally, we evaluate the optimal decision policies in Section 3.4, prior to providing a summary of the main results in Section 3.5.

3.1 Background

Optimal scheduling in energy harvesting sensor networks is an active research topic. We refer to Yick et al. [70] and Lu et al. [71] and the references therein for a discussion of key issues and developments in WSNs, addressing the different challenges including storage capacity, energy replenishment, network services, deployment, etc. We restrict the discussion below to Markovian models.

Markovian models have been studied by various authors, one of the first contributions being [62] where Susu et al. propose a finite birth-death Markov chain to model energy harvesting sensor nodes, a birth and death corresponding to en-

ergy harvesting and energy consumption respectively. The same energy harvesting process is considered by Jornet and Akyildiz [72], but the authors allow for more rapid energy consumption, a transmission corresponding to a deterministic jump downwards. Seyedi and Sikdar [45] propose a Markov model to study the trade-off between energy consumption and packet error probability. Dong et al. [73] consider the Bernoulli energy harvesting process to obtain the near-optimal energy control policy in energy harvesting communication network where Ventura et al. [74] propose a Markov model that harvests energy from the same source, or a combination of different sources. Most contributions study a single sensor node in isolation, notable exceptions being [75, 60]. Authors study various properties of the data retrieval time in EH-WSNs, while minimising the energy consumption for the sensors. Studying the complete network allows for assessing the probability of a node failing to detect an event owing to a lack of energy, which is a key design consideration for body sensor networks.

Some research focuses on energy conservation by controlling the communication system. For example, Raghunathan et al. [76] study the energy consumption in WSNs and find that the energy cost required for sensing the information or for computation is negligible compared to the transmission cost. Hence, data compression can be used to minimise energy consumption and extend the overall lifetime of the network [77, 11]. As there is also significant energy consumption when the sensor node is idle, switching off the sensor node can save the battery and thus extend the lifetime. In such strategies, the WSN node periodically wakes up to transmit data and then sleeps by powering off to conserve the energy. WSN technology must efficiently manage the frequency of on- and off-times of the node. Such a control strategy is studied by Sharma et al. [78] for an energy harvesting sensor node that periodically transmits data. The authors discuss the existence of an optimal transmission policy but do not calculate it. Morsi et al. [79] calculate an on-off transmission policy either assuming a finite or infinite energy buffer. The same control problem is considered in [80, 81] in a deterministic setting: data arrivals and the amount of harvested energy are known in advance. Policies obtained from such model can be a benchmark but given the random nature of energy harvesting, the results cannot be attained in a random setting. Ozel et al. [82] consider optimal scheduling for transmissions over a time varying channel. In an offline setting, the authors show the optimality of an adaptive directional water-filling algorithm for throughput maximisation whereas they rely on stochastic dynamic programming to solve for the optimal online policy.

We briefly discuss literature on MDPs in WSNs. Various authors introduce MDPs for studying optimal transmission policies in wireless sensor networks, see the recent survey [56] and the references. Fernandez et al. [83] use the term "importance of message" for the value of the message and propose a stochastic approximation algorithm to find out the optimal transmission policy. The optimal policy is a threshold policy under reasonable assumptions on battery dynamics. Lei et al. [44] discuss energy-aware threshold transmission policies by modelling the energy state transitions by a continuous time Markov chain. Three different scenarios are considered where batteries are recharged and/or replaced. Transmis-

sion policies depend on the state of the channel as well as on the value of the message. Michelusi et al. [46] models energy harvesting as a Markov process with two states, i.e., a good and a bad state. The authors adapt the transmission probabilities to the state of the battery, deriving the optimal policy using policy iteration. The optimal policy accounts for the data at the sensor node and the amount of energy at the time of decision making. Some authors further focus on control policies when the energy harvesting distribution is unknown and the system can learn from past observations. [84, 85] discuss the optimal power control policies for EH-WSN by formulating the problem as a partially observable Markov decision process (POMDP). The authors consider an ARQ-based packet transmission protocol, their goal being to find the optimal transmit power for each packet transmission.

Various applications involve WSNs with mobile sinks such as agricultural areas [86], continuous object tracking [87] etc. Mobile sinks are generally used to reduce the energy consumption [39] or overcome the hot spot effect [36]. Some studies show that the mobile sink can significantly improve the network lifetime [88, 89]. In such WSNs, sensor nodes gather the information from the environment and transmit their positional information gradually to the sink. The sink can use this information to adjust its position in the network for shortest path [90] or maximising the network throughput [91, 92, 93]. Angelopoulos et al. [94] considers a WSN with a mobile sink and moving nodes where the significance of the local information is measured with the help of ranking function which degrades over time. Thus, information at the node is replaced by new updated information. Data replacement is also used to train the networks with a specific application that detects abnormal activities like intruders in a restricted environment. Li et al. [95] compares different techniques to replace the missing data in WSNs.

3.2 Mathematical Model

We focus on a single sensor node with energy harvesting capability in a sensor network where data is collected by a mobile sink as depicted in Figure 3.1. The sensor has an on-board battery for storing harvested energy as well as the capability for storing sensed information. We assume that time is discrete. That is, time is divided into fixed length intervals (slots) and transmissions from the sensor node are synchronised with respect to slot boundaries. Note that the current model differs from the models in the previous chapter in terms of the mathematical framework under consideration, as well as in terms of its applications. Unlike the models in the previous chapter, we now use the controlled framework to model the WSN and also assume that the VoI is non-additive in nature.

The dynamics of the sensor node are governed by three independent stochastic processes. The first process describes how energy is harvested. Assuming that energy can be discretised into chunks of energy, let H_n denote the number of *energy chunks* or energy units harvested during the kth slot. The sequence $\{H_k, k \in \mathbb{N}\}$ constitutes a sequence of independent Bernoulli random variables.

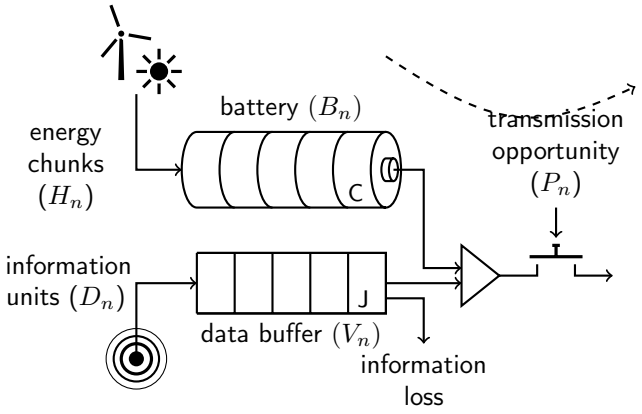

Figure 3.1: WSN Model

Let p_e denote the probability that a chunk of energy arrives during a slot. The second process describes the value (importance) of the information that is sensed during a slot. Let D_n denote the value of information sensed during the kth slot. We express the value of information as a discrete number of units. The process $\{D_n, n \in \mathbb{N}\}$ is a sequence of independent and identically distributed non-negative discrete random variables. The sensed information can have a value of at most J units, $\mathsf{P}[D_n > J] = 0$, and we denote the common probability mass function of the D_n's by $d_j = \mathsf{P}[D_n = j]$, $j = 0, \ldots, J$. For further use, we also introduce the corresponding distribution function $\bar{d}_j = \mathsf{P}[D_n \leq j] = \sum_{j' \leq j} d_{j'}$. The third process describes when the sensor node can pass on its information to the mobile sink. Let T_n be the indicator that there is a transmission opportunity at the kth slot boundary. The sequence $\{T_n, n \in \mathbb{N}\}$ constitutes a sequence of independent Bernoulli random variables, p_t denoting the probability that there is a transmission opportunity at a slot boundary.

We can now describe the sensor node dynamics in terms of these random variables. Let B_n be the battery level (in terms of energy chunks) at the nth slot boundary. We assume that a single chunk of energy is required to transmit information to the mobile sink and that the on-board battery can store C chunks of energy at most. Energy chunks are lost when the battery capacity is exceeded. In view of these assumptions, we find that the battery level at the $(n+1)$st slot boundary can be expressed as,

$$B_{n+1} = \min(B_n + H_n - U_n, C)\,.$$

Here U_n is the indicator that there is a transmission at the kth slot boundary. This random variable depends on the availability of the mobile sink T_n, on the battery level B_n as well as on the value of the information V_k as discussed below. In particular, transmissions are not possible when there is no energy, which means that $B_n = 0$ implies $U_n = 0$.

The evolution of the value of information V_n is the combination of an infor-

mation loss process and an information replacement process. To capture the loss of information over time, we assume that the value of information decreases by one information unit per slot. In addition, we assume that the information at the sensor node is replaced by newly sensed information whenever the value of newly sensed information units exceeds the value of information at the sensor node. Finally, whenever the information is passed on to the mobile sink, the information is deleted at the sensor node. In view of these assumptions, we can express the value of information at the $(n+1)$st slot boundary as follows,

$$V_{n+1} = \begin{cases} D_{n+1} & \text{for } U_n = 1\,, \\ \max(D_{n+1}, (V_n - 1)) & \text{for } U_n = 0\,. \end{cases} \tag{3.1}$$

Here U_n is again the indicator that there is a transmission at the nth slot boundary.

When there is no transmission opportunity, $T_n = 0$, there obviously is no transmission, hence $U_n = 0$. When there is a transmission opportunity, $T_n = 1$, the decision on transmitting depends on the current value of information, as well as on the battery level. Thus we can write U_n mathematically as,

$$U_n = \begin{cases} 0 & \text{for } B_n = 0 \text{ or } T_n = 0\,, \\ \pi(B_n, V_n, T_n) & \text{otherwise.} \end{cases}$$

Where π is the transmission policy that indicates the decision taken by the node at time slot n. As there is only energy consumption when there is a transmission, it can be beneficial to postpone transmissions when there is limited value of information at the sensor node. Therefore, we study the optimal transmission policy by modelling the sensor node as a Markov decision process (MDP).

3.2.1 Markov decision process framework

In order to define the MDP, we must specify its state space, action set, transition probabilities and rewards. We explain each of the components in detail below.

(a) **State Space:** In view of the modelling assumptions above, the state of the sensor node at the nth slot boundary is described by the battery level B_n and the value of information V_n. These discrete random variables are positive and bounded by C (battery capacity) and J (maximum of the sensed value of information), respectively. In addition, as the decision to transmit or defer transmission depends on the availability of a transmission opportunity, we additionally track T_n as well.

Summarising, the state is described by the vector $(B_n, V_n, T_n) \in \mathscr{S} \triangleq \mathscr{B} \times \mathscr{V} \times \mathscr{T}$, where,

- $\mathscr{B} = \{0, 1, 2, \cdots, C\}$ is the set of battery states,
- $\mathscr{V} = \{0, 1, 2, \cdots, J\}$ is the set of the value of information states.
- $\mathscr{T} = \{0, 1\}$ is the set of the transmission opportunity states.

(b) **Action Set:** There are at most two possible actions: transmitting (action 1) or not transmitting (action 0). The sensor node cannot transmit in the absence of energy ($B_n = 0$) or in the absence of a transmission opportunity ($T_n = 0$), hence for $s \in \mathscr{S}_0 = \mathscr{B} \times \mathscr{V} \times \{0\} \cup \{0\} \times \mathscr{V} \times \mathscr{T}$, the only possible action is not to transmit: the action set is a singleton $\mathscr{A}_s = \{0\}$ for $s \in \mathscr{S}_0$. For $s \in \mathscr{S}_1 = \mathscr{S} \setminus \mathscr{S}_0$, there is a transmission opportunity as well as energy such that the action set includes both possible actions: $\mathscr{A}_s = \{0,1\}$ for $s \in \mathscr{S}_1$.

For further use, let $\pi : \mathscr{S} \to \{0,1\}$ denote a policy of the sensor node, that is a mapping from the state space to the action space $\{0,1\}$. A policy π is admissible if $\pi(s) \in \mathscr{A}_s$ for all $s \in \mathscr{S}$.

(c) **Transition Probabilities:** Let $q(s'|s) = q((i',j',k')|(i,j,k))$ represent the transition probability that state $s' = (i',j',k')$ is visited from state $s = (i,j,k)$ for $s \in \mathscr{S}_0$. We here suppress the action from the notation as for $s \in \mathscr{S}_0$ only action 0 is available. Note first that the transition probabilities of the transmission opportunity process are given by

$$p^o(k') = \begin{cases} 1 - p_t & \text{for } k' = 0\,, \\ p_t & \text{for } k' = 1\,, \end{cases}$$

which can also be written as $p^o(k') = p_t^{k'}(1-p_t)^{1-k'}$. Recalling that the entries of the state vector correspond to the battery level, the value of information and the indicator of the transmission opportunity respectively, we find,

$$q((i',j',k')|(i,j,k)) = \begin{cases} d_{j'} p_e p^o(k') & \text{for } i' = i+1 \text{ and } j' \geq j\,, \\ \bar{d}_{j-1} p_e p^o(k') & \text{for } i' = i+1 \text{ and } j' = j-1\,, \\ d_{j'} \bar{p}_e p^o(k') & \text{for } i' = i < C \text{ and } j' \geq j\,, \\ \bar{d}_{j-1} \bar{p}_e p^o(k') & \text{for } i' = i < C \text{ and } j' = j-1 \\ d_{j'} p^o(k') & \text{for } i' = i = C \text{ and } j' \geq j\,, \\ \bar{d}_{j-1} p^o(k') & \text{for } i' = i = C \text{ and } j' = j-1\,, \\ 0 & \text{otherwise,} \end{cases} \tag{3.2}$$

for $s \in \mathscr{S}_0$ and $s' \in \mathscr{S}$.

For $s \in \mathscr{S}_1$, let $p(s'|s,a) = p((i',j',k')|(i,j,k),a)$ represent the transition probability that state $s' = (i',j',k')$ is visited from state $s = (i,j,k)$ when action $a \in \{0,1\}$ is chosen. For $a = 0$, the evolution of the state is similar to

the evolution when there is no transmission opportunity. Hence, we have,

$$p((i',j',k')|(i,j,k),0) = \begin{cases} d_{j'} p_e p^o(k') & \text{for } i' = i+1 \text{ and } j' \geq j\,, \\ \bar{d}_{j-1} p_e p^o(k') & \text{for } i' = i+1 \text{ and } j' = j-1\,, \\ d_{j'} \bar{p}_e p^o(k') & \text{for } i' = i < C \text{ and } j' \geq j\,, \\ \bar{d}_{j-1} \bar{p}_e p^o(k') & \text{for } i' = i < C \text{ and } j' = j-1 \\ d_{j'} p^o(k') & \text{for } i' = i = C \text{ and } j' \geq j\,, \\ \bar{d}_{j-1} p^o(k') & \text{for } i' = i = C \text{ and } j' = j-1\,, \\ 0 & \text{otherwise,} \end{cases} \tag{3.3}$$

for $s \in \mathscr{S}_1$ and $s' \in \mathscr{S}$. Finally, for $a = 1$, we find,

$$p((i',j',k')|(i,j,k),1) = \begin{cases} d_{j'} p_e p^o(k') & \text{for } i' = i\,, \\ d_{j'} \bar{p}_e p^o(k') & \text{for } i' = i-1\,, \\ 0 & \text{otherwise,} \end{cases} \tag{3.4}$$

for $s \in \mathscr{S}_1$ and $s' \in \mathscr{S}$.

(d) **Reward:** We define the immediate reward in state $s \in S$ as the value of information that is transmitted to the mobile sink. That is, the reward in state $s \in \mathscr{S}_0$ is zero. For $s = (i,j,k) \in \mathscr{S}_1$ the reward equals j if $a = 1$ while there is no reward for $a = 0$. Let $R_\pi(s)$ be the immediate reward in state $s = (i,j,k)$ for policy π, we then have,

$$R_\pi(i,j,k) = \begin{cases} 0 & \text{for } \pi((i,j,k)) = 0 \\ j & \text{for } \pi((i,j,k)) = 1\,. \end{cases}$$

The immediate reward only depends on the state and the action.

3.2.2 Policy evaluation

We focus on the infinite horizon control problem, assuming that a stationary policy is applied. Let $v_\pi(s)$ be the uniformly discounted value-to-go from state s under policy π,

$$v_\pi(s) = v_\pi(i,j,k) = \mathrm{E}\left[\sum_{n=0}^{\infty} \alpha^n R_\pi(B_n, V_n, T_n) \middle| B_0 = i, V_0 = j, T_0 = k \right],$$

where α is a discounting factor. Further, let $v^*(s)$ be the optimal value-to-go from state s,

$$v^*(s) = \max_\pi v_\pi(s)\,,$$

where the maximum is taken over all admissible policies π. The optimal value-to-go and optimal policy can be found by solving the Bellman equations, which read,

$$v^*(s) = \sum_{s' \in \mathscr{S}} \alpha q(s'|s) v^*(s')$$

for $s \in \mathscr{S}_0$, and,

$$v^*(s) = \max\left(j + \alpha \sum_{s' \in \mathscr{S}} p(s'|s,1) v^*(s'), \sum_{s' \in \mathscr{S}} p(s'|s,a=0) \alpha v^*(s') \right)$$

for $s = (i,j,k) \in \mathscr{S}_1$.

To solve the Bellman equations, we rely on policy iteration [96]. To this end, starting from an initial policy π_0, we iteratively improve the policy. In each iteration $n = 0, 1, \ldots$ we first solve the system of equations,

$$v_{\pi_n}(s) = \begin{cases} \sum_{s' \in \mathscr{S}} q(s'|s) \alpha v_{\pi_n}(s') & \text{for } s \in \mathscr{S}_0\,, \\ j\pi_n(s) + \alpha \sum_{s' \in \mathscr{S}} p(s'|s, \pi_n(s)) v_{\pi_n}(s') & \text{for } s \in \mathscr{S}_1\,. \end{cases} \tag{3.5}$$

We can then adjust the policy in the policy improvement step,

$$\pi_{n+1}(s) = \arg\max_\pi \left(j\pi(s) + \alpha \sum_{s' \in \mathscr{S}} p(s'|s, \pi(s)) v_{\pi_n}(s') \right).$$

In view of the above, we have $\pi_{n+1}(s) = 0$ for $s \in \mathscr{S}_0$ and

$$\pi_{n+1}(s) = 1\left\{ j + \alpha \sum_{s' \in \mathscr{S}} p(s'|s,1) v_{\pi_n}(s') > \alpha \sum_{s' \in \mathscr{S}} p(s'|s,0) v_{\pi_n}(s') \right\} \tag{3.6}$$

for $s \in \mathscr{S}_1$, where $1\{\cdot\}$ is the indicator function.

3.2.3 Quasi birth death structure

The major computational effort in solving the MDP problem is the evaluation of (3.5). Note however that – regardless of the policy – the transitions of the battery level are skip-free in both directions: the battery level either remains the same or can only go up or down one level during a slot. This in turn means that the matrix corresponding to the system of equations (3.5) has a tridiagonal block structure or quasi-birth-death (QBD) structure, blocks grouping transitions from battery level i to battery level i'. As the battery level is skip free, the blocks are non-zero only for $i' \in \{i-1, i, i+1\}$ (hence the matrix is block-tridiagonal).

The block structure allows for efficiently solving the system of equations by linear level reduction [97]. To this end, let $\mathbf{v}_\pi(i,k)$ be the column vector with elements $v_\pi(i,j,k)$ for $j = 0, \ldots, J-1$. From equation (3.5), we then find that these vectors adhere,

$$\begin{aligned} \mathbf{v}_\pi(i,0) = {} & \alpha \bar{p}_t \bar{p}_e A \mathbf{v}_\pi(i,0) + \alpha p_t \bar{p}_e A \mathbf{v}_\pi(i,1) \\ & + \alpha \bar{p}_t p_e A \mathbf{v}_\pi(i+1,0) + \alpha p_t p_e A \mathbf{v}_\pi(i+1,1)\,, \end{aligned} \tag{3.7}$$

for $k = 0$ and for $i = 0, \ldots, C-1$, while for $k = 0$ and $i = C$ we have,

$$\mathbf{v}_\pi(C,0) = \alpha \bar{p}_t A \mathbf{v}_\pi(C,0) + \alpha p_t A \mathbf{v}_\pi(C,1)\,. \tag{3.8}$$

Similarly, for $k = 1$, we find,

$$\begin{aligned}\mathbf{v}_\pi(0,1) &= \alpha\bar{p}_t\bar{p}_e A\mathbf{v}_\pi(0,0) + \alpha p_t\bar{p}_e A\mathbf{v}_\pi(0,1)\\ &\quad + \alpha\bar{p}_t p_e A\mathbf{v}_\pi(1,0) + \alpha p_t p_e A\mathbf{v}_\pi(1,1)\,, \end{aligned} \tag{3.9}$$

$$\begin{aligned}\mathbf{v}_\pi(i,1) &= \Pi(i)\theta + \alpha\Pi(i)\bar{p}_t\bar{p}_e B\mathbf{v}_\pi(i-1,0) + \alpha\Pi(i)p_t\bar{p}_e B\mathbf{v}_\pi(i-1,1)\\ &\quad + \alpha\Pi(i)\bar{p}_t p_e B\mathbf{v}_\pi(i,0) + \alpha\Pi(i)p_t p_e B\mathbf{v}_\pi(i,1) + \alpha\bar{\Pi}(i)\bar{p}_e\bar{p}_t A\mathbf{v}_\pi(i,0)\\ &\quad + \alpha\bar{\Pi}(i)\bar{p}_e p_t A\mathbf{v}_\pi(i,1) + \alpha\bar{\Pi}(i)p_e\bar{p}_t A\mathbf{v}_\pi(i+1,0)\\ &\quad + \alpha\bar{\Pi}(i)p_e p_t A\mathbf{v}_\pi(i+1,1)\,, \end{aligned} \tag{3.10}$$

$$\begin{aligned}\mathbf{v}_\pi(i,1) &= \Pi(i)\theta + \alpha\Pi(i)\bar{p}_t\bar{p}_e B\mathbf{v}_\pi(i-1,0) + \alpha\Pi(i)p_t\bar{p}_e B\mathbf{v}_\pi(i-1,1)\\ &\quad + \alpha\Pi(i)\bar{p}_t p_e B\mathbf{v}_\pi(i,0) + \alpha\Pi(i)p_t p_e B\mathbf{v}_\pi(i,1) + \alpha\bar{\Pi}(i)\bar{p}_e\bar{p}_t A\mathbf{v}_\pi(i,0)\\ &\quad + \alpha\bar{\Pi}(i)\bar{p}_e p_t A\mathbf{v}_\pi(i,1) + \alpha\bar{\Pi}(i)p_e\bar{p}_t A\mathbf{v}_\pi(i+1,0)\\ &\quad + \alpha\bar{\Pi}(i)p_e p_t A\mathbf{v}_\pi(i+1,1) \end{aligned} \tag{3.11}$$

for $i = 1,\ldots,C-1$ and finally for $i = C$, we obtain,

$$\begin{aligned}\mathbf{v}_\pi(C,1) &= \Pi(i)\theta + \alpha\Pi(i)\bar{p}_t\bar{p}_e B\mathbf{v}_\pi(C-1,0) + \alpha\Pi(i)p_t\bar{p}_e B\mathbf{v}_\pi(C-1,1)\\ &\quad + \alpha\Pi(i)\bar{p}_t p_e B\mathbf{v}_\pi(C,0) + \alpha\Pi(i)p_t p_e B\mathbf{v}_\pi(C,1)\\ &\quad + \alpha\bar{\Pi}(i)\bar{p}_t A\mathbf{v}_\pi(C,0) + \alpha\bar{\Pi}(i)p_t A\mathbf{v}_\pi(C,1)\,, \end{aligned} \tag{3.12}$$

where $\theta = [0,1,2,\ldots,J]'$ is a column vector with $J+1$ entries, with $\Pi(i)$ the $(J+1)\times(J+1)$ diagonal matrix with diagonal entries $\pi(i,j,1)$ $(j = 0,\ldots,J-1)$, with $\bar{\Pi}(i)$ the $(J+1)\times(J+1)$ diagonal matrix with diagonal entries $1-\pi(i,j,1)$ $(j = 0,\ldots,J-1)$, and where the $(J+1)\times(J+1)$ matrices A and B are defined as follows,

$$\boldsymbol{\mathcal{A}} = \begin{bmatrix} d_0 & d_1 & d_2 & d_3 & \cdots & d_J \\ \bar{d}_0 & d_1 & d_2 & d_3 & \cdots & d_J \\ 0 & \bar{d}_1 & d_2 & d_3 & \cdots & d_J \\ 0 & 0 & \bar{d}_2 & d_3 & \cdots & d_J \\ \vdots & \vdots & \vdots & \vdots & \ddots & \vdots \\ 0 & 0 & 0 & 0 & \cdots & d_J \end{bmatrix}, \quad \boldsymbol{\mathcal{B}} = \begin{bmatrix} d_0 & d_1 & d_2 & d_3 & \cdots & d_J \\ d_0 & d_1 & d_2 & d_3 & \cdots & d_J \\ d_0 & d_1 & d_2 & d_3 & \cdots & d_J \\ \vdots & \vdots & \vdots & \vdots & \ddots & \vdots \\ d_0 & d_1 & d_2 & d_3 & \cdots & d_J \end{bmatrix}.$$

We further introduce the column vectors $\mathbf{v}_\pi(i) = [\mathbf{v}_\pi(i,0)', \mathbf{v}_\pi(i,1)']'$. From equations (3.7) and (3.9), we find,

$$\mathbf{v}_\pi(0) = \alpha\bar{p}_e \begin{bmatrix} \bar{p}_t\boldsymbol{\mathcal{A}} & p_t\boldsymbol{\mathcal{A}} \\ \bar{p}_t\boldsymbol{\mathcal{A}} & p_t\boldsymbol{\mathcal{A}} \end{bmatrix} \mathbf{v}_\pi(0) + \alpha p_e \begin{bmatrix} \bar{p}_t\boldsymbol{\mathcal{A}} & p_t\boldsymbol{\mathcal{A}} \\ \bar{p}_t\boldsymbol{\mathcal{A}} & p_t\boldsymbol{\mathcal{A}} \end{bmatrix} \mathbf{v}_\pi(1)\,. \tag{3.13}$$

Analogously, equations (3.7) and (3.10) yield,

$$\begin{aligned}\mathbf{v}_\pi(i) &= \begin{bmatrix} 0 \\ \Pi(i)\theta \end{bmatrix} + \alpha\bar{p}_e \begin{bmatrix} 0 & 0 \\ \bar{p}_t\Pi(i)\boldsymbol{\mathcal{B}} & p_t\Pi(i)\boldsymbol{\mathcal{B}} \end{bmatrix} \mathbf{v}_\pi(i-1) - \alpha\bar{p}_e\\ &\quad \begin{bmatrix} 0 & 0 \\ \Pi(i)\bar{p}_t\boldsymbol{\mathcal{A}} & \Pi(i)p_t\boldsymbol{\mathcal{A}} \end{bmatrix} \mathbf{v}_\pi(i) + \alpha p_e \begin{bmatrix} 0 & 0 \\ \Pi(i)\bar{p}_t\boldsymbol{\mathcal{B}} & \Pi(i)p_t\boldsymbol{\mathcal{B}} \end{bmatrix} \mathbf{v}_\pi(i) \end{aligned}$$

$$+\alpha\bar{p}_e\begin{bmatrix}\bar{p}_t\mathcal{A} & p_t\mathcal{A}\\ \bar{p}_t\mathcal{A} & p_t\mathcal{A}\end{bmatrix}\mathbf{v}_\pi(i)+\alpha p_e\begin{bmatrix}\bar{p}_t A & p_t\mathcal{A}\\ \bar{\Pi}(i)\bar{p}_t\mathcal{A} & \bar{\Pi}(i)p_t\mathcal{A}\end{bmatrix}\mathbf{v}_\pi(i+1)\,, \quad (3.14)$$

whereas equations (3.8) and (3.12) lead to,

$$\begin{aligned}\mathbf{v}_\pi(C) = &\begin{bmatrix}0\\ \Pi(C)\theta\end{bmatrix}+\alpha\bar{p}_e\begin{bmatrix}0 & 0\\ \bar{p}_t\Pi(C)\mathcal{B} & p_t\Pi(C)\mathcal{B}\end{bmatrix}\mathbf{v}_\pi(C-1)\\ &+\alpha p_e\begin{bmatrix}0 & 0\\ \Pi(C)\bar{p}_t\mathcal{B} & \Pi(C)p_t\mathcal{B}\end{bmatrix}\mathbf{v}_\pi(C)+\alpha\begin{bmatrix}\bar{p}_t\mathcal{A} & p_t\mathcal{A}\\ \bar{\Pi}(C)\bar{p}_t\mathcal{A} & \bar{\Pi}(i)p_t\mathcal{A}\end{bmatrix}\mathbf{v}_\pi(C)\,.\end{aligned} \quad (3.15)$$

The former set of matrices confirm the QBD structure of the system of equations, as $\mathbf{v}_\pi(i)$ is expressed in terms of $\mathbf{v}_\pi(i-1)$, $\mathbf{v}_\pi(i)$ and $\mathbf{v}_\pi(i+1)$ for all i.

3.2.4 Linear level reduction

As mentioned above, the structural property of the system of equations allows for solving the system of equations efficiently by linear level reduction [97]. Let the $2(J+1)\times 2(J+1)$ matrices F_0 and G_0, and the $2(M+1)$ column vector h_0 be defined as,

$$\begin{aligned}\mathcal{F}_0 &= \left(\mathcal{I}-\alpha\bar{p}_e\begin{bmatrix}\bar{p}_t\mathcal{A} & p_t\mathcal{A}\\ \bar{p}_t\mathcal{A} & p_t\mathcal{A}\end{bmatrix}\right)^{-1},\\ \mathcal{G}_0 &= \mathcal{F}_0\alpha p_e\begin{bmatrix}\bar{p}_t\mathcal{A} & p_t\mathcal{A}\\ \bar{p}_t\mathcal{A} & p_t\mathcal{A}\end{bmatrix},\\ \mathbf{h}_0 &= [0,0,\ldots,0]'\,.\end{aligned} \quad (3.16)$$

Here $\mathcal{I}$ is the $2(J+1)\times 2(J+1)$ identity matrix. Hence, we have $\mathbf{v}_\pi(0) = G_0\mathbf{v}_\pi(1)+h_0$. For $0<i<C$, we again have $\mathbf{v}_\pi(i)=\mathcal{G}_i\mathbf{v}_\pi(i+1)+h_i$ where

$$\begin{aligned}\mathcal{G}_i &= \alpha p_e\mathcal{F}_i\begin{bmatrix}\bar{p}_t\mathcal{A} & p_t\mathcal{A}\\ \bar{\Pi}(i)\bar{p}_t\mathcal{A} & \bar{\Pi}(i)p_t\mathcal{A}\end{bmatrix} \quad \text{and,}\\ \mathbf{h}_i &= \mathcal{F}_i\left(\begin{bmatrix}0\\ \Pi(i)\theta\end{bmatrix}+\alpha\bar{p}_e\begin{bmatrix}0 & 0\\ \bar{p}_t\Pi(i)B & p_t\Pi(i)B\end{bmatrix}\mathbf{h}_{i-1}\right)\end{aligned} \quad (3.17)$$

with,

$$\begin{aligned}\mathcal{F}_i = \Bigg(&\mathcal{I}-\alpha p_e\begin{bmatrix}0 & 0\\ \Pi(i)\bar{p}_t\mathcal{B} & \Pi(i)p_t\mathcal{B}\end{bmatrix}-\alpha\bar{p}_e\begin{bmatrix}\bar{p}_t\mathcal{A} & p_t\mathcal{A}\\ \bar{p}_t\mathcal{A} & p_t\mathcal{A}\end{bmatrix}\\ &+\alpha\bar{p}_e\begin{bmatrix}0 & 0\\ \Pi(i)\bar{p}_t\mathcal{A} & \Pi(i)p_t\mathcal{A}\end{bmatrix}-\alpha\bar{p}_e\begin{bmatrix}0 & 0\\ \bar{p}_t\Pi(i)\mathcal{B} & p_t\Pi(i)\mathcal{B}\end{bmatrix}\mathcal{G}_{i-1}\Bigg)^{-1}.\end{aligned}$$

Finally, for battery level C, we have,

$$\mathbf{v}_\pi(C) = \Bigg(\boldsymbol{\mathcal{I}} - \alpha\bar{p}_e \begin{bmatrix} 0 & 0 \\ \bar{p}_t\Pi(C)\boldsymbol{\mathcal{B}} & p_t\Pi(C)\boldsymbol{\mathcal{B}} \end{bmatrix} \boldsymbol{\mathcal{G}}_{C-1} - \alpha p_e \begin{bmatrix} 0 & 0 \\ \Pi(C)\bar{p}_t\boldsymbol{\mathcal{B}} & \Pi(C)p_t\boldsymbol{\mathcal{B}} \end{bmatrix} - \alpha \begin{bmatrix} \bar{p}_t\boldsymbol{\mathcal{A}} & p_t\boldsymbol{\mathcal{A}} \\ \bar{\Pi}(C)\bar{p}_t\boldsymbol{\mathcal{A}} & \bar{\Pi}(i)p_t\boldsymbol{\mathcal{A}} \end{bmatrix}\Bigg)^{-1} \Bigg(\begin{bmatrix} 0 \\ \Pi(C)\theta \end{bmatrix} + \alpha\bar{p}_e \begin{bmatrix} 0 & 0 \\ \Pi(C)\bar{p}_t\boldsymbol{\mathcal{B}} & \Pi(C)p_t\boldsymbol{\mathcal{B}} \end{bmatrix} \mathbf{h}_{C-1}\Bigg). \quad (3.18)$$

We find $\mathbf{v}_\pi(C)$ by this last equation, and can then recursively calculate all $\mathbf{v}_\pi(i)$ as we have $\mathbf{v}_\pi(i) = \boldsymbol{\mathcal{G}}_i\mathbf{v}_\pi(i+1) + \mathbf{h}_i$ for $i < C$.

3.2.5 Summary and computational complexity

Summarising, we obtain the optimal policy π using the following algorithm.

1. Start with an initial policy π_0. As we have $\pi_0(s) = 0$ for $s \in \mathscr{S}_0$, we only need to choose an action for all $s \in \mathscr{S}_1$. Set $n = 0$.
2. Given $\pi = \pi_n$, we calculate $\mathbf{v}_\pi(i)$ for $i = 0,\ldots,C$ as follows:
   (a) Calculate $\boldsymbol{\mathcal{F}}_0$, $\boldsymbol{\mathcal{G}}_0$ and $\mathbf{h}_0$ in accordance with equation (3.16).
   (b) Calculate $\boldsymbol{\mathcal{F}}_i$, $\boldsymbol{\mathcal{G}}_i$ and $\mathbf{h}_i$ for $i = 1,\ldots,C-1$ in accordance with equation (3.17).
   (c) Calculate $\mathbf{v}_\pi(C)$ using equation (3.18).
   (d) Recursively calculate $\mathbf{v}_\pi(i)$ for $i = C-1,\ldots,0$ using $\mathbf{v}_\pi(i) = \boldsymbol{\mathcal{G}}_i\mathbf{v}_\pi(i+1) + h_i$.

   Finally, set $\mathbf{v}_{\pi_n}(i) = \mathbf{v}_\pi(i)$ for $i = 0,\ldots,C$.
3. We can now update the policy. For each $s \in \mathscr{S}_0$, set $\pi_{n+1}(s) = 0$. For each $s \in \mathscr{S}_1$ calculate $\pi_{n+1}(s)$ in accordance with equation (3.6).
4. If $\pi_{n+1} = \pi_n$, return π_n, if not, set $n \leftarrow n+1$ and return to 2.

As policy iteration ensures that the policy improves in every step, the number of iterations is bounded and the algorithm is guaranteed to converge in a finite number of iterations [29]. Each iteration requires the solution of the system of linear equations, which has complexity $O(CJ^3)$, see [97] for a general discussion on QBDs or [98] for a discussion on QBDs in the context of solving MDPs.

3.3 Properties of value function

In this section, we discuss some properties of the value function. These properties are proved theoretically by the standard approach of mathematical induction. At first, we assume that the problem is a finite horizon problem with n stages and we prove the property by induction. Then, by sending n to infinity to complete the proof. For ease of notation, we suppress the policy in the notation of $v(s)$.

Theorem 3.1. *v(s) is a non-decreasing function of the energy as well as of the value of information for $s \in \mathscr{S}_1$.*

Proof. We will use induction to prove this theorem. With a slight abuse of notation, let $v(s;n)$ be the optimal value function when the decision horizon consists of n stages. Then, we can write the value function as,

$$v(s;n{+}1) = \max\left(j + \alpha \sum_{s' \in \mathscr{S}} p(s'|s,a=1) v(s';n), \sum_{s' \in \mathscr{S}} p(s'|s,a=0) \alpha v(s';n) \right).$$

For $t = 0$, $v(i,j,k;1) = j$ for $i > 0$. Thus, the hypothesis is true for $t = 0$ as $v(i,j,k;1) - v(i-1,j,k;1) = 0$ for $i > 0$. Let's assume that hypothesis is true for t, then

$$\begin{aligned} v(i,j,k;n{+}1) = \\ \max\Bigg(& j + \alpha p^o(k') \Bigg(\sum_{j'=0}^{J} d'_j \Big(p_e\, v(i,j',k';n) + \bar{p}_e\, v(i{-}1,j',k';n) \Big) \Bigg), \\ & \alpha p^o(k') \Bigg(p_e \sum_{j'=j}^{J} d_{j'} v(i{+}1,j',k';n) + \bar{p}_e \sum_{j'=j}^{J} d_{j'} v(i,j',k';n) \\ & \qquad + p_e \bar{d}_{j-1} v(i{+}1,j{-}1,k';n) + \bar{p}_e \bar{d}_{j-1} v(i,j{-}1,k';n) \Bigg) \Bigg). \end{aligned}$$

Note that each argument in the max function is a weighted sum of non-decreasing functions. So, each argument is a non-decreasing function as well. Thus, $v(i,j,k;n)$ is a non-decreasing function in terms of the energy since the maximum of two non-decreasing function is a non-decreasing function. Taking the limit for t going to infinity, we obtain the desired monotonicity of the value function in terms of the energy.

Similarly, for $n = 0$, $v(i,0,k;1) = 0$ and $v(i,j,k;1) = j$ for $j > 0$. Thus, the hypothesis is true for $n = 0$ as $v(i,j,k;1) - v(i,j{-}1,k;1) = 1$ for $j > 0$. Note that $v(i,j,k;1) = 0$ for $j < 0$ by convention. If the hypothesis is true for n, then by the same set of arguments as above, we can show that $v(s)$ is a non-decreasing function of the value of information. □

Theorem 3.2. *For $s \in \mathscr{S}_1$, the value function is bounded in energy as well as in value of information. That is,*

$$v(i{+}1,j,k) - v(i,j,k) \leq 1 \text{ and } v(i,j{+}1,k) - v(i,j,k) \leq 1.$$

Proof. We again use induction to prove the statement. Recall that $v(s;n)$ is the optimal value function when the decision horizon has t stages,

$$v(s;n{+}1) = \max\left(j + \alpha \sum_{s' \in \mathscr{S}} p(s'|s,a=1) v(s';n), \sum_{s' \in \mathscr{S}} p(s'|s,a=0) \alpha v(s';n) \right).$$

Let us verify the hypothesis for $n=0$: $v(i,j{+}1,k;1)-v(i,j,k;1)=j{+}1-j=1\leq(j{+}1)$ and $v(i{+}1,j,k;1)-v(i,j,k;1)=j-j=0\leq 1$. Thus, the hypothesis is true for $n=0$. Now assume that the hypothesis is true for n. For further use, we define $v_a(s;n)$ as the value function when action a is chosen in state s and define $\mathscr{D}v_{aa'}$ to be the difference between $v_a(s;n)$ and $v_{a'}(s';n)$ for $a,a'\in\{0,1\}$. In the first part of the proof, we show that the value function is bounded in terms of energy and in the later part, we prove the boundedness in terms of the VoI. Four different sub-cases exists depending on the optimal action chosen when the battery level is $(i{+}1)$ and i. We now explore each sub-case and show that the difference is bounded by 1.

Case 1: In the first case, we assume that action 1 is chosen when the battery level is $(i{+}1)$ as well as when the battery level is i:

$$\begin{aligned}
\mathscr{D}v_{11} &= v_1(i{+}1,j,k;n{+}1)-v_1(i,j,k;n{+}1)\\
&=\sum_{s'\in\mathscr{S}}p(s'|(i{+}1,j,k),a=1)\alpha v(s';n)-\sum_{s'\in\mathscr{S}}p(s'|(i,j,k),a=1)\alpha v(s';n)\\
&=j+\alpha p^o(k')\Big(p_e\sum_{j'=0}^{J}d_{j'}v(i{+}1,j',k';n)+\bar{p}_e\sum_{j'=0}^{J}d_{j'}v(i,j',k';n)\Big)\\
&\quad -j+\alpha p^o(k')\Big(p_e\sum_{j'=0}^{J}d_{j'}v(i,j',k';n)+\bar{p}_e\sum_{j'=0}^{J}d_{j'}v(i{-}1,j',k';n)\Big)\\
&=\alpha p^o(k')\Bigg(p_e\sum_{j'=0}^{J}d_{j'}(v(i{+}1,j',k';n)-v(i,j',k';n))\\
&\quad +\bar{p}_e\sum_{j'=0}^{J}d_{j'}\Big(v(i,j',k';n)-v(i{-}1,j',k';n)\Big)\Bigg)\\
&\leq \alpha p^o(k')(p_e\,1+\bar{p}_e\,1)\leq 1\,.
\end{aligned}$$

Case 2: In the second case, action 0 is chosen when the battery level is $(i+1)$ as well as when the battery level is i:

$$\begin{aligned}
\mathscr{D}v_{00} &= v_0(i{+}1,j,k;n{+}1)-v_0(i,j,k;n{+}1)\\
&=\sum_{s'\in\mathscr{S}}p(s'|(i{+}1,j,k),a=0)\alpha v(s';n)-\sum_{s'\in\mathscr{S}}p(s'|(i,j,k),a=0)\alpha v(s';n)\\
&=\alpha p^o(k')\Big(p_e\sum_{j'=j}^{J}d_{j'}v(i{+}2,j',k';n)+\bar{p}_e\sum_{j'=j}^{J}d_{j'}v(i{+}1,j',k';n)\\
&\quad +p_e\bar{d}_{j-1}v(i{+}2,j{-}1,k';n)+\bar{p}_e\bar{d}_{j-1}v(i{+}1,j{-}1,k';n)\Big)\\
&\quad -\alpha p^o(k')\Big(p_e\sum_{j'=j}^{J}d_{j'}v(i{+}1,j',k';n)+\bar{p}_e\sum_{j'=j}^{J}d_{j'}v(i,j',k';n)\\
&\quad +p_e\bar{d}_{j-1}v(i{+}1,j{-}1,k';n)+\bar{p}_e\bar{d}_{j-1}v(i,j{-}1,k';n)\Big)
\end{aligned}$$

$$\leq \alpha p^o(k')\Big(p_e \sum_{j'=j}^{J} d_{j'}\,1 + \bar{p}_e \sum_{j'=j}^{J} d_{j'}\,1 + p_e \bar{d}_{j-1}\,1 + \bar{p}_e \bar{d}_{j-1}\,1\Big) \leq 1\,.$$

Case 3: In the third case, action 0 is chosen when the battery level is $(i{+}1)$ and action 1 is chosen when the battery level is i. We need the boundedness of the value function in terms of the VoI at n to show that the difference in the value function is bounded in this case:

$$\begin{aligned}
\mathscr{D}v_{01} &= v_0(i{+}1,j,k;n{+}1) - v_1(i,j,k;n{+}1) \\
&= \sum_{s'\in\mathscr{S}} p(s'|(i{+}1,j,k),a=0)\alpha v(s';n) - \sum_{s'\in\mathscr{S}} p(s'|(i,j,k),a=1)\alpha v(s';n) \\
&= -\alpha p^o(k')\Big(p_e \sum_{j'=j}^{J} d_{j'} v(i{+}1,j',k';n) + \bar{p}_e \sum_{j'=j}^{J} d_{j'} v(i,j',k';n) \\
&\quad + p_e \bar{d}_{j-1} v(i{+}1,j{-}1,k';n) + \bar{p}_e \bar{d}_{j-1} v(i,j{-}1,k';n)\Big) \\
&\quad - j - \alpha p^o(k')\Big(p_e \sum_{j'=0}^{J} d_{j'} v(i{+}1,j',k';n) + \bar{p}_e \sum_{j'=0}^{J} d_{j'} v(i,j',k';n)\Big) \\
&= -j + \alpha p^o(k')\Bigg(p_e \sum_{j'=0}^{j-1} d_{j'}\Big(v(i{+}1,j{-}1,k';n) - v(i{+}1,j',k';n)\Big) \\
&\quad + \bar{p}_e \sum_{j'=0}^{j-1} d_{j'}\Big(v(i,j{-}1,k';n) - v(i,j',k';n)\Big)\Bigg) \\
&\leq -j + \alpha p^o(k')\Big(p_e \sum_{j'=0}^{j-1} d_{j'}(j') + \bar{p}_e \sum_{j'=0}^{j-1} d_{j'}(j')\Big) \\
&\leq -j + \alpha p^o(k')(j{-}1) \leq 1\,.
\end{aligned}$$

Case 4: In the final case, action 1 is chosen when the battery level is $(i{+}1)$ and action 0 is chosen when the battery level is i:

$$\begin{aligned}
\mathscr{D}v_{10} &= v_1(i{+}1,j,k;n) - v_0(i,j,k;n) \\
&= v_1(i{+}1,j,k;n) - v_1(i,j,k;n) + v_1(i,j,k;n) - v_0(i,j,k;n) \\
&\leq v_1(i{+}1,j,k;n) - v_1(i,j,k;n) \leq 1\,.
\end{aligned}$$

Note that the first inequality is due to the fact that $v_1(i,j,k;n) < v_0(i,j,k;n)$ since action 0 is the optimal action in (i,j,k). For all the four sub-cases, we find that value function is bounded in terms of the energy available in the system at time stage n. By letting n go to infinity, we complete the first part of the proof. We now prove that the value function is also bounded in terms of the VoI in the system. There are again four different sub-cases here depending on the optimal action chosen when the VoI is j and $(j{+}1)$.

Case 1: In the first case, we assume that action 1 is chosen when the VoI is $(j+1)$ and j:

$$\begin{aligned}
\mathscr{D}v_{11} &= v_1(i,j{+}1,k;n{+}1) - v_1(i,j,k;n{+}1) \\
&= (j{+}1) + \sum_{s'\in\mathscr{S}} p(s'|(i,j{+}1,k),a=1)\alpha v(s';n) \\
&\quad - j - \sum_{s'\in\mathscr{S}} p(s'|(i,j,k),a=1)\alpha v(s';n) \\
&= 1 + \alpha p^o(k')\Big(p_e \sum_{j'=0}^{J} d_{j'} v(i,j',k';n) + \bar{p}_e \sum_{j'=0}^{J} d_{j'} v(i{-}1,j',k';) \\
&\quad - p_e \sum_{j'=0}^{J} d_{j'} v(i,j',k';n) + \bar{p}_e \sum_{j'=0}^{J} d_{j'} v(i{-}1,j',k';n)\Big) \\
&= 1
\end{aligned}$$

Case 2: In the second case, action 0 is chosen when the VoI is $(j+1)$ as well as when the VoI is j:

$$\begin{aligned}
\mathscr{D}v_{00} &= v_0(i,j{+}1,k;n{+}1) - v_0(i,j,k;n{+}1) \\
&= \sum_{s'\in\mathscr{S}} p(s'|(i,j{+}1,k),a=0)\alpha v(s',t) - \sum_{s'\in\mathscr{S}} p(s'|(i,j,k),a=0)\alpha v(s',t) \\
&= \alpha p^o(k')\Big(p_e \sum_{j'=j+1}^{J} d_{j'} v(i{+}1,j',k';n) + \bar{p}_e \sum_{j'=j+1}^{J} d_{j'} v(i,j',k';n) \\
&\quad + p_e \bar{d}_j v(i{+}1,j,k';n) + \bar{p}_e \bar{d}_j v(i,j,k';n)\Big) \\
&\quad - \alpha p^o(k')\Big(p_e \sum_{j'=j}^{J} d_{j'} v(i{+}1,j',k';n) + \bar{p}_e \sum_{j'=j}^{J} d_{j'} v(i,j',k';n) \\
&\quad + p_e \bar{d}_{j-1} v(i{+}1,j{-}1,k';n) + \bar{p}_e \bar{d}_{j-1} v(i,j{-}1,k';n)\Big) \\
&= \alpha p^o(k')\Big(p_e \bar{d}_{j-1} v(i+1,j,k';n) + \bar{p}_e \bar{d}_{j-1} v(i,j,k';n) \\
&\quad - p_e \bar{d}_{j-1} v(i{+}1,j{-}1,k';n) - \bar{p}_e) \bar{d}_{j-1} v(i,j{-}1,k';n)\Big) \\
&\leq \alpha p^o(k')\Big(p_e \bar{d}_{j-1} 1 + \bar{p}_e \bar{d}_{j-1} 1\Big) \leq \alpha p^o(k') \bar{d}_{j-1} 1 \leq 1
\end{aligned}$$

Case 3: In the third case, action 1 is chosen when the VoI is $(j+1)$ and action 0 is chosen when the VoI is j. We need the boundedness of the value function in terms of the energy at $n-1$ to show that the difference in the value function is bounded in this case:

$$\begin{aligned}
\mathscr{D}v_{01} &= v_0(i,j{+}1,k;n{+}1) - v_1(i,j,k;n{+}1) \\
&= \sum_{s'\in\mathscr{S}} p(s'|(i,j+1,k),a=0)\alpha v(s';n)
\end{aligned}$$

$$
\begin{aligned}
&- j - \sum_{s' \in \mathscr{S}} p(s'|(i,j,k),a=0)\alpha v(s';n) \\
&= \alpha p^o(k')\Big(p_e \sum_{j'=j+1}^{J} d_{j'} v(i{+}1,j',k';n) + \bar{p}_e \sum_{j'=j+1}^{J} d_{j'} v(i,j',k';n) \\
&\quad + p_e \bar{d}_j v(i{+}1,j,k';n) + \bar{p}_e \bar{d}_j v(i,j,k';n)\Big) \\
&\quad - j - \alpha p^o(k')\Big(p_e \sum_{j'=0}^{J} d_{j'} v(i,j',k';n) + \bar{p}_e \sum_{j'=0}^{J} d_{j'} v(i{-}1,j',k';n)\Big) \\
&= -j + \alpha p^o(k')\Big(p_e \sum_{j'=0}^{J} d_{j'}\Big(v(i{+}1,j',k';n) - v(i,j',k';n)\Big) \\
&\quad + \bar{p}_e \sum_{j'} d_{j'}\Big(v(i,j',k';n) - v(i{-}1,j',k';n)\Big) \\
&\quad + p_e \sum_{j'=0}^{j} d_{j'}\Big(v(i{+}1,j,k';n) - v(i{+}1,j',k';n)\Big) \\
&\quad + \bar{p}_e \sum_{j'=0}^{j} d_{j'}(v(i,j,k',t) - v(i,j',k',t))\Big)\Big) \\
&\leq -j + \alpha p^o(k')(1+j) \leq 1
\end{aligned}
$$

Case 4: In the final case, action 1 is chosen when the VoI is $(j+1)$ and action 0 is chosen when the VoI is j:

$$
\begin{aligned}
\mathscr{D}v_{10} &= v_1(i,j{+}1,k;n) - v_1(i,j,k;n) + v_1(i,j,k;n) - v_0(i,j,k;n) \\
&\leq v_1(i,j{+}1,k;n) - v_1(i,j,k;n) \leq 1
\end{aligned}
$$

Again note that the first inequality is due to the fact that $v_1(i,j,k;n) < v_0(i,j,k;n)$ since action 0 is the optimal action in state (i,j,k). For all four subcases, we find that the value function is bounded in terms of the VoI in the system at time stage t. By letting n go to infinity, we complete the second part of the proof. □

3.4 Numerical examples and discussion

We now investigate the structure of the optimal policy with respect to the different system parameters. To study the optimal policy for different transmission opportunity probabilities p_t, we fix the maximum capacity of the battery to $C = 100$ energy chunks and the VoI is at most $J = 100$ information units, the distribution being,

$$d_i = p(1-p)^i,$$

for $0 < i \leq J$ with $p = 0.1$ and $d_0 = 1 - \sum_{k=1}^{J} d_k$.

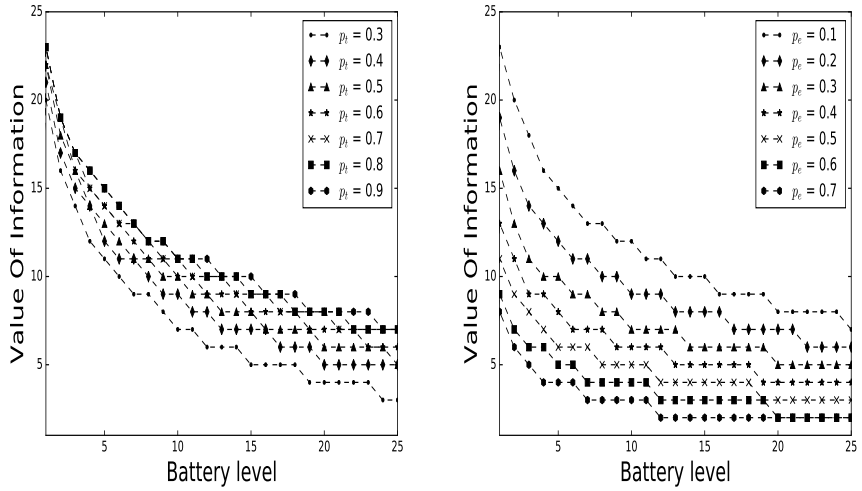

(a) varying p_t (b) varying p_e

Figure 3.2: Optimal policy (a) for varying Transmission opportunity p_t (b) Varying harvesting energy probability p_e as indicated.

The optimal policy obtained is a deterministic threshold policy. As the system has only one action available when there is no transmission opportunity, we analyse the policy for the reduced state space $\mathscr{S}_1$. The optimal threshold is two dimensional, meaning that for a fixed VoI we always transmit beyond a certain battery level and that for a fixed battery level we always transmit beyond a certain number of information units.

Figures 3.2(a) and 3.2(b) depict the threshold for the VoI as a function of the battery state for a fixed discounting factor $\alpha = 0.9$. Figure 3.2(a) fixes the probability of an energy arrival $p_e = 0.1$ and shows the threshold for various transmission opportunity probabilities as indicated. Figure 3.2(b) fixes the probability of a transmission opportunity $p_t = 0.9$ and shows the threshold for different energy arrival probabilities as indicated.

It can be seen from both figures that the threshold decreases for increasing battery levels. This is not unexpected. When only little energy is available, the decision to transmit affects future transmissions more if there is but a little energy so that one only transmits if there is a lot of information. If more energy available, the effect on future transmissions is smaller. Moreover, an additional increase will then hardly influence the threshold.

Figure 3.2(a) further reveals that the threshold increases for increasing values of p_t. If there are many transmission opportunities, the chance to send more data units later on increases as the next transmission opportunity is not far away in time. It is also observed that the threshold for higher transmission opportunity probabil-

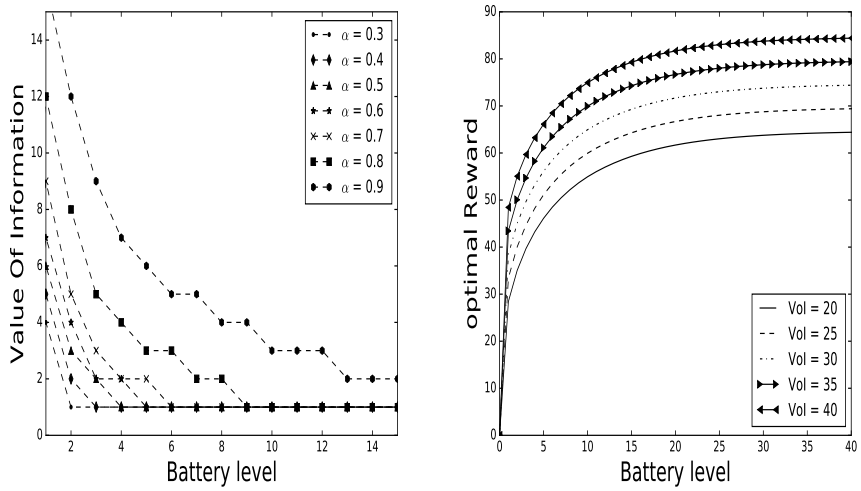

Figure 3.3: (a) Optimal policy for a varying discounting factor and (b) reward at the optimal policy as indicated.

ities can be equal to the threshold at lower transmission opportunity probabilities but cannot be less. In addition, Figure 3.2(b) shows that boosting the energy harvesting capability yields lower thresholds. Higher p_e implies that availability of energy at future transmission opportunities is more likely so that one can send even when there is less data. If the battery has enough energy, a further increase in harvesting capability cannot improve the optimal reward and thus the threshold does not vary significantly.

Figure 3.3(a) shows the VoI threshold versus the battery level for different discounting factors as indicated. We fix the transmission opportunity probability $p_t = 0.9$ and energy arrival probability $p_e = 0.1$, while all the other parameters are kept the same. A higher discounting factor means that more importance is given to the future rewards. That is, when the discounting factor is high, the system is more likely to conserve the energy for messages that may arrive in the future with a higher VoI which implies that the threshold for sending the VoI is higher as well. Further notice that the threshold for low discounting factors can equal the threshold for a higher discounting factor but cannot exceed that threshold. Figure 3.3(b) shows the reward $v^*(i, j, 1)$ for the optimal policy versus the battery level i for different values of the value of information j as indicated. We retain the parameters of Figure 3.3(a), and additionally fix the discounting factor to $\alpha = 0.9$. We observe that for a fixed VoI, the optimal reward is a non-decreasing function of the battery level. This behaviour of the value function has been already confirmed by the theoretical analysis in Section 3.3. Results not depicted here show that if we fix the battery level, the optimal expected reward is non-decreasing for different

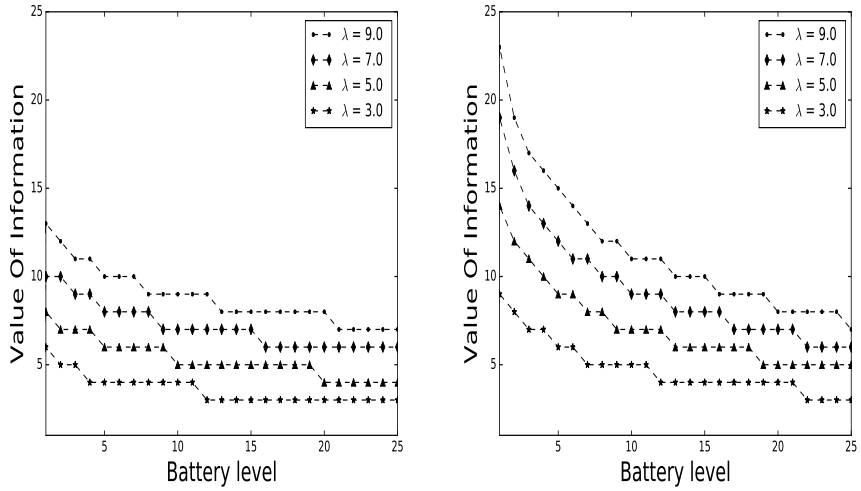

(a) Poisson (b) Geometric

Figure 3.4: Optimal policy for (a) Poisson (b) geometric VoI distribution for different values of mean (λ) of data arrival as indicated.

VoI as well.

We now focus on the effects of the distribution of the Value of Information on the optimal policy. To this end, Figure 3.4(a) and 3.4(b) depict the threshold for (truncated) Poisson and (truncated) geometrically distributed VoI, respectively. Different values for the mean number of information units (λ) are assumed as indicated. We assume that the battery can store up to $C = 50$ chunks and that the VoI is bounded by $J = 50$. Moreover, the discounting factor is equal to $\alpha = 0.9$, the transmission opportunity probability is assumed to be $p_t = 0.9$ and the energy arrival probability is fixed to $p_e = 0.1$. Comparing Figure 3.4(a) and 3.4(b) reveals that the distribution of the VoI affects the threshold policy significantly. This is not unexpected, as the chance to replace the current VoI with a better VoI depends on the distribution, and not only on its mean.

Optimal data collection

To conclude, we study the optimal collection probability p_t, assuming that (i) the sensor node applies the optimal policy and (ii) there is a cost related to data collection.

To this end, we calculate the mean value of information collected per time slot as a function of p_t. For every value of p_t, we first find the optimal policy in accordance with Section 3. Given this policy, we obtain the Markov chain for the

optimally controlled sensor node. We have the transition probabilities,

$$\tau(s'|s) = \begin{cases} \sum_{s' \in \mathscr{S}} q(s'|s) & \text{for } s \in \mathscr{S}_0\,, \\ \sum_{s' \in \mathscr{S}} p(s'|s, \pi^*(s)) & \text{for } s \in \mathscr{S}_1\,, \end{cases} \tag{3.19}$$

with $q(s'|s)$ and $p(s'|s)$ as defined in equations (3.2) - (3.4). Let $\psi(s)$ be the stationary probability of being in state s. That is, $\psi(s)$ is the normalised solution of the system of equations,

$$\psi(s') = \sum_{s \in \mathscr{S}} \tau(s'|s)\psi(s)\,,$$

for $s' \in \mathscr{S}$. Note that the system of equations above is again a QBD. Hence, we can again rely on linear level reduction to calculate these probabilities in $O(CJ^3)$, see Latouche and Ramaswami [97].

Once we have found $\psi(s)$, the mean reward per time slot can be expressed as,

$$\bar{V} = \sum_{s=(i,j,k) \in \mathscr{S}} \psi(s)\, j\pi(s)\,.$$

We now investigate the optimal data collection probability for the sensor node at hand, similarly as in Chapter 2 for the uncontrolled sensor node. We assume that there is a cost c associated to data collection so that the average value after collection equals,

$$\bar{V}_p = -cp_t + \bar{V}\,. \tag{3.20}$$

Note that we hereby assume that the cost can be expressed in terms of information units.

We can now study the impact of transmission opportunity probability on the average VoI collected from a sensor node operating under its optimal policy. We fix the battery capacity to 50 chunks and the range of VoI is 1 to 50 i.e., $C = 50, J = 50$.

Figure 3.5(a) fixes the energy arrival probability to 0.4 and plots $\bar{V}_p$ for different discounting factors whereas Figure 3.5(b) fixes the discounting factor to 0.4 and shows the average VoI collected from the node for different energy arrival probabilities. The cost of collection is assumed to be 2 i.e., $c = 2$. We can observe clearly that $\bar{V}_p$ increases for increasing transmission opportunities and then decreases again. This can be explained by the fact that by increasing p_t one first increases the value of data one can collect. However, once p_t is sufficiently high, hardly any additional value can be collected by further increasing p_t. In contrast the collection cost does increase so that the overall value decreases.

The small jumps in the figures are present due to a change of the optimal policy at particular transmission opportunity probabilities. As a consequence, the curve representing $\bar{V}_p$ is not concave due to these jumps and multiple optimal transmission opportunity probabilities may exist for which $\bar{V}_p$ attains its maximum value. It is also observed that the optimal transmission opportunity is more sensitive to changes in p_e than to changes in the discounting factor.

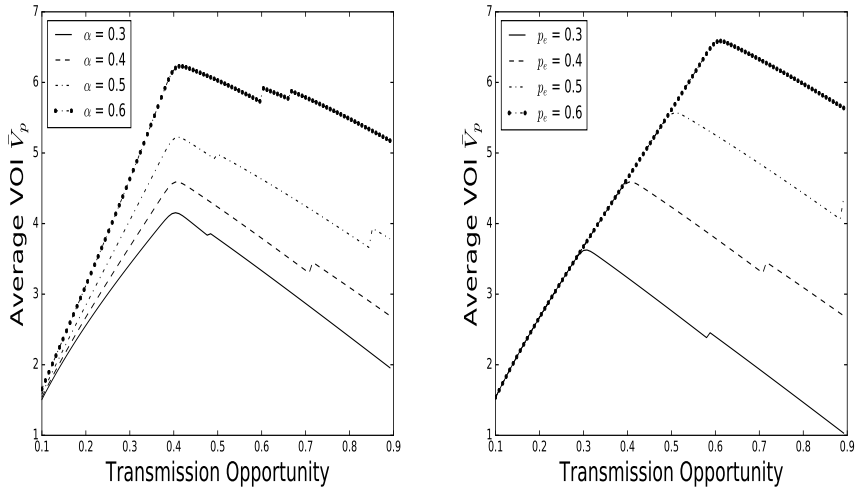

Figure 3.5: Value of information collected from node for (a) varying discounting factor and (b) varying energy harvesting probability

3.5 Summary

We proposed a two-queue Markov model for a wireless sensor node. The non-additive nature of the Value of Information plays an important role in decision making. We formulated the problem as Markov decision process and found the exact solution by policy iteration. Numerical results show that the optimal transmission policy is a threshold policy. Further observations show that the threshold for the value of the information is most sensitive to the battery level when there is but few energy: the node transmits more selectively when there is less energy. We also studied the behaviour of the optimal reward and mean value of information collected from a node under the optimal policy. Here, we found the pervasive structural property that the optimal reward is non-decreasing in terms of the battery level as well as in terms of the VoI.

4

Large-scale wireless sensor networks with interacting nodes

WSNs have a variety of mechanisms according to which nodes coordinate with each other to transfer information from where it is sensed towards the sink where it is processed. Most of these mechanisms are multi-hop mechanisms, that is, mechanisms that rely on nodes relaying information towards the sink. Such mechanisms have many advantages including redundancy, scalability and a larger coverage. Indeed, each sensor node has the potential to act as a relay node and if some node in the network fails to operate at some time, the information can be routed through an alternate path. Recall that gathering and transmitting the information make up most of a node's power consumption in WSNs. Hence, with multihop mechanisms, a large portion of the battery power is expended in relaying information to other sensor nodes. As many WSNs are battery-powered, it is important to ensure that the network lifetime (the time the network can operate autonomously until the batteries or the sensor nodes themselves need to be replaced) is sufficiently long. Thus, the optimal transmission policies and efficient routing schemes are crucial in the design and modelling of WSNs. See [99] for the detailed discussion on different routing schemes in WSNs. These authors also highlight the different advantages and performance issues of each scheme.

From a modelling perspective, the main challenge for assessing such networks lies with the interaction between the nodes. If interaction is the key determinant of the performance of the sensor network, then nodes cannot be studied in isolation. Over the past few years, there has been a lot of work in modelling WSNs by controlled stochastic processes. A popular approach is the dynamic programming framework, which provides multiple advantages over its alternatives such as optimal resource utilisation, balanced design of different objectives including efficient energy utilisation and optimal data collection. However, the method requires to store the "value function" for each state which often leads to high memory utilisa-

tion. Moreover, large sizes of the state space cause a marked increase in complexity of the dynamic programming equations, or equivalently, a marked increase in the computational resources that are needed to obtain the exact solution. Hence, many attempts have been made to solve large stochastic control problems through various approximation techniques [100]. For example, De Farias et al [101] study linear approximations to large scale stochastic control problems while Chen et al. [102] approximate dynamic programming through fluid and diffusion models. Le Boudec et al. [103] use a set of deterministic equations also referred to as a *mean-field* approach. These techniques provide a powerful approach to handle the high complexity in large scale WSNs [104]. Also some other recent works such as [105, 106] handle the high complexity by analysing the performance of communication protocols and end-to-end delay in WSNs with mean-field approximations. Moreover, Gast et al [107] discuss the mean-field approximation for generic Markov decision processes and show that the approximation converges almost surely as the number of nodes tends to infinity. These authors also provide several examples and show that the optimal control of the mean-field system is the same as the limit of the optimal control of the original problem. This property then implies that the optimal control in the limit is a good approximation for the optimal control in the pre-limit.

In this chapter, we focus on the optimal transmission policy for a sensor network with a large number of sensor nodes. In particular, we focus on maximising the VoI available for collection by a mobile sink, while keeping the energy consumption at minimum. Various energy problems in large scale networks have been already investigated, see for example [108, 109], which use game theory and mean-field games. The authors provide a solution by solving a coupled system of Fokker-Planck-Kolmogorov (FPK) equations and Hamiltonian-Jacobi-Bellman (HJB) equations. However, the numerical solution is highly complex and does not consider the impact of the quality of information on the transmission decisions. We therefore define a stochastic model for WSNs where each node in the network can be in a finite number of information states, such that the combined states of all nodes make up the state space for the Markov description of the complete network. We then formulate the optimisation problem that offers a systematic approach to obtain energy-aware transmission policies. However, as mentioned earlier, such problems prove to be very difficult to solve as the number of nodes in the network increases. To overcome these issues, we adopt a mean-field approximation and convert the problem into a deterministic control problem. We use Pontryagin's minimum principle to get the solution for the resulting HJB equation. The main challenge we face is that these equations are fully coupled and we have more than one control variable. Moreover, the constraints on the state and control variables make the problem more difficult. In order to handle these challenges, we first characterise the optimal control and show that the solution always exists on the boundary. Then we remove the constraints on the state variables by showing that they are always satisfied. Lastly, in the numerical section we consider the specific case of a network with three control variables and provide the full characterisation of the optimal transmission policy. It is worth mentioning that the optimal policy

in this case is a threshold-type policy and hence is easy to implement in practice.

The remainder of this chapter is organised as follows. The next Section 4.1 introduces the stochastic model and its mean-field approximation. In Section 4.2, we focus on some numerical examples. Finally, we conclude and summarise our results in Section 4.3.

4.1 Model Description

We consider a network with N interacting sensor nodes, each node being equipped with on-board memory to store sensor information. The sensor is aware of the value that the information brings to decision making, which is expressed in terms of the Value of Information (VoI). We assume that the VoI is an integer value between 0 and J, where 0 corresponds to the absence of information, and J to the maximum VoI. The sensor data is periodically collected by a mobile sink that randomly polls sensor nodes. Therefore, data collection by the sink is optimal if the nodes keep as much VoI as possible in the network.

We model the network by a multi-dimensional Markov process, where the state of the Markov process is completely described by the VoI at the nodes. The VoI at the nodes changes according to the following three different processes:

- The VoI decreases if there is no new information from the environment. The VoI decreases by one unit with rate ℓ_0^N, independently for each sensor node.
- The VoI increases if there is new information from the environment with a value higher than the current VoI at the node. For each sensor node, new sensing data with VoI j arrives with rate ℓ_j^N, $j \in \{1,\dots,J\}$.
- The VoI changes if two nodes in the network meet each other. Two nodes meet with rate γ^N. When this is the case, there are two different scenarios:
  - If both nodes decide to send their information, then the information is lost due to a collision and no exchange is possible. Similarly, if both nodes decide to receive at the same time, there is no information transfer.
  - If one sends and another receives, then data is sent. However, the exchange of data only affects the VoI of the receiving node if the sender has a higher VoI than the receiver.

  A node decides to send its information depending on the corresponding VoI. If the VoI is j, a node will send with probability η_j, $j \in \{1,\dots,J\}$.

Hence, the evolution of the VoI at a particular node is the combination of an information loss process and an information replacement process. The information loss process causes each node to depreciate the value of information over time. Likewise, the information replacement process models the appearance of newly sensed or relayed information, and the already available information gets replaced

whenever the value of newly sensed or relayed information exceeds the old VoI at the sensor node. Note that this means the VoI process operates in a non-additive way: when new more valuable information arrives at a node, the resulting VoI of the node is the value of the arriving information, and not the sum of the values of the old and the new information or anything of the kind.

4.1.1 Markov model

We first characterise the Markovian network model in terms of time-shifted Poisson processes. This characterisation then facilitates studying the mean-field limit in the next subsection. Let $X_n^N(t)$ denote the value of the information (VoI) at the nth node at time t. The VoI in the network at time t is then described by the vector $\mathbf{X}^N(t) = (X_1^N(t), X_2^N(t), \ldots, X_N^N(t))$. In view of the assumptions above, the future evolution of the VoI in the network does not depend on the past VoI, given the present VoI, and hence the process $\mathbf{X}^N(t)$ constitutes a Markov process.

We can now introduce the occupation process $\mathbf{M}^N(t) = [M_j^N(t)]_{j=0}^J$ in terms of the VoI process $\mathbf{X}^N(t)$. The jth element of $\mathbf{M}^N(t)$ counts the number of nodes that carry VoI j at time t,

$$M_j^N(t) = \sum_{n=1}^{N} 1_{\left\{X_n^N(t)=j\right\}},$$

for $j \in \{0, 1, \ldots, J\}$. As we do not distinguish between sensor nodes, our assumptions on the sensor network also imply that $\mathbf{M}^N(t)$ constitutes a Markov process as well. In particular, if the process is in state $\mathbf{M}^N(t) = \mathbf{m} = [m_j]_{j=0}^J$, the state of the occupation process changes according to the following rates:

- The VoI at any node drops with rate ℓ_0^N, and hence the VoI at nodes with VoI j drops with rate $\ell_0^N m_j$ for $j \in \{1, \ldots, J\}$. As there is one more node with VoI $j-1$ and one less with VoI j after the drop, the new state is $\mathbf{m} - \mathbf{e}_j + \mathbf{e}_{j-1}$, with $\mathbf{e}_j = [1_{\{i=j\}}]_{i=0}^J$.

- New information with value i arrives at each and every node with rate ℓ_i^N, for $i \in \{1, \ldots, J\}$. Hence the VoI at nodes with VoI j changes with rate $\ell_i^N m_j$ for $j \in \{0, \ldots, i-1\}$. As there is one more node with VoI i and one less with VoI j after the arrival, the new state is $\mathbf{m} - \mathbf{e}_j + \mathbf{e}_i$.

- Finally, nodes meet with rate γ^N, and hence a random (tagged) node with VoI j meets another node with rate $\gamma^N m_j N^{-1}$. This other node then carries VoI $i > j$ with probability $m_i(N-1)^{-1}$, and the VoI of the tagged node changes to i provided that the tagged node does not send (with probability $1-\eta_j$) and the other node does send (with probability η_i). The new state is then $\mathbf{m} - \mathbf{e}_j + \mathbf{e}_i$.

The former description of the transition rates then allows for expressing $M_j^N(t)$ in terms of Poisson processes. Let D_j, $A_{i,j}$ and $Q_{i,j}$ denote independent unit-rate

Poisson processes, for $i, j \in \{0, \ldots, J\}$. We then express $M_j^N(t)$ as follows,

$$\begin{aligned}
M_0^N(t) &= D_1\left(\ell_0^N \int_0^t M_{j+1}^N(u)du\right) - \sum_{i=1}^{J} A_{0,i}\left(\ell_i^N \int_0^t M_0^N(u)du\right) \\
&\quad - \sum_{i=1}^{J} Q_{0,i}\left(\gamma^N \eta_i(1-\eta_0)\int_0^t \frac{M_0^N(u)}{N}\frac{M_i^N(u)}{N-1}du\right) \\
M_j^N(t) &= D_{j+1}\left(\ell_0^N \int_0^t M_{j+1}^N(u)du\right) - D_j\left(\ell_0^N \int_0^t M_j^N(u)du\right) \\
&\quad + \sum_{i=1}^{j-1} A_{i,j}\left(\ell_j^N \int_0^t M_i^N(u)du\right) - \sum_{i=j+1}^{J} A_{j,i}\left(\ell_i^N \int_0^t M_j^N(u)du\right) \\
&\quad - \sum_{i=j+1}^{J} Q_{j,i}\left(\gamma^N \eta_i(1-\eta_j)\int_0^t \frac{M_j^N(u)}{N}\frac{M_i^N(u)}{N-1}du\right) \\
M_J^N(t) &= -D_j\left(\ell_0^N \int_0^t M_J^N(u)du\right) + \sum_{i=1}^{J-1} A_{i,j}\left(\ell_J^N \int_0^t M_i^N(u)du\right), \qquad (4.1)
\end{aligned}$$

for $j = 1, \ldots, J-1$. The process D_j counts the number of times the VoI drops from level j to $j-1$ (over all nodes), the process $A_{i,j}$ counts the transitions from level i to level j, due to arriving sensor information. Finally, the process $Q_{j,i}$ counts the transitions from level j to level i due to an exchange of information.

4.1.2 Mean-field limit

Define the scaled process $m_j^N(t) = M_j^N(Nt)N^{-1}$, where we scale the parameters as follows

$$\ell_j^N = \frac{\ell_j}{N}, \quad \gamma^N = \gamma.$$

With this scaling, the total rate of sensor information in the network and the contact rate remain constant. Evaluating (4.1) in Nt and dividing by N, yields the following after some manipulations,

$$\begin{aligned}
m_0^N(t) &= \frac{1}{N}D_1\left(N\ell_0 \int_0^t m_1^N(u)du\right) - \sum_{i=1}^{J} \frac{1}{N}A_{0,i}\left(N\ell_i \int_0^t m_0^N(u)du\right) \\
&\quad - \sum_{i=1}^{J} \frac{1}{N}Q_{0,i}\left(N\gamma\frac{N}{N-1}\eta_i(1-\eta_0)\int_0^t m_0^N(u)m_i^N(u)du\right), \\
m_j^N(t) &= \frac{1}{N}D_{j+1}\left(N\ell_0 \int_0^t m_{j+1}^N(u)du\right) - \frac{1}{N}D_j\left(N\ell_0 \int_0^t m_j^N(u)du\right) \\
&\quad + \sum_{i=1}^{j-1} \frac{1}{N}A_{i,j}\left(N\ell_j \int_0^t m_i^N(u)du\right) - \sum_{i=j+1}^{J} \frac{1}{N}A_{j,i}\left(N\ell_i \int_0^t m_j^N(u)du\right) \\
&\quad - \sum_{i=j+1}^{J} \frac{1}{N}Q_{j,i}\left(N\gamma\frac{N}{N-1}\eta_i(1-\eta_j)\int_0^t m_j^N(u)m_i^N(u)du\right),
\end{aligned}$$

$$m_j^N(t) = -\frac{1}{N} D_j \left(N\ell_0 \int_0^t m_j^N(u)du \right) + \sum_{i=1}^{J-1} \frac{1}{N} A_{i,j} \left(N\ell_j \int_0^t m_i^N(u)du \right). \quad (4.2)$$

Now, for $j \in \{0,1,\ldots,J\}$, assume that $m_j^N(0)$ converges to a deterministic limit $m_{j,0}$ for $N \to \infty$, almost surely. Then, let $m_j(t)$ be the unique solution of the system of differential equations,

$$m_0'(t) = \ell_0 m_{j+1}(t) - \sum_{i=j+1}^{J} \ell_i m_j(t) - \sum_{i=j+1}^{J} \gamma\eta_i(1-\eta_j) m_i(t) m_j(t), \quad (4.3)$$

$$m_j'(t) = \ell_0 m_{j+1}(t) - \ell_0 m_j(t) + \ell_j \sum_{i=1}^{j-1} m_i(t) - \sum_{i=j+1}^{J} \ell_i m_j(t) \quad (4.4)$$

$$- \sum_{i=j+1}^{J} \gamma\eta_i(1-\eta_j) m_i(t) m_j(t),$$

$$m_J'(t) = -\ell_0 m_j(t) + \ell_j \sum_{i=1}^{J-1} m_i(t), \quad (4.5)$$

with initial condition $m_j(0) = m_{j,0}$.

Integrating both sides of (4.5) and subtracting it from (4.2) yields,

$$m_j^N(t) - m_j(t) = d_{j+1}^N(t) - d_j^N(t) + \sum_{i=1}^{j-1} a_{i,j}^N(t) - \sum_{i=j+1}^{J} a_{j,i}^N(t) - \sum_{i=j+1}^{J} q_{j,i}^N(t),$$

for $j = 1,\ldots,J-1$ with

$$d_j^N(t) = N^{-1} D_j \left(N\ell_0 \int_0^t m_j^N(u)du \right) - \ell_0 \int_0^t m_j^N(u)du$$

$$a_{i,j}^N(t) = N^{-1} A_{i,j} \left(N\ell_j \int_0^t m_i^N(u)du \right) - \ell_j \int_0^t m_i^N(u)du$$

$$q_{j,i}^N(t) = N^{-1} Q_{j,i} \left(N\gamma \frac{N}{N-1} \eta_i(1-\eta_j) \int_0^t m_j^N(u) m_i^N(u)du \right)$$

$$- \gamma\eta_i(1-\eta_j) \int_0^t m_j^N(u) m_i^N(u)du.$$

Hence, the difference between $m_j^N(t)$ and $m_j(t)$ in the interval $[0,T]$ is bounded by,

$$\sup_{t\in[0,T]} |m_j^N(t) - m_j(t)| \le \sup_{t\in[0,T]} |d_{j+1}^N(t)| + \sup_{t\in[0,T]} |d_j^N(t)| + \sum_{i=1}^{j-1} \sup_{t\in[0,T]} |a_{i,j}^N(t)|$$

$$+ \sum_{i=j+1}^{J} \sup_{t\in[0,T]} |a_{j,i}^N(t)| + \sum_{i=j+1}^{J} \sup_{t\in[0,T]} |q_{j,i}^N(t)|.$$

Moreover, the terms on the right-hand side converge to 0 almost surely by the functional strong law of large numbers for Poisson processes such that

$\sup_{t\in[0,T]} |m_j^N(t) - m_j(t)| \to 0$ for $N \to \infty$. Indeed, we have for $d_j^N(t)$,

$$\lim_{N\to\infty} \sup_{t\in[0,T]} |d_j^N(t)| = \lim_{N\to\infty} \sup_{t\in[0,T]} \left| \frac{1}{N} D_j \left(N\ell_0 \int_0^t m_j^N(u)du \right) - \ell_0 \int_0^t m_j^N(u)du \right|$$
$$\leq \lim_{N\to\infty} \sup_{t\in[0,\ell_0 T]} \left| \frac{1}{N} D_j(Nt) - t \right| = 0\,,$$

where the first inequality follows from the bound,

$$\ell_0 \int_0^t m_j^N(u)du \leq \ell_0 t\,.$$

The proofs for the other terms and for the cases $j = 0$ and $j = J$ are entirely similar and therefore omitted. Thus, we have shown that the probability of observing a significant difference between any single trajectory of the Markov process and the solution of the ODE goes to zero as N grows to infinity. We refer to the set of ordinary differential equations 4.5 as the limit ODE and this set provides an accurate approximation of the mean occupancy vector $m(t)$ when the number of nodes in the network are finite but sufficiently large.

4.1.3 The HJB equation and optimal control

The aim is to keep the VoI as high as possible while keeping the exchange of information to a minimum. Therefore, we define the following cost function,

$$U = \int_0^T \sum_{j=0}^{J} (c\,\eta_j(t) - r_j)\, m_j(t)dt\,, \tag{4.6}$$

where, r_i is the reward for transmitting i VoI and c is a constant cost incurred if the node decides to transmit the information. Here $\eta_j(t)$ is the control, that is, the probability to transmit at time t and VoI level j. As $\eta_j(t)$ is probability, we impose,

$$0 \leq \eta_j(t) \leq 1\,. \tag{4.7}$$

Moreover, as there is no reward for transmitting zero VoI, it is natural to assume that r_0 is zero.

Recall the $m_j(t)$ denotes the fraction of nodes carrying VoI j, and hence we have,

$$\begin{aligned} 0 \leq m_j(t) \leq 1\,,\\ \sum_{j=1}^{J} m_j(t) \leq 1\,. \end{aligned} \tag{4.8}$$

These constraints will be imposed for now, but will follow from the remaining calculations.

We now focus on obtaining the closed-loop optimal control using the HJB equations based on Bellman's optimality principle. This principle states that regardless of previous decisions (controls), the remaining decisions must constitute

the optimal policy. This simply means that any part of the optimal trajectory is optimal. We provide the HJB equations for the system at hand and obtain the control as a function of the state variables. To this point, we introduce the following Hamiltonian of the system,

$$H(m,\eta,\lambda) = \sum_j (c\,\eta_j - r_j) m_j + \sum_j \lambda_j \Bigg(m_{j+1}\,\ell_0 + \ell_j \sum_{i=0}^{j-1} m_i - m_j \Bigg(\ell_0 + \sum_{i=j+1}^{J} \ell_i \Bigg) - \sum_{i>j} \gamma m_i\, m_j\, (1-\eta_j)\,\eta_i \Bigg), \quad (4.9)$$

where λ_j is Lagrangian multiplier for the constraint m_j' and where we suppress the time-parameter t from the notation for convenience. Note that the functions λ_j are also called the co-state variables and they relate to the state variable as $\lambda' = -\partial H/\partial m$. The solution (m^*, η^*, λ^*) corresponding to the optimal control, then satisfies the HJB equations, i.e.,

$$H(m^*(t), \eta^*(t), \lambda^*(t)) = 0\,. \quad (4.10)$$

Given $(m^*, \eta*, \lambda^*)$, the scalar cost is,

$$U^* = \int_0^T \sum_{j=0}^{J} (c\,\eta_j^*(t) - r_j)\, m_j^*(t) dt\,.$$

In the expressions above, we can assume without loss of generality that the optimal control at VoI level 0 is 0 as there is no reward of sending data that carries no VoI. Therefore, we do not include index 0 in the optimal control vector $\eta^* = [\eta_j^*]_{j=1}^J$. Likewise, as we have $\sum m_j = 1$, we define the optimal state trajectory vector as $m^* = [m_j^*]_{j=0}^{J-1}$.

We are interested in finding the optimal control for any initial state vector $[m_{j,0}]_{j=0}^J$. In general, the equation (4.10) is a non-linear partial differential equation and obtaining its solution can prove to be challenging. We use Pontryagin's minimum principle to find the optimal control. With a slight abuse of notation, suppose $\eta^* = (\eta_1^*, \eta_2^*, \cdots, \eta_J^*)$ is the optimal control over the interval $[t,T]$ and $m^* = (m_0^*, m_2^*, \cdots, m_{J-1}^*)$ is the optimal state at time t. Formally, Pontryagin's minimum principle states the following three conditions for optimality.

1. **Hamiltonian:** The optimal state trajectory $m^*(t)$, optimal control $\eta^*(t)$ and corresponding co-state variables $\lambda^*(t)$ must minimise the Hamiltonian H such that,
$$H(m^*, \eta^*, \lambda^*) \leq H(m^*, \eta, \lambda^*)\,,$$
for any $\eta = [\eta_1, \ldots, \eta_J]$ satisfying (4.7).

2. **State and co-state Equations:**
$$m_i' = H_{\lambda_i}(m, \eta, \lambda)\,,$$

$$\lambda_i' = -H_{m_i}(m, \eta, \lambda)\,.$$

where H_{λ_i} (H_{m_i}) is the derivative of the Hamiltonian with respect to λ_i (m_i).

3. **Terminal Condition:** for all time $t \in [0,T]$ and for all permissible control inputs η, $H(T) = 0$.

We find the critical point by differentiating the Hamiltonian with respect to the controls and equating to zero, i.e., $\partial H/\partial \eta = 0$. This yields a system of linear equations so can be written in matrix form as $\mathbf{A}\,\eta^* = \mathbf{b}$, where the coefficient matrix $\mathbf{A} = (a_{ij})$ can be expressed as,

$$a_{ij} = \begin{cases} \lambda_i m_{j+1} & i > j\,, \\ \lambda_j m_j & i < j\,, \\ 0 & i = j\,, \end{cases} \tag{4.11}$$

for $i, j \in \{1, 2, \cdots, J\}$ and $\mathbf{b} = (b_i)$ with,

$$b_i = b_{i-1} + \lambda_{i-1} m_{i-1}\,, \tag{4.12}$$

for $i \in \{2, 3, \cdots, J\}$ and with $b_1 = -c + \lambda_0 m_0$.

Proposition 4.1. *Let η^* to be the optimal solution that minimises the total cost of the transmission in the network given by function (4.6) with $0 \leq \eta_j^* \leq 1$. Then, the optimal solution η^* always lies on the boundary of $[0,1]^J$.*

Proof. We consider the last two equations of the system given in (4.11) and (4.12),

$$\sum_{j=1}^{J-1} \lambda_j m_j \eta_j^* = b_{J-1} + \lambda_{J-1} m_{J-1} \tag{4.13}$$

and,

$$\sum_{j=1}^{J-2} \lambda_j m_j \eta_j^* + \lambda_{J-1} m_J \eta_J^* = b_{J-1} \tag{4.14}$$

Subtracting (4.13) from (4.14),

$$\lambda_{J-1} m_{J-1} \eta_{J-1}^* - \lambda_{J-1} m_J \eta_J^* = \lambda_{J-1} m_{J-1}\,.$$

or, equivalently,

$$\eta_{J-1}^* = 1 + \left(\frac{m_J}{m_{J-1}}\right) \eta_J^*\,. \tag{4.15}$$

It can easily be seen from the relation above that for any $\eta_J^* \in (0,1]$, the critical point will lie outside the feasible region. Since, the relation between η_J^* or η_{J-1}^* can only be satisfied at the extreme values, it is sufficient to conclude that there is no critical point inside the feasible region and the optimal solution exists on the boundary. □

The above proposition states that the optimal control lies on the boundary and therefore we have to evaluate each boundary point in order to obtain the optimal transmission policy. This may simplify the analysis but we still have constraints on the state variables, which should be handled by means of an additional analysis [110]. However, when we analyse the ODE of state variables for any control η, the state constraints in (4.7) are automatically satisfied throughout the finite interval $[0,T]$. Thus, we can ignore the state constraints and the optimisation problem can be solved as an unconstrained optimisation problem.

Proposition 4.2. *For any $\eta \in [0,1]^J$, the state functions $m_1, m_2, \cdots m_J : [0,T] \to \mathbb{R}^J$ that satisfy the state equations and initial conditions, always satisfy the constraints in* (4.8).

Proof. To prove this proposition, we look into the direction field of the state function and show that the state constraints $m_1, \cdots, m_J \geq 0$, are always satisfied. From equation (4.5), it is easy to see that $m'_j = m_{j+1}\,\ell_0 + \ell_j \sum_{i=0}^{j-1} m_i$ when $m_j = 0$. Note that the rates $\ell_j \geq 0$, for all $j \in \{1,\ldots,J\}$. Thus, for any feasible control η, the state function m'_j is positive at the boundary $m_j = 0$ meaning all the state variables would be non-negative throughout the time horizon.

Now consider $\sum_{j=0}^{J-1} m'_j$,

$$\begin{aligned}
\sum_{j=0}^{J-1} m'_j &= \sum_{j=0}^{J-1} \Bigg(m_{j+1}\,\ell_0 + \ell_j \sum_{i=0}^{j-1} m_i - m_j \Bigg(\ell_0 + \sum_{i=j+1}^{J} \ell_i \Bigg) \\
&\qquad - \sum_{i>j} \gamma m_i m_j (1-\eta_j)\,\eta_i \Bigg) \\
&= -\ell_0 m_0 + \ell_0 m_J + \sum_{i=0}^{J-2} m_i \sum_{j=i+1}^{J-1} \ell_j - \sum_{i=0}^{J-1} m_i \sum_{j=i+1}^{J-1} \ell_j \\
&\qquad - \sum_{j=0}^{J-1} \sum_{i=j+1}^{J} \gamma m_i m_j (1-\eta_j)\,\eta_i \\
&= -\ell_0 m_0 + \ell_0 m_J - m_{J-1}\ell_J - \sum_{j=0}^{J-1} \sum_{i=j+1}^{J} \gamma m_i m_j (1-\eta_j)\,\eta_i \\
&= -\ell_0 m_0 - m_{J-1}\ell_J - \sum_{j=0}^{J-1} \sum_{i=j+1}^{J} \gamma m_i m_j (1-\eta_j)\,\eta_i ,
\end{aligned}$$

where $m_J = 1 - \sum_{j=0}^{J-1} m_j = 0$, and where we already know that all m_j are non-negative. Thus, $\sum_{j=0}^{J-1} m_j \leq 1$. This constraint is stronger than the individual upper bound on the state variable $m_j \leq 1$ and therefore, we can say that the state function always satisfies the constraints in (4.7). □

4.1.4 Three State System

In this section, we focus on a system with three levels of VoI and analyse the behaviour of the optimal transmission policy. We assume that the information coming to the sensor node can be divided into two categories; regular information (VoI = 1) and high importance information (VoI = 2). When there is no information, the information state of the node is represented by VoI = 0. There are N sensor nodes in the network, and hence the state space of the Markov model is $\{0,1,2\}^N$. In practice, whether the controller can achieve the aim of keeping the maximum VoI depends on the optimal transmission policies. Recall that there is a basic trade-off between cost of transmission and the VoI in the network. We define the optimisation problem for the three state system formally as follows. Find the control (η_1^*, η_2^*), with

$$0 \leq \eta_1^*, \eta_2^* \leq 1\,,$$

such that,

$$\min_{\eta} U = \int_0^T \sum_{j=0}^{2} (c\,\eta_j(t) - r_j)\, m_j(t) dt\,, \tag{4.16}$$

subject to,

$$m_j' = m_{j+1}\ell_0 + \ell_j \sum_{i=0}^{j-1} m_i - m_j\left(\ell_0 + \sum_{i=j+1}^{2} \ell_i\right) - \sum_{i=j+1}^{2} m_i\,, m_j(1-\eta_j)\eta_i\,,$$

for $j = 0, 1$.

From proposition (4.1) and (4.2), we can ignore the constraints on controls and state variables of the optimisation problem and use Pontryagin's minimum principle for unconstrained problems in order to get the optimality conditions. We already know that the optimal control lies on the boundary and we have to evaluate each boundary point in order to obtain the optimal transmission policy. We further analyse the cost function at each boundary point and find an upper bound on the optimal transmission policy. We now investigate the structure of the Hamiltonian function and observe a special property of the transmission policy. It also helps to identify any redundant policies, to reduce the computational complexity.

Proposition 4.3. *Let $\eta^* := (\eta_1^*, \eta_2^*)$ be the optimal control that minimises the total cost of the transmission in the network given by* (4.16) *with $0 \leq \eta_1^*, \eta_2^* \leq 1$. Then, the solution is of bang-bang*[1] *form. Moreover, the optimal policy follows a threshold-type structure.*

Proof. We define the Hamiltonian of the system as,

$$H(m, \eta, \lambda) = \sum_{j=0}^{2} (c\eta_j - r_j) m_j$$

[1] In optimal control theory, sometimes a control is restricted to be between a lower and an upper bound. If the solution (the optimal control) switches from one extreme to other then that control is referred to as a bang-bang solution. It never takes the value in between the bounds.

$$+\lambda_1\left(m_1\,\ell_0 - m_0\left(\ell_0+\sum_{i=1}^{2}\ell_i\right) - m_0\,m_1\,\eta_1 - m_0\,m_2\,\eta_2\right)$$
$$+\lambda_2\left(m_2\,\ell_0+\ell_1 m_0 - m_1(\ell_0+\ell_2) - m_1\,m_2\,(1-\eta_1)\,\eta_2\right). \quad (4.17)$$

From proposition (4.1), we already know that the critical point lies outside the feasible region. To minimise the Hamiltonian, we have to evaluate expression in (4.17) at each boundary point. Note that the Hamiltonian in (4.17) has only one term of degree 2, which is $m_1\,m_2\,(1-\eta_1)\,\eta_2$. Thus at any boundary, if one of the optimal controls is fixed, then the Hamiltonian H is linear in terms of the other control. As a result, the minimum can again occur at the extreme points. In other words, the optimal policy is of bang-bang form; that is, it possesses four possible values and can switch abruptly between them.

We now show that the Hamiltonian at $(\eta_1 = 1, \eta_2 = 0)$ can not be minimum. Let $\tilde{H}$ be the Hamiltonian at $(\eta_1 = 0, \eta_2 = 0)$ as,

$$\tilde{H} = \sum_{j=0}^{2} -r_j\,m_j + \lambda_1\left(m_1\,\ell_0 - m_0\left(\ell_0+\sum_{i=1}^{2}\ell_i\right)\right)$$
$$+\lambda_2\left(m_2\,\ell_0+\ell_1 m_0 - m_1(\ell_0+\ell_2)\right).$$

Now we define the Hamiltonian at other three corner points in terms of $\tilde{H}$ as,

$$H_{\eta_1\eta_2}(m,\eta,\lambda) = \begin{cases} \tilde{H} + c\,m_2 - \lambda_1\,(m_0\,m_2) - \lambda_2\,(m_1\,m_2)\,, & \eta_1 = 0,\ \eta_2 = 1\,; \\ \tilde{H} + m_1\,(c - \lambda_1\,m_0)\,, & \eta_1 = 1,\ \eta_2 = 0\,; \\ \tilde{H} + (c - \lambda_1\,m_0)\,(m_1 + m_2)\,, & \eta_1 = 1,\ \eta_2 = 1\,. \end{cases}$$

It is easy to see from the expression above that $\tilde{H} < H_{10}$ if $(c - \lambda_1\,m_0) > 0$, and also that $H_{11} = H_{10} + m_2(c - \lambda_1\,m_0)$. Thus, $H_{11} < H_{10}$ if $(c - \lambda_1\,m_0) < 0$. Therefore, the optimal transmission policy switches between $(0,0)$, $(0,1)$ and $(1,1)$. At any time instance, there exists no j such that $\eta^*_{j+1} < \eta^*_j$. In other words, our system satisfies a threshold policy. □

4.2 Numerical Examples and Discussion

In this section, we numerically study the optimal behaviour of the state and control variables for a system with three VoI levels. We assume that the rewards for transmitting the VoI are $r_2 = 2$, $r_1 = 1$ and $r_0 = 0$. We fix the cost of transmission to $c = 1$ and plot the solution for the transient analysis in Figure 4.1(a) and Figure 4.1(b). We make the natural assumption that the rate of loss of information is less than that of the arrival rate of new information. Moreover, the information with high VoI arrives less frequently as compared to the information with low VoI. In

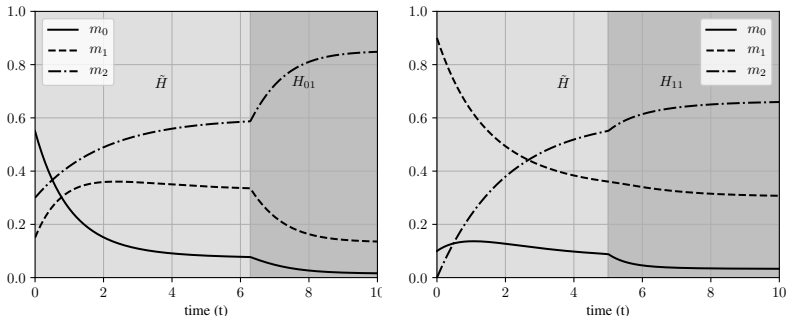

(a) $m_1(0) = 0.15, m_0(0) = 0.55$ (b) $m_1(0) = 0.1, m_0(0) = 0.9$

Figure 4.1: Transient analysis: Evaluation of the optimal controllers and the according state trajectories as function of time t

particular, we set $\ell_1 = 0.6$, $\ell_2 = 0.3$ and $\ell_0 = 0.2$. We already know that the solution in the transient case is of bang-bang type, which is also seen in the figure.

The solution depends on the initial values of state ($m_i(0)$) and co-state variables ($\lambda_i(0)$). We set the time horizon for the system to $T = 10$. Figure 4.1 depicts the trajectory of the number of nodes carrying particular VoIs. Depending on the trajectory, we observe a change in the optimal transmission policy. Moreover, state trajectories vary with respect to the initial conditions which may lead to different optimal transmission policies. We fix the initial state of to $m_0(0) = 0.55$, $m_1(0) = 0.15$ in Figure 4.1(a) and plot the state trajectories. For convenience, we denote the optimal policy with (η_1^*, η_2^*). Note that the optimal control η_0^* is always zero and thus we avoid it from the notation of optimal policy. It is observed from the figure that the optimal control policy is initially $(0,0)$ and later switches to $(0,1)$. This is due to the switching condition described in Proposition 4.3. We can see from the Figure 4.1(b) that different initial conditions, $m_0(0) = 0.9$, $m_1(0) = 0.1$, lead to different optimal transmission policies which switch from $(0,0)$ to $(1,1)$. Initially, there are a lot of nodes in the network without any VoI and therefore the optimal control is zero, i.e. allowing no exchange of information. Thus, the network defers the transmission decision until there is sufficient information from the environment. At a certain time, the control switches abruptly and allows the exchange of information. The number of nodes containing higher VoI then grows rapidly. Moreover, as we assumed that the rate of loss of information is less than the rate of new VoI coming to the system, we see that the state trajectory of nodes carrying no VoI is decreasing throughout time.

We now observe the behaviour of the state vector when there is already a sufficient VoI in the network. We modify the transition rates to $\ell_2 = 0.1$, $\ell_1 = 0.2$ and $\ell_0 = 0.3$. The reward and cost of transmission are kept the same as above. Figure 4.2(a) depicts the optimal control and the optimal state with initial condi-

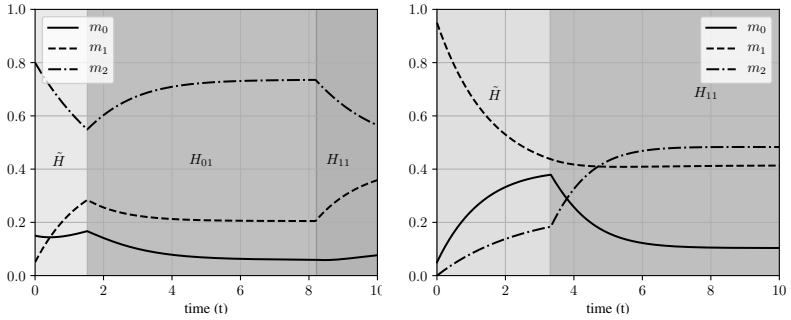

(a) $m_1(0) = 0.05, m_0(0) = 0.15$ (b) $m_1(0) = 0.95, m_0(0) = 0.05$

Figure 4.2: Transient analysis: Evaluation of the optimal controls and the according state trajectories as function of time t

tions $m_0(0) = 0.05$, $m_1(0) = 0.15$. In other words, we assume that the network already contains considerable VoI ($m_2(0) = 0.8$). It is easy to see that the optimal transmission policy changes two times that is, $(0,0) \to (0,1) \to (1,1)$. Note that, the rate of loss of information in this example is higher than the arrival rate of new information. Thus, in the first region, when there is no exchange of information, it is expected that the VoI in a node frequently degrades. As a result, the trajectory of m_2 is decreasing. However, once the network allows the exchange of information, the optimal trajectory depends on the trade-off between reward and cost of transmission. Figure 4.2(b) depicts the optimal control and the optimal state vector when the network already has many nodes with VoI $m_0(0) = 0.05$, $m_0(0) = 0.95$. In this case, the optimal control switches only once from $(0,0)$ to $(1,1)$.

Figure 4.3 depicts the optimal control as a function of the rate the information degrades (a) and as a function of the arrival rate of new VoI. For consistency, we retain all the parameter of Figure 4.1(b). We observe the optimal policy at a particular time instance $t = 6$. It is interesting to see in Figure 4.3(a) that the optimal control η_1^* switch from 0 to 1 as ℓ_0 increases. Thus, the system tries to compensate for the loss of information by increasing VoI through an exchange process. However, η_1^* again drops to zero if ℓ_0 is too high. There is a fixed cost associated with each transmission and the higher ℓ_0 means VoI degrades quickly. Thus, the possible gain of increasing VoI through exchange process no longer compensates the frequent transmission cost. In such cases, the optimal strategy throughout the finite time horizon is not to allow any transmissions. Figure 4.3(b) fixes the rate of loss of information $\ell_0 = 0.2$ and vary ℓ_1. The number of nodes in the network containing regular information increases with ℓ_1. Note that the optimal control η_1^* switches only once when rate ℓ_1 is above the certain value. We can further confirm from the Figure 4.1(b) that the optimal controls η_1^* and η_2^* are 1 at time $t = 6$ with rates $\ell_1 = 0.6$ and $\ell_0 = 0.2$.

Figure4.4 depicts more general behaviour of the optimal transmission policy

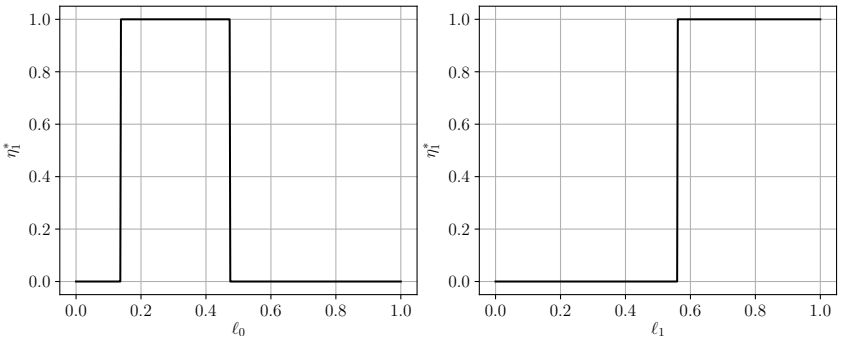

(a) The rate of loss of information (ℓ_0) (b) The rate of arrival of new VoI (ℓ_1)

Figure 4.3: Evaluation of optimal controls versus rate of loss of information and rate of arrival of new VoI respectively

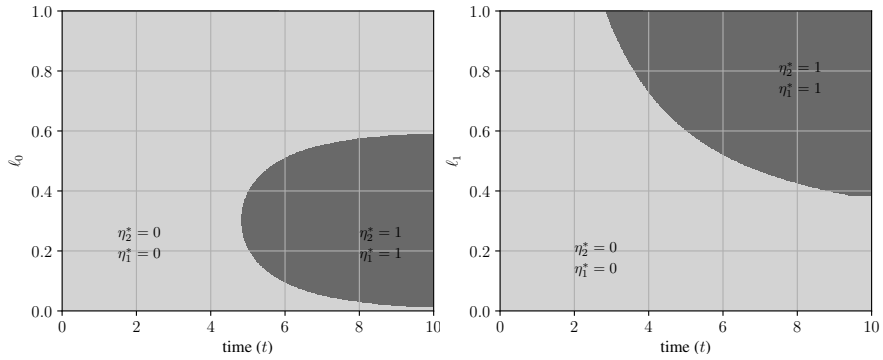

(a) (b)

Figure 4.4: Optimal transmission policy as a function of (a) rate of loss of information (ℓ_0) and (b) rate of arrival of new VoI versus time (ℓ_1)

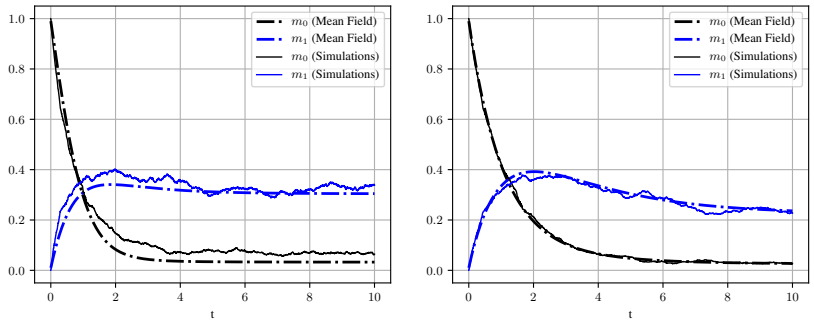

(a) $(\eta_0^*, \eta_1^*, \eta_2^*) = (0,1,1)$ (b) $(\eta_0^*, \eta_1^*, \eta_2^*) = (0,0,0)$

Figure 4.5: Comparison of mean-field limit and simulations

with respect to the different transition rates. Figure 4.4(a) shows the effect the degradation rate of the information has on the optimal transmission policy. The control switches from $(0,0)$ to $(1,1)$ at a time t that depends on the rate ℓ_0. The different shaded regions in the figures describe the respective optimal policies. A similar analysis for ℓ_1 is shown in fig.4.4(b).

Finally, we verify the mean-field approximation by means of stochastic simulation. To compare the result of simulations with the mean-field limits, we keep the parameters same as in Figure 4.1. The time for the simulation model is scaled appropriately with system size i.e., $1/N$. We further assume that the number of nodes in the network is $N = 1000$.

Figure 4.5 compares the trajectories of the state variables m_0 and m_1 of the mean-field approximation and as generated by stochastic simulation. We compare the trajectories for different transmission policies. Figure 4.5(a) depicts the result for optimal policy $(1,1)$ whereas Figure 4.5(b) shows the comparison when the network does not allow any exchange of information i.e., $(0,0)$. Initially, all the nodes in the network are assumed to have zero value of information. As time increases, the nodes get more information either from the environment or from the interaction with their neighbouring nodes. Thus, m_0 starts decreasing before stabilising at a different time according to different optimal policies as shown in the figure. Since the rate of loss of information is very low, it is expected that the network has more nodes containing regular or high importance information over time. It can be readily seen from both figures that the mean-field approximation gives an accurate approximation for the evolution of both m_0 and m_1.

4.3 Summary

We model a WSN with a large number of nodes by a mean-field approximation. We consider the quality of information by introducing VoI and show that it plays an important role in transmission decisions. Furthermore, we have studied the system with three levels of information in full detail and analyse its transient behaviour. The optimal transmission policy in such a network is of bang-bang type and also follows a threshold structure. Such policy is very easy to implement in practice for large WSNs. In the numerical section, we study the impact of different parameters on the optimal policy. Finally, we validate our mean-field approximation through stochastic simulations by comparing the performance of the simulated system to the mean-field limit.

5

Underwater wireless sensor networks

Underwater sensor networks are different from their terrestrial counterparts in many aspects, including size, cost, deployment and memory. Moreover, the slow propagation speed of signals in an underwater environment leads to challenging performance evaluation problems. In this chapter, we propose a stochastic model to evaluate the performance of the depth based routing protocol, which is a popular location-free routing protocol for underwater sensor networks. Compared to simulation studies of underwater sensor networks from literature, our performance evaluation study can calculate various important performance metrics faster and thereby offer considerable support during the design of such networks.

Over the last two decades, underwater applications like seabed management, sea-mine detection, environmental monitoring, etc. have motivated the adoption of Underwater Wireless Sensor Networks (UWSNs) as a communication infrastructure. As a consequence, many research effort has been devoted to study their performance and derive guidelines for their design. In contrast to most terrestrial wireless networks, UWSNs widely adopt acoustic communication as its intrinsic properties like low signal interference and large transmission coverage make it suitable for the underwater environment. Like their terrestrial counterparts, UWSNs adopt multi-hop routing protocols that aim at delivering the harvested data packets to on-surface sink nodes. The design of these routing protocols must account for the energy consumption of the network — battery replacement is considered unfeasible or prohibitively expensive — as well as for common performance indices like the expected end-to-end delay, the packet delivery probability and the network throughput.

Among routing protocols for UWSNs, an important role is played by localisation-free protocols [111]. These assume that nodes only know their depth (and potentially that of their neighbours) when taking routing decisions. Such protocols are mostly adopted for networks with high node mobility, channel fading etc. as they are capable of finding new routes for each transmission. While such protocols provide a high network resilience, this may come at the expense of con-

siderable energy consumption caused by redundant packet transmissions and the hidden terminal problem. Therefore, it is crucial that the parameters of the protocol are configured to balance the various performance indices. For a given cost, the optimal configuration achieves the best trade-off between energy consumption, mean end-to-end delay, throughput, delivery probability, etc.

One of the most widely used localisation-free routing protocols is Depth Based Routing (DBR) [112]. It uses the depth information of nodes to build a route from the source sensor node to the on-surface sink. The nodes estimate their depth by on-board pressure sensors and add this information to any packet they send out, so that all receivers can calculate the depth difference between themselves and the transmitter. DBR adopts a receiver-based forwarding scheme in which the potential forwarders are chosen on the basis of the depth difference between the sender and the receiver. In order to reduce redundant transmissions, DBR introduces the concept of a packet holding time, i.e., a time that a potential forwarder waits before sending the packet. The holding time is inversely proportional to the depth difference between sender and receiver. For a given transmission range, this mechanism enables the protocol to cover the longest distance towards the surface at each forwarding step, as receivers further away from the surface wait longer and then drop the packet if they overhear the communication of the nodes closer to the surface. The optimal configuration of DBR depends on a set of parameters, among which a pivotal importance is played by the choice of the transmission power and the holding time. Specifically, the transmission power determines the distance over which the packet can be received correctly, which in turn affects the number of hops needed to reach the sink, the overall energy consumption, the packet delivery probability and the end-to-end delay. In general, there is a trade-off between long and short distance transmissions, i.e., too many hops to the destination lead to high end-to-end delays while too few require a high transmission power that consumes the nodes' batteries too fast.

We study this trade-off by proposing and analysing a numerically tractable stochastic model that can capture the dynamics of DBR. We further show that one can efficiently calculate the main performance metrics including the mean end-to-end delay, the delivery probability and the expected energy consumption. In comparison to simulation, these performance measures can be calculated much faster, which in turn allows for speeding up the optimising procedure to find the optimal configuration of the UWSN. With respect to previous work that addresses the problem of assessing DBR performance, this is the first analytical model taking into account node deployment and mobility, as well as the intrinsic properties of acoustic transmissions including the path loss and the bit error rate. The model is validated by comparing its results with the estimates obtained by resorting to stochastic simulations.

The remainder of this chapter is organised as follows. In Section 5.1, we relate the contribution of this chapter to the literature by discussing related work. Section 5.2 then presents the stochastic model and the numerical algorithm to efficiently calculate the key performance measures of the model. We illustrate our approach by some numerical examples in Section 5.3, before summarising our findings in

Section 5.4.

5.1 Related work

In the last decade, the performance analysis of UWSNs and their optimisation and control have drawn the attention of many researchers (see, e.g., [113]), simulation rather than analytical models being the primary tool to study performance. In general, simulation models can be very accurate, however, obtaining performance metrics is often time consuming and their adoption for optimisation purposes can be very expensive. Among the analytical models, Guan et al. [114] examine the spatial and temporal uncertainty of the underwater acoustic channel and develop a statistical model that is used to propose a novel distributed MAC scheme with an optimised transmission strategy. Pignieri et al. [115] propose an analytic model for channels in underwater networks. In these papers, neither the computation of the mean end-to-end delay and energy consumption nor the impact of the routing protocols on the networks performance is considered.

The energy consumption is higher in UWSNs due to longer distances that need to be crossed and due to complex signal processing (see, e.g., [116, 117, 118] for some works that improve the energy consumption at the physical and MAC layers). Since the communication speed is equal to the speed of sound, the propagation delay is also much higher than the speed in the terrestrial networks. De Souze et al. [119] propose a model to analyse the energy consumption in multihop UWSNs. Some works study stochastic scheduling of data transmissions to deal with network latency while accounting for energy consumption. Among these, Marinakis et al. [120] formulate the channel access problem in terms of directed graphs and provide a heuristic to obtain the minimum latency. However, the acoustic absorption (as in Thorp's experimental formula [121]) and routing protocols in the computation of the transmission loss are abstracted out. Similarly, Li et al. [122] develop a new routing protocol based on a Markov model used to optimise the trade-off between the packet delivery probability and the energy consumption. While the authors provide an energy-aware routing path selection, the unreliability of the links and the impact of node mobility on data transmissions are ignored. The optimality of opportunistic protocols in UWSNs is considered in [123].

In UWSNs, full localisation schemes are difficult to implement since nodes consume considerable energy to access the localisation services. Yu et al. [124] propose a Weighting Depth and Forwarding Area Division DBR routing protocol that accounts for the depth difference of two hops: not only the depth difference of the current hop but also the depth difference of the next expected hop. It achieves an improved packet delivery ratio as it tackles the issue of coverage holes during transmission towards the sink. More recent work from Rehman et al. [125] proposes an energy efficient cooperative opportunistic routing protocol that improves the network lifetime by applying fuzzy logic for relay node selection towards the network sink. Chao et al. [126] minimise the expected number of transmissions for

successful delivery of a packet to the sink. In [127], the authors proposed a novel routing scheme called Channel Aware routing protocol (CARP) in which reliable communication between the hops is preferred on the basis of the transmission history of the nodes. Shadow zones in the network are also identified and network throughput is increased. Xie et al. [128] propose a Segmented data transport protocol (SDRT), which mainly employs block-by-block packet transmission. They combine FEC and ARQ to formulate their hybrid approach along with improving the channel utilisation. Some other works [129, 130] exploit extra capabilities of a node, e.g., the ability to move autonomously in order to minimise the energy consumption in the deployed sensor network.

5.2 DBR and its Stochastic Model

In this section, we present DBR and introduce a stochastic model to assess its performance. In contrast to previous work that relies on simulation, we provide an algorithm to efficiently calculate various performance indices, including the distribution of the number of hops it takes to send from a point other than the bottom of the network to a surface node, the level dependent energy consumption and the mean end-to-end delay. As the model accounts for the impact of node deployment and the high transmission loss of the acoustic channel, it can be used to understand the behaviour of DBR at the network level. We now describe the mechanism of DBR in detail.

5.2.1 Depth based routing

DBR [112] is a packet forwarding protocol for UWSNs that uses depth information to relay information from underwater sensors to data sinks at the surface. In DBR, every node has a pressure sensor that enables the node to estimate its depth, while the nodes are in general unaware of their exact 3D position.

The key determinant that decides which node will forward the information is the depth difference between the sender and the receiving node. More precisely, when a node transmits a packet, it includes its own depth information in the header. Among the (possible multiple) nodes that correctly receive the packet, the next forwarder is decided by two mechanisms. First, a *depth threshold* is installed. This is the minimum depth difference that allows a receiver node to become an eligible forwarder. Secondly, with the aim of maximising the distance covered by one hop, a depth-difference dependent *holding time* is introduced. That is, every packet to be forwarded is kept at the receiver node for a time interval that decreases linearly with the depth difference between the sender (as indicated in the packet header) and itself. In this way, nodes closer to the surface have shorter holding times and actually forward the packet if they correctly receive the packet. Once a node overhears a re-transmission of a packet that is stored in its *priority queue*, it removes this packet and cancels its holding time in order to prevent redundant transmissions.

Notation	Definition
U	Total number of deployed nodes in the network
L	Total number of depth levels in the network for a node
Δ_d	Total depth of the network
Δ_w	Total width of the network
M	Number of horizontal positions on a particular level for a node
S	Horizontal position of the source node at the bottom level of the network
T	Horizontal position of the sink node at the top level of the network
(i,j)	Location of a node with position j at level i in the network
b_j	Probability that the node occupies position j at a particular level in the network
$d_{ij}^{i'j'}$	Euclidean distance between nodes at locations (i,j) and (i',j')
T_r	Transmission Range of a node
N^{ij}	Set of nodes within the transmission range of node at (i,j)
$p_m(d)$	Probability that the packet is successfully delivered over distance d
$P_{ij}^{i'j'}$	Acceptance probability of a packet from location (i,j) to (i',j')
$h_k(i,j)$	Probability that packet is accepted at (i,j) in k-hops
$D_P(i,j;i',j')$	Propagation delay when the packet is sent from (i,j) to (i',j')
$D_H(i,j;i',j')$	Holding time when the packet is sent from (i,j) to (i',j')
w_{ij}^k	Mean delay of k-hop communication to reach (i,j)
$c_{ij}^k(i',j')$	Mean energy consumption at position (i',j') from (i,j) in k-hop communication

Table 5.1: List of Notations used in the model

In accordance with [112], the holding time D_H for a certain depth difference d can be expressed as follows,

$$D_H(d) = \left(\frac{2\tau}{\delta}\right)(T_r - d),$$

where T_r is the maximal transmission range of a node, τ is the maximum propagation delay of one hop, i.e., $\tau = T_r/v_0$ where v_0 denotes the sound propagation speed in water, and δ is a scaling factor that is chosen in order to achieve optimal performance of the network and to minimise the hidden terminal problem. We choose $\delta = T_r/4$ in the remainder in accordance with literature [112].

5.2.2 Node location model

For the sake of readability, we present a model for DBR in a two-dimensional environment. The extension to 3 dimensions is straightforward and summarised in

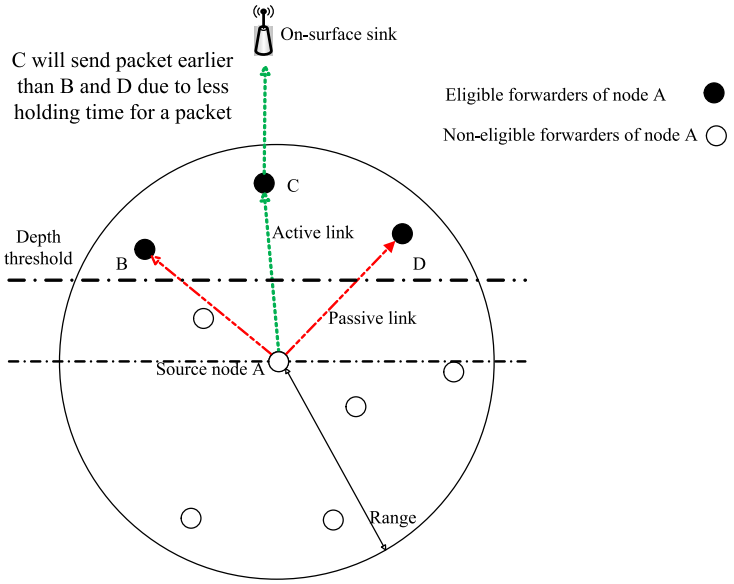

Figure 5.1: Methodology of DBR

Section 5.2.7.

We consider an UWSN with U nodes. The target or sink node is located at the surface level whereas the source node is located at the bottom. While assuming fixed positions for source and sink, we allow for movement of the nodes that relay the information. In particular, we divide the total depth difference Δ_D between source and sink into $L+1$ depth levels, level 0 being the level of the source and level L being the level of the sink. One node is present at each depth level, we have $U = L+1$, which randomly moves in the horizontal direction. Figure 5.1 demonstrates the methodology for DBR.

The nodes can move, but remain at a fixed depth level. To simplify the analysis, we divide the range Δ_W in which the nodes move horizontally into M slots with the same length, and assume that the node is always located at one of the $M+1$ slot boundaries (which we label from 0 to M). The horizontal position of the node at each level is assumed to be an independent random variable. Let b_j denote the probability that the node is in horizontal position j. We here assume that the distribution of the horizontal position of the node is independent of the level ($j \in \{0,1,\ldots,M\}$). In the remainder, the notation "node (i,j)" refers to the node at level i and horizontal position j. For ease of reference, we enlist the major notations of the model in Table 5.1.

5.2.3 Delivery probability of a node

We consider the underwater acoustic channel that is described in [131]. The path loss $A(d,f)$ of the acoustic channel over a Euclidean distance d for a signal having frequency f can be expressed as,

$$A(d,f) = d^s a(f)^d .$$

The path loss $A(d,f)$ is expressed in decibels referenced to 1 micro-Pascal (dB re 1 μPa) where d is expressed in km and f in kHz [132]. The spreading factor s describes the geometry of the propagation; a spreading factor $s = 2$ corresponds to spherical spreading while a spreading factor $s = 1$ corresponds to cylindrical spreading. Finally, the absorption coefficient $a(f)$ depends on the frequency and is expressed in dB/km using Thorp's experimental formula, see [121].

We can then express the average Signal-to-Noise ratio (SNR) over the distance d in terms of the path loss,

$$\Gamma(d) = \frac{e_b}{N_0 A(d,f)} = \frac{e_b}{N_0 d^s a(f)^d} .$$

Here, e_b and N_0 are constants that represent the average transmission energy per bit and noise power density of the additive white Gaussian noise channel. We assume binary phase shift keying modulation which is widely used in acoustic modems [133]. In accordance with [134], the bit error probability over distance d can then be expressed as,

$$q_e(d) = \frac{1}{2}\left(1 - \sqrt{\frac{\Gamma(d)}{1+\Gamma(d)}}\right) .$$

For a data packet with m bits, the probability that the packet is successfully delivered over a distance d therefore equals,

$$p_m(d) = (1 - q_e(d))^m .$$

For ease of notation, we introduce notation for the Euclidean distance between nodes. Let $d_{ij}^{i'j'}$ represent the distance between nodes (i,j) and (i',j'),

$$d_{ij}^{i'j'} = \sqrt{\left(\frac{\Delta_D}{L}\right)^2 (i-i')^2 + \left(\frac{\Delta_W}{M}\right)^2 (j-j')^2} .$$

In addition, let $N^{ij} = \{(i',j') : d_{ij}^{i'j'} \leq T_r\}$ be the set of nodes within transmission range of node (i,j).

In DBR, a packet is accepted by a node at position (i',j') if (i) node (i',j') is in the transmission range of the sender node (i,j), (ii) node (i',j') successfully receives the packet and (iii) all the nodes located in N^{ij} that are above (i',j') do not

accept the packet. Let $P_{ij}^{i'j'}$ denote the probability that a data packet is successfully received at (i', j') when sent from (i, j), we then have,

$$P_{ij}^{i'j'} = b_{j'}\, p_m \left(d_{ij}^{i'j'}\right) \prod_{\ell=i'+1}^{L} \left(1 - Q(\ell; i, j)\right),$$

for $(i', j') \in N^{ij}$ and where $Q(\ell; i, j)$ is the probability that the packet is successfully delivered at level ℓ,

$$Q(\ell; i, j) = \sum_{k=0}^{M} b_k\, p_m \left(d_{ij}^{\ell k}\right) 1_{\{(\ell,k)\in N^{ij}\}}.$$

Here $1_{\{\cdot\}}$ denotes the indicator function which equals 1 if its argument is true, and 0 if its argument is false. In other words, the sum above only includes nodes within the transmission range of the node at position (i, j).

5.2.4 Analysis of k-hop communication

We now focus on the number of hops needed for the data to be successfully delivered from source to sink. We first calculate the probability that any node in the network accepts the data packet from the source in one hop. Clearly nodes situated at an immediate upper level of the source will have zero probability to receive the data in one or more hops, as only direct communication is possible. Let S be the horizontal position of the source at the bottom level and T be the horizontal position of the sink at the surface level of the network. Let $h_k(i, j)$ represent the probability that the data is accepted by node (i, j) in k hops. The one-hop probability can be written as,

$$h_1(i, j) = \sum_{i'=1}^{i-1} \sum_{j'=1}^{M} P_{i'j'}^{ij}\, P_{0S}^{i'j'}.$$

Note that the terms in the sum are only non-zero for $(i', j') \in N^{0S} \cup N^{ij}$.

Similarly, the delivery probability in two hops can be written as:

$$h_2(i, j) = \sum_{i'=1}^{i-1} \sum_{j'=1}^{M} P_{i'j'}^{ij}\, h_1(i', j'),$$

while the delivery probability of k hop communication can be written by induction as,

$$h_k(i, j) = \sum_{i'=1}^{i-1} \sum_{j'=1}^{M} P_{i'j'}^{ij}\, h_{k-1}(i', j').$$

Given the values $h_k(i, j)$, we can now easily express the delivery probability at the sink. Indeed, the packet reaches the sink if it is delivered in any number of hops,

$$\bar{h} = \sum_{k=0}^{L} h_k(L, T).$$

For these calculations as well as for the delay and energy consumption calculations below, we implicitly make the simplifying assumption that the position of the nodes at the different levels is independent from hop to hop. This is indeed an approximation: the acceptance at a certain level depends on the position of the nodes at higher levels, as it is more probable to accept at a level if nodes at higher levels are at a larger horizontal distance from the transmitter. While we retain the position of the node that accepted the packet, we resample the positions of the nodes at higher levels. We will verify by simulation that this simplification does not void our results in Section 5.3.

5.2.5 Computation of the mean end-to-end delay

The propagation speed of the acoustic signal in water is $v_0 = 1500\,\mathrm{m/s}$ which is much lower than that of terrestrial radio-frequency based signals. Thus, the propagation delay is significant in UWSN and can have a considerable impact on the performance of the system. Apart from the propagation delay, we also need to account for the effect of holding times which depend on the depth difference between sending and receiving nodes. Let $D_P(i,j;i',j')$ and $D_H(i,j;i',j')$ denote the propagation and holding time delays when the packet is sent from (i,j) to (i',j'), then,

$$D_P(i,j;i',j') = \frac{d_{ij}^{i'j'}}{v_0},$$

and,

$$D_H(i,j;i',j') = \frac{2\tau}{\delta}\left(T_r - \frac{\Delta_D}{L}(i'-i)\right),$$

for $i' > i$ and $(i',j') \neq (L,T)$. Furthermore, $D_H(i,j;L,T) = 0$, as there is no holding time at the sink.

In order to find the mean delay, each possible path of the network needs to be explored. To this end, let $W_{i,j}$ denote the waiting time for a packet to reach (i,j) and let $H_{i,j}$ denote the number of hops it takes. We now calculate the mean delays w_{ij}^k, given that it takes k hops to reach (i,j),

$$w_{ij}^k = E\left[W_{i,j}1_{\{H_{i,j}=k\}}\right].$$

We again use a recursive scheme, similar to that for the delay calculations, for calculating the acceptance probability for the data packets in k hops. To start, we find the delay for one hop communication,

$$w_{ij}^1 = \sum_{i'=1}^{i-1}\sum_{j'=0}^{M}\Big(D_H(0,S;i',j') + D_P(0,S;i',j') + D_H(i',j';i,j) + D_P(i,j;i',j')\Big)P_{0S}^{i'j'}P_{i'j'}^{ij}.$$

To calculate w_{ij}^k for $k > 1$, we condition on the position of the last hop. That is, to reach (i, j) in k hops, we need to reach some (i', j') in $k-1$ hops, and then reach (i, j) by direct communication. The waiting time is then the sum of the waiting time to reach (i', j') and the transmission and holding times to reach (i, j) from (i', j'),

$$w_{ij}^k = \sum_{i'=1}^{i-1} \sum_{j'=0}^{M} \Big(w_{i'j'}^{k-1} + D_H(i', j'; i, j) h_{k-1}(i', j') + D_P(i', j'; i, j) h_{k-1}(i', j') \Big) P_{i'j'}^{ij} .$$

Finally, we can calculate the mean end-to-end waiting time, conditional on the packet reaching the sink, by summing over the number of hops that it takes to reach (L, T), and by dividing by the probability that the packet reaches the sink,

$$\bar{W} = \frac{1}{\bar{h}} \sum_{k=0}^{L} w_{LT}^k .$$

5.2.6 Energy consumption

In order to study the expected energy consumption in the network, we recursively calculate the energy consumption for all node positions in the network to transmit to a particular node in a fixed number of hops. More precisely, let $C_{ij}(i', j')$ denote the energy consumption in position (i', j') for transmitting from the source to node (i, j) and let $H_{i,j}$ denote the number of hops to transmit to node (i, j) as before, we then study the mean energy consumption given the number of hops,

$$c_{ij}^k(i', j') = E\left[C_{ij}(i', j') 1_{\{H_{i,j}=k\}} \right] .$$

Note that $c_{ij}^k(i', j') = 0$ for $i \leq i'$ since nodes above (i, j) cannot forward to (i, j).

To start with one hop communication, we have

$$c_{ij}^1(i', j') = \gamma P_{i'j'}^{ij} P_{0S}^{i'j'} .$$

Here γ denotes the amount of energy a single transmission takes. That is, $C_{ij}(i', j') = \gamma$ if the single forwarding hop is in position (i', j') and $C_{ij}(i', j') = 0$ if this is not the case.

We further calculate the values $c_{ij}^k(i', j')$ for $k > 0$ recursively. There is energy consumption at position (i', j') if it is reached in $k-1$ hops, followed by direct communication, or if (i', j') is part of a $(k-1)$-hop path to some intermediate node (above level i'), from which (i, j) is reached. We have,

$$c_{ij}^k(i', j') = \gamma h_k(i', j') P_{i'j'}^{ij} + \sum_{\ell=i'+1}^{i-1} \sum_{m=0}^{M} c_{\ell m}^{k-1}(i', j') P_{\ell m}^{ij} .$$

We can finally calculate the energy consumption at each level in the network, by summing over the number of hops to reach the destination, and by summing over the different positions at the same level,

$$c(i) = \sum_{k=0}^{L} \sum_{m=0}^{M} c_{LT}^{k}(i,m)\,.$$

5.2.7 Extension to 3 dimensions

We briefly discuss how the model can be extended to 3 dimensions (3D). We still consider an UWSN with $L+1$ nodes with sink at the surface and source at the bottom. While assuming fixed positions for source and sink, we allow for movement of the nodes that relay the information. In particular, we divide the total depth difference Δ_D between source and sink into $L+1$ depth levels, level 0 being the level of the source and level L being the level of the sink.

At each horizontal level, the node can be in M positions. As the horizontal level is a plane, there are e.g. M positions on a square grid, or M discrete positions evenly distributed on a disk. The distance calculations are the key difference between the 2D and 3D model. For ease of notation, we introduce a common coordinate system on all levels, and let $(x(j),y(j))$ denote the (horizontal) coordinates of position j. The distance between node j on level i and node j' on level i' can then be expressed as follows,

$$d_{ij}^{i'j'} = \sqrt{\left(\frac{\Delta_D}{L}\right)^2 (i-i')^2 + (x(j)-x(j'))^2 + (y(j)-y(j'))^2}\,.$$

Given this modification of the distance calculations, the remainder of the calculations remain valid. Note however that the summations in Sections 5.2.3 till 5.2.6 now run over all positions in a horizontal plane.

5.3 Numerical Results

In this section, we numerically study different performance measures of the model at hand. We assume that the total depth of the network is $\Delta_D = 500$m with $L = 50$ depth levels. Note that there is only one sensor node at each depth level meaning there are 50 nodes in the network. We keep the values of the numerical parameters in line with the values in [112]: we set $s = 2$, $v_0 = 1500\,\mathrm{m/s}$, $\delta = T_r/4$ and $\tau = T_r/v_0$. Finally, we assume data packets of 50 bytes. These parameter values are used in all plots.

5.3.1 Delivery probabilities

We first investigate the delivery probabilities for direct communication. The source is fixed at bottom level of the network at horizontal position S. We assume that

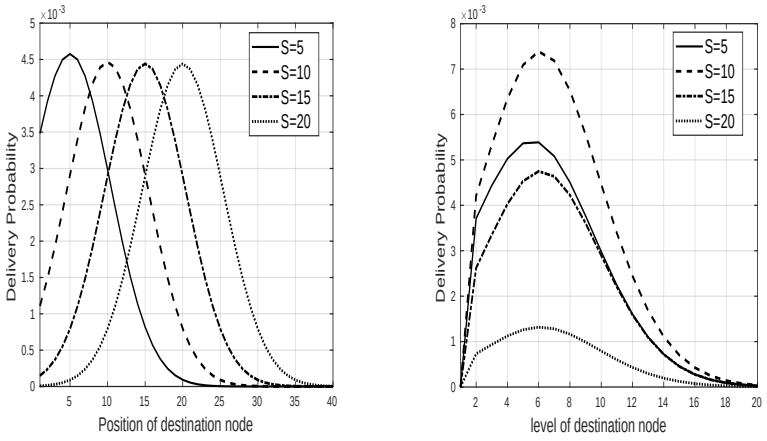

(a) (b)

Figure 5.2: Delivery probability for direct transmission from source to sink (a) for different horizontal positions of the destination and (b) for different levels of destination

each node can move horizontally to $M = 50$ locations over a range of $\Delta_W = 500$m, each horizontal position being equally likely. We further choose the transmission energy such that $e_b/N_0 = 57$dB, and assume that the transmission range is only bounded by transmission errors ($T_r = \infty$).

Figure 5.2(a) shows the delivery probability by a direct transmission from the source to a node at level 10 vs. the horizontal position of this node for different source positions S as indicated. As expected, the maximal delivery probability is obtained when source and destination are aligned, as this corresponds to the shortest distance between these nodes.

Figure 5.2(b) shows the same delivery probability, but we now fix the horizontal position of the destination node at 10 and vary its depth level. Again, different source positions S are assumed as indicated. There is an outspoken optimal depth level: at first the delivery probability is small as it is likely that the packet will be delivered to higher nodes. The delivery probability therefore first increases with the depth level. However, if the depth level is already high, the chance to successfully transmit is low. Hence, the delivery probability decreases with increasing depth levels.

For the remaining plots, we assume that the node can move into $M = 15$ slots spanning a range $\Delta_W = 150$m. We set the transmission range to one-fifth of the total range of the network i.e., $T_r = \Delta_D/5 = 100$m and fix the horizontal position of the source and sink: $S = T = 10$.

We now focus on the number of hops needed for the data to be delivered at the sink. Note that the number of hops cannot exceed the number of depth levels

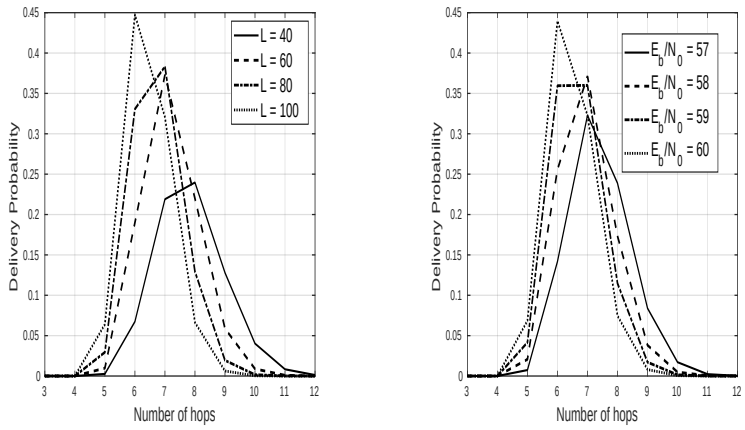

(a) (b)

Figure 5.3: Delivery probability (a) for different total number of depth levels and (b) for different e_b/N_0

as no downward transmissions are allowed in DBR. Figure 5.3(a) and Fig 5.3(b) depict the probability mass function of the number of hops needed to deliver the packet from source to sink. In 5.3(a), we depict the probability mass function for networks with different levels L. In 5.3(a), we depict the probability mass function for different transmission powers e_b/N_0.

From the figures, we can observe that the delivery probability is zero for the first 4 hops, which is not surprising as the transmission range is 100m. Moreover, most of the probability mass is between 5 and 9 hops, which is again in line with the transmission range. Finally, it is seen that end-to-end communication with fewer hops is more likely if there are more nodes (i.e., by increasing L, see Figure 5.3(a)), or if the transmission power increases (see Figure 5.3(b)).

5.3.2 Mean end-to-end delay

Figure 5.4 depicts the mean delay conditioned on the number of hops required for the data to reach the sink. Figure 5.4(a) fixes e_b/N_0 to 57dB and shows the mean delay for different numbers of depth levels L between the source and the sink. On the other hand Figure 5.4(b) fixes the number of depth levels to $L = 50$ and varies the transmission power as indicated. It is readily seen that the conditional end-to-end delay grows almost linearly with the number of hops, and is largely insensitive to changes in transmission power and the number of depth levels. This is not entirely unexpected as the end-to-end delay is largely dominated by the holding times at the nodes.

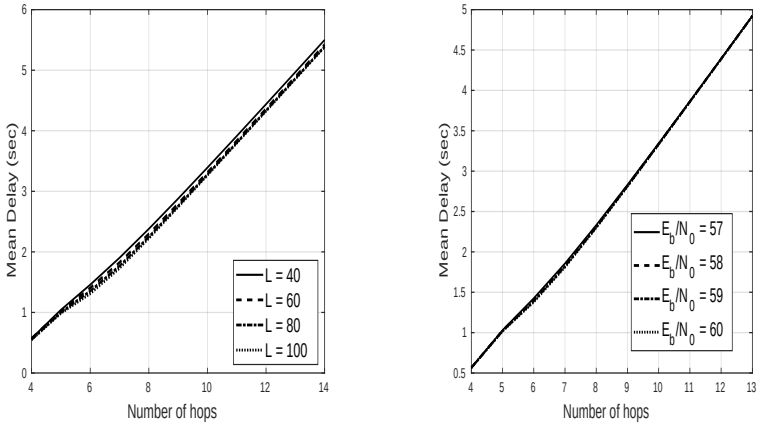

(a) (b)

Figure 5.4: Mean Delay (a) for different total number of depth levels and (b) for different e_b/N_0

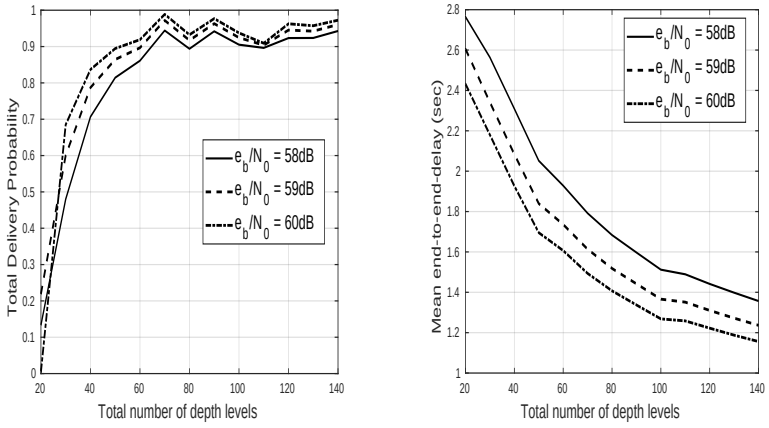

(a) (b)

Figure 5.5: Total delivery probability and mean end-to-end delay

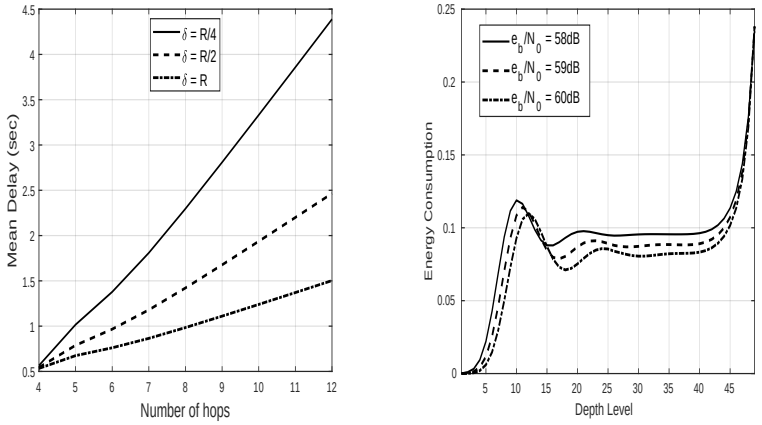

(a) (b)

Figure 5.6: Mean Delay and Energy consumption

In Figure 5.5, we depict the delivery probability at the sink and the corresponding mean end-to-end delay (conditional on the packet reaching the sink). We again set the total depth to $\Delta_D = 500$m and vary the number of depth levels. As we fix the total depth, increasing the number of levels means that the depth difference between adjacent levels decreases. Figure 5.5(a) depicts the delivery probability at the sink vs. the number of depth levels for different e_b/N_0 as indicated. It can be seen from the figure that the total delivery probability in general increases when the number of depth levels increases. This is expected as we add additional sensors, making it less likely that the packet is lost. The curve is not monotone increasing though, which can be explained by the interplay between the depth levels and the fixed transmission range T_r. Figure 5.5(b) shows that the mean end-to-end delay decreases when the total number of depth levels increases. Note that the total depth of the network is fixed. As the depth difference between adjacent levels decreases, it is expected that the mean end-to-end delay decreases as well. Moreover, while the delivery probability increases with e_b/N_0, it has the opposite effect on the mean end-to-end delay.

In Figure 5.6(a), we study the effect of the scaling parameter δ on the mean delay. The parameter δ is key for the holding times. Larger δ implies shorter holding times at each intermediate node and thus reduces the mean delay. Figure 5.6(a) depicts the mean end-to-end delay, conditional on the number of hops. As previously noted, the end-to-end delay grows approximately linearly with the number of hops. It can now clearly be seen that the slope of the conditional end-to-end delay depends on δ.

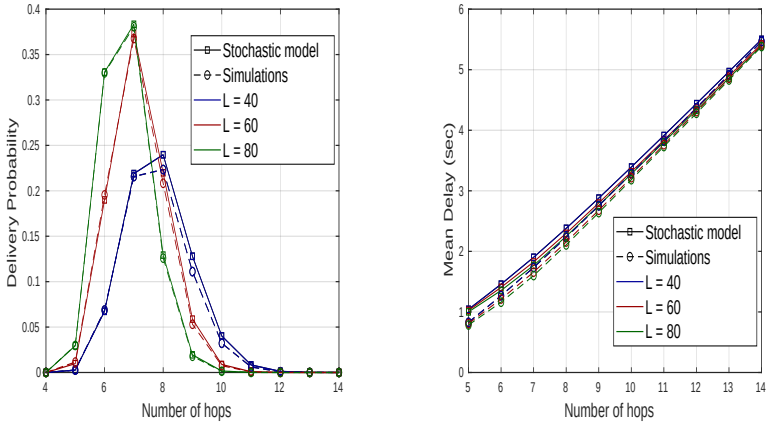

(a) (b)

Figure 5.7: Comparison of stochastic model and Monte-Carlo simulation for hops distribution and Mean delay

5.3.3 Energy consumption

Finally, Figure 5.6(b) depicts the energy consumption at the different depth levels of the network. We assume that the amount of energy for one transmission is $\gamma = 1$, so that the plot depicts the mean number of times the nodes at each level participate in the transmission. Ideally, one aims for uniform energy expenditure so that the life time of all nodes is approximately equal. It is however clear from the figure that the energy consumption at levels close to both source and sink is higher, compared to the energy consumption by nodes in the middle of the network. This suggests that it is beneficial to increase the density of the nodes near sink and source.

5.3.4 Model validation by simulation

We now evaluate the performance of the model through simulations and compare its time complexity with the stochastic model.

Recall that the analytical model made the following simplifying assumption. The position of the nodes above a transmitting node, is assumed independent of their positions during preceding transmissions. In reality, these positions may largely remain the same, and therefore we need to verify that this assumption does not compromise the accuracy of our results. To this end, we compare our results with results obtained by Monte Carlo simulation, where it is assumed that the positions of the nodes do not change throughout the multi-hop transmission of the packet.

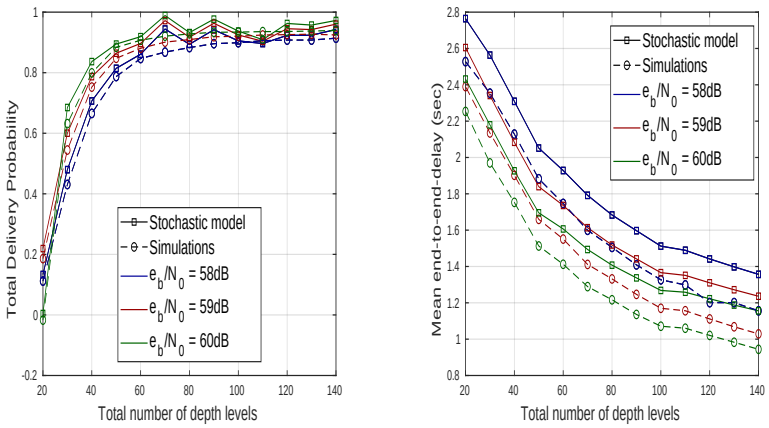

(a) (b)

Figure 5.8: Comparison of stochastic model and Monte-Carlo simulation for Total delivery probability and Mean end-to-end delay

In particular, the details of the simulation study are as follows. We consider K replications of a multi-hop transmission from source to sink. For each replication, we first randomly draw the positions of the nodes at all levels. We then calculate the performance measures using the analytical model of Section 4, for the given fixed node positions. As the positions of the nodes are fixed, the calculations of Section 4 are exact. Each replication yielding values for the various performance measures, we finally calculate the sample averages, and corresponding confidence intervals for these performance measures.

Analytic and simulation results are numerically compared in Figs. 5.7 and 5.8. We keep the same size of the network: a depth of 500 m and a width of 150 m. The number of available positions that a node can take at a particular depth level are fixed to $M = 15$ in accordance with the stochastic model. We sample $K = 1000$ times, which is sufficient to obtain a confidence 95% confidence interval of $\pm 0.5\%$ the sample mean. Although the source and sink can be randomly located at bottom and surface level of the network respectively, we place them both at a position 10 for consistency in the experiment. All the other network parameters are similar to those in the stochastic model.

Figure 5.7(a) depicts the comparison of the number of hops distribution where Figure 5.7(b) shows the comparison of the mean delay for different number of deployed nodes in the network. Furthermore, Figure 5.8(a) depicts the total delivery probability and Figure 5.8(b) shows the mean end-to-end delay for both models. It can be seen from the figure that the difference between the results obtained by simulation and analytically is negligible.

To compare the efficiency of the analytical model and the simulation model, we compare their time complexity. For the stochastic model, most of the time is spent on the calculation of the delivery probability and hops distributions. In the worst case scenario, the time complexity of the stochastic model is $O(L^3M^2)$, where L is the number of depth levels in the network and M is the number of positions that a node can take horizontally. For the simulation study, we only sample the positions of the nodes, and then calculate the performance measures by the analytic approach to reduce the variance of the Monte-Carlo simulation. This technique is referred to as variance reduction by conditioning, see e.g. [135]. Hence, the time complexity of a single iteration is $O(L^3)$, which corresponds to the complexity of the stochastic model with $M = 1$ (as the nodes are at a fixed position in each iteration). For moderate M, the number of samples K that are needed in the Monte Carlo simulations considerably exceeds M^2, which implies that the stochastic model can calculate the various performance measures faster, even after applying the variance reduction technique (which also relies on the model).

5.4 Summary

We propose a numerically tractable stochastic model for the performance evaluation of DBR. In particular, we consider four performance metrics: the hop-distribution, the packet delivery probability, the expected energy consumption and the expected end-to-end delay. The model is validated by comparing the average performance indices obtained by its analysis with the estimates obtained by a stochastic simulation. By a numerical example, we illustrate that our model can be used to assess the impact of various network configuration parameters (e.g., the transmission power and the scaling factor δ defined by DBR) on these indices. Our analysis showed that the number of hops in the route can dramatically affect the performance of the protocol. The proposed model can be further used for optimisation purposes given the limited computational effort required, in comparison to underwater sensor network simulations.

6

Conclusion

In this dissertation, we investigated the performance of wireless sensor networks through various stochastic models. In order to formulate stochastic models, we first identified the most important processes that determine the performance of the WSN and properly quantified the uncertainties in these processes. We solve these models by adapting probabilistic techniques and gain important insights into the design and performance of the network. In certain instances, we exploited the special structure of some processes in order to obtain a solution more quickly. Such theoretical analyses often lead to interesting properties of the optimal solution. To conclude this dissertation, we now summarise our contributions below.

Chapter 2 contains a basic model for a sensor node in isolation, followed by a series of extensions and refinements, which relaxed some of the initial assumptions on the sensing and energy harvesting processes. The value of information (VoI) for all the models in that chapter were additive in nature. We provided recursive equations for the battery and VoI dynamics in a sensor node. The set of recursions allowed us to determine the first two moments of the value of information that is collected by a mobile sink. We showed that there exists a stationary ergodic process representing the battery and VoI. Moreover, we also proved the convergence of the battery and VoI processes, irrespective of the initial conditions. We closed the discussion on the basic model by providing an extensive numerical study in order to understand the behaviour of the collected VoI with respect to different system parameters. The immediate extension of the model was inspired by the assumption of energy utilisation for sensing the information. We extended the assumptions of the basic model by allowing that the node ability is aware of the presence or absence of information and compared the results with the previous model. We also extended this model by incorporating time correlation in the energy harvesting process. This is achieved by formulating the harvesting process as N-state Markov modulated process. We provided the equations for different performance measure of the generalised model and numerically analysed the network for the interrupted Poisson process which is nothing but a two-state Markov modulated process. We clearly observed that correlation has a considerable impact on the performance of the node. In particular, we observed that longer active and

inactive periods of energy harvesting adversely affects the mean value of information collected by the mobile sink. Also, if the harvesting process is bursty, i.e., harvesting is concentrated in a few time slots followed by a large number of inactive slots, then the mobile sink collects less VoI. In all these models, we allowed for temporal unavailability of the mobile sink by introducing a transmission opportunity process, i.e., the sink is in range of the sensor node in particular time slot with a fixed probability. The numerical study depicts that the mean VoI is a concave function of this transmission opportunity. This is a very strong insight from the perspective of a network designer. It can be used to find the optimal trajectory of the mobile sink maximising the sum of the values of information collected by the sink.

Chapters 3 and 4 then investigated how to optimally control WSNs. In contrast to Chapter 2, we assumed that the VoI process is a combination of an information loss process and an information replacement process. In particular, information gets replaced if newly sensed information has a higher VoI than the current information and it decreases by one unit if no new information arrives. This is a popular assumption when the age of information is more important than its amount. Chapter 3 presented a stochastic recursion for a sensor node in isolation. We formulated the performance problem within the framework of discrete-time infinite-horizon Markov decision processes, and solved it by a standard policy iteration algorithm. We however exploited the special quasi-birth-death structure of the transition matrix of the Markov decision process to facilitate its solution. The numerical results showed that the optimal transmission policy is a threshold policy in terms of both the battery level and the VoI, which is highly sensitive to the battery level.

In general, WSNs contain a large number of interacting nodes, each node being in some state, such that the states of all nodes combined make up the state space of a Markov chain. We considered interaction among nodes in Chapter 4. The sensor nodes in the network can obtain a new value, either directly from the environment or from interaction with other nodes in the network which hold a higher VoI. The exchange of information through interaction causes considerable energy expenditure from the nodes. Solving such a network becomes practically impossible due to the curse of dimensionality. We therefore formulated the mean-field limit of the Markov model at hand which, heavily reduced the computational effort needed to obtain the optimal control of the network. In the mean-field limit, the optimisation problem was reduced to a continuous-time deterministic optimal control problem. We proved the convergence of the mean-field model theoretically and obtained the optimal transmission policy by solving Hamiltonian-Jacobi-Bellman equations. We also provided a detailed analysis on the structure of optimal policy as well as some numerical results.

Lastly, we considered underwater wireless sensor networks in Chapter 5. In particular, we addressed the performance evaluation of multi-hop underwater communication by developing a stochastic model for the depth-based routing protocol in UWSNs. We mainly calculated three performance measures: the number-of-hops distribution, the mean end-to-end delay and the energy consumption in the network. The numerical analysis of these performance indices exhibited powerful

insights on node deployment under water. For example, the energy consumption near the sink is higher meaning more nodes should be deployed closer to sink. We also validated our results through stochastic simulations.

Finally, we mention some possible future research directions. While the models in Chapter 2 considered a sensor node in isolation, we already mentioned that these could be used to evaluate mobile sink routing. Given a certain path, the mobile sink will be in range for some part of the trajectory and out of range for the remainder of the path. For the models in Chapter 2, sink availability was assumed independent from slot to slot. This assumption may already offer a good approximation for the amount of information that can be collected by the mobile sink. The model can however also be refined to capture the sink availability process more accurately. The mean-field limit of Chapter 4 studies the VoI information process in a WSN without energy harvesting. The methodology may also extend to EH-WSN. Then the state of each node not only includes the VoI, but also the battery state, and communication is not possible if there is no energy.

Bibliography

[1] X. Ren, W. Liang, W. Xu, Data collection maximization in renewable sensor networks via time-slot scheduling, IEEE Transactions on Computers 64 (7) (2015) 1870–1883.

[2] L. Atzori, A. Iera, G. Morabito, The internet of things: a survey, Computer Networks 54 (15) (2010) 2787–2805.

[3] J. Gubbi, R. Buyya, S. Marusic, M. Palaniswami, Internet of things (iot): a vision, architectural elements, and future directions, Future generation computer systems 29 (2013) 1645–1660.

[4] H. M. Ammari, N. Gomes, M. Jacques, B. Maxim, D. Yoon, A survey of sensor network applications and architectural components, Adhoc & Sensor Wireless Networks 25 (1–2) (2015) 1–44.

[5] H. Sundmaeker, P. Guillemin, P. Friess, S. Woelfflé, Vision and challenges for realising the internet of things, European commission, 2010.

[6] S. Sudevalayam, P. Kulkarni, Energy harvesting sensor nodes: Survey and implications, IEEE Communications Surveys and Tutorials 13 (3) (2011) 443–461.

[7] G. J. Pottie, W. J. Kaiser, Wireless integrated network sensors, Communications of the ACM 43 (5) (2000) 51–58.

[8] M. A. Razzaque, S. Dobson, Energy-Efficient Sensing in Wireless Sensor Networks Using Compressed Sensing, Sensors 14 (2) (2014) 2822–2859.

[9] J. Polastre, J. Hill, D. Culler, Versatile low power media access for wireless sensor networks, in: Proceedings of the 2nd international conference on Embedded networked sensor systems, ACM, 2004, pp. 95–107.

[10] W. R. Heinzelman, A. Chandrakasan, H. Balakrishnan, Energy-efficient communication protocol for wireless microsensor networks, in: Proceedings of the 33rd annual Hawaii international conference on system sciences, Vol. 00, 2000, pp. 3005–3014.

[11] G. Anastasi, M. Conti, M. Di Francesco, A. Passarella, M. D. Francesco, A. Passarella, Energy conservation in wireless sensor networks: A survey, Ad Hoc Networks 7 (3) (2009) 537–568.

[12] X. Wang, G. Xing, Y. Zhang, C. Lu, R. Pless, C. Gill, Integrated coverage and connectivity configuration in wireless sensor networks, in: Proceedings of the 1st international conference on Embedded networked sensor systems, ACM, 2003, pp. 28–39.

[13] S. Ganeriwal, I. Tsigkogiannis, H. Shim, V. Tsiatsis, M. B. Srivastava, D. Ganesan, Estimating clock uncertainty for efficient duty-cycling in sensor networks, IEEE/ACM Transactions on Networking 17 (3) (2009) 843–856.

[14] J. A. Paradiso, T. Starner, Energy scavenging for mobile and wireless electronics, IEEE Pervasive Computing 4 (1) (2005) 18–27.

[15] F. K. Shaikh, S. Zeadally, Energy harvesting in wireless sensor networks: A comprehensive review, Renewable & Sustainable Energy Reviews 55 (2016) 1041–1054.

[16] V. Sachidananda, A. Khelil, N. Suri, Quality of information in wireless sensor networks: A survey, ICIQ (to Appear.

[17] C. Bisdikian, L. M. Kaplan, M. B. Srivastava, On the quality and value of information in sensor networks, ACM Transactions on Sensor Networks 9 (4) (2013) 48.

[18] E. C.-H. Ngai, P. Gunningberg, Quality-of-information-aware data collection for mobile sensor networks, Pervasive and Mobile Computing 11 (2014) 203–215.

[19] M. reza Akhondi, A. Talevski, S. Carlsen, S. Petersen, Applications of wireless sensor networks in the oil, gas and resources industries, in: 2010 24th IEEE International Conference on Advanced Information Networking and Applications, IEEE, 2010, pp. 941–948.

[20] M. S. Al-Fares, Z. Sun, Self-organizing routing protocol to achieve QoS in wireless sensor network for forest fire monitoring, in: 2009 IEEE 9th Malaysia International Conference on Communications (MICC), 2009, pp. 211–216.

[21] M. V. Ramesh, N. Vasudevan, J. Freeman, Real time landslide monitoring via wireless sensor network, in: EGU General Assembly Conference Abstracts, Vol. 11, 2009, p. 14061.

[22] S. Verma, N. Chug, D. V. Gadre, Wireless sensor network for crop field monitoring, in: 2010 International Conference on Recent Trends in Information, Telecommunication and Computing, IEEE, 2010, pp. 207–211.

[23] M. Hefeeda, H. Ahmadi, A probabilistic coverage protocol for wireless sensor networks, in: 2007 IEEE International Conference on Network Protocols, IEEE, 2007, pp. 41–50.

[24] H. Zhang, J. C. Hou, Maintaining sensing coverage and connectivity in large sensor networks, Ad Hoc and Sensor Wireless Networks 1 (1-2) (2005) 89–124.

[25] G. Tolle, J. Polastre, R. Szewczyk, D. Culler, N. Turner, K. Tu, S. Burgess, T. Dawson, P. Buonadonna, D. Gay, et al., A macroscope in the redwoods, in: Proceedings of the 3rd international conference on Embedded networked sensor systems, ACM, 2005, pp. 51–63.

[26] S. Akoush, A. Sameh, Mobile user movement prediction using Bayesian learning for neural networks, in: Proceedings of the 2007 international conference on Wireless communications and mobile computing, ACM, 2007, pp. 191–196.

[27] R. Serfozo, Basics of applied stochastic processes, Springer Science & Business Media, 2009.

[28] S. M. Ross, Introduction to probability models, Academic press, 2014.

[29] M. L.Puterman, Markov Decision Processes: Discrete Stochastic Dynamic Programming, John Wiley & Sons, 2014.

[30] F. Baccelli, F. I. Karpelevich, M. Y. Kelbert, A. A. Puhalskii, A. N. Rybko, Y. M. Suhov, A mean-field limit for a class of queueing networks, Journal of Statistical Physics 66 (3-4) (1992) 803–825.

[31] K. Patil, D. Fiems, The value of information in energy harvesting sensor networks, Operations Research Letters 46 (3) (2018) –.

[32] K. Patil, K. De Turck, D. Fiems, Optimal data collection in wireless sensor networks with correlated energy harvesting, Annals of Telecommunication (2018) 1–12.

[33] K. Patil, K. De Turck, D. Fiems, Optimal data collection in hybrid energy-harvesting sensor networks, in: International Conference on Analytical and Stochastic Modeling Techniques and Applications, Springer, 2016, pp. 239–252.

[34] K. Patil, K. De Turck, D. Fiems, A two-queue model for optimising the value of information in energy-harvesting sensor networks, Performance Evaluation 119 (2018) 27–42.

[35] K. Patil, M. Jafri, D. Fiems, A. Marin, Stochastic modeling of depth based routing in underwater sensor networks, Ad Hoc Networks 89.

[36] Z. Zhou, C. Du, L. Shu, G. Hancke, J. Niu, H. Ning, An Energy-Balanced Heuristic for Mobile Sink Scheduling in Hybrid WSNs, IEEE Transactions on Industrial Informatics 12 (1) (2016) 28–40.

[37] Y. Bi, J. Niu, L. Sun, W. Huangfu, Y. Sun, Moving schemes for mobile sinks in wireless sensor networks, in: 2007 IEEE International Performance, Computing, and Communications Conference, 2007, pp. 101–108.

[38] C. Tunca, S. Isik, M. Y. Donmez, C. Ersoy, Distributed mobile sink routing for wireless sensor networks: A survey, IEEE Communications Surveys and Tutorials 16 (2) (2014) 877–897.

[39] B. Nazir, H. Hasbullah, Mobile sink based routing protocol (msrp) for prolonging network lifetime in clustered wireless sensor network, in: 2010 International Conference on Computer Applications and Industrial Electronics, IEEE, 2010, pp. 624–629.

[40] Y. Gu, Y. Ji, J. Li, B. Zhao, Eswc: Efficient scheduling for the mobile sink in wireless sensor networks with delay constraint, IEEE Transactions on Parallel & Distributed Systems 24 (7) (2013) 1310–1320.

[41] S.-C. Huang, H.-Y. Chang, A farmland multimedia data collection method using mobile sink for wireless sensor networks, Multimedia Tools and Applications 76 (19) (2017) 19463–19478.

[42] Y. Yang, Y. Miao, A path planning method for mobile sink in farmland wireless sensor network, in: 2017 IEEE 2nd Information Technology, Networking, Electronic and Automation Control Conference (ITNEC), IEEE, 2017, pp. 1157–1160.

[43] M. Taherian, M. Maeen, M. Haghparast, Promoting the Quality Level of Signaling in Railway Transportation System Taking Advantage from Wireless Sensor Networks Technology, Computers 6 (3).

[44] J. Lei, R. Yates, L. Greenstein, A generic model for optimizing single-hop transmission policy of replenishable sensors, IEEE Transactions on Wireless Communications 8 (2) (2009) 547–551.

[45] A. Seyedi, B. Sikdar, Energy efficient transmission strategies for Body Sensor Networks with energy harvesting, The 42nd Annual Conference on Information Sciences and Systems 58 (7) (2008) 2116–2126.

[46] N. Michelusi, K. Stamatiou, M. Zorzi, Transmission policies for energy harvesting sensors with time-correlated energy supply, IEEE Transactions on Communications 61 (7) (2013) 2988–3001.

[47] P. Lee, Z. A. Eu, M. Han, H.-P. Tan, Empirical modeling of a solar-powered energy harvesting wireless sensor node for time-slotted operation, in: 2011 International Wireless Communications and Mobile Computing Conference, IEEE, 2011, pp. 179–184.

[48] C. K. Ho, P. D. Khoa, P. C. Ming, Markovian models for harvested energy in wireless communications, Proc. IEEE ICCS (2010) 311–315.

[49] M. Y. Naderi, S. Basagni, K. R. Chowdhury, Modeling the residual energy and lifetime of energy harvesting sensor nodes, in: 2012 IEEE Global Communications Conference (GLOBECOM), IEEE, 2012, pp. 3394–3400.

[50] E. De Cuypere, K. De Turck, D. Fiems, Stochastic modelling of energy harvesting for low power sensor nodes, in: 7th International Conference on Queueing Theory Network Application Proceeding, 2012, pp. 1–6.

[51] E. De Cuypere, K. De Turck, D. Fiems, A queueing model of an energy harvesting sensor node with data buffering, Telecommunication Systems 67 (2) (2018) 281–295.

[52] E. Gelenbe, Y. M. Kadioglu, Energy loss through standby and leakage in energy harvesting wireless sensors, in: 2015 IEEE 20th International Workshop on Computer Aided Modelling and Design of Communication Links and Networks (CAMAD), 2015, pp. 231–236.

[53] E. Gelenbe, A Sensor Node with Energy Harvesting, ACM SIGMETRICS Performance Evaluation Review 42 (2) (2014) 37–39.

[54] L. Tan, S. Tang, Energy harvesting wireless sensor node with temporal death: Novel models and analyses, IEEE/ACM Transactions on Networking 25 (2) (2017) 896–909.

[55] I. Dimitriou, S. Alouf, A. Jean-Marie, A Markovian queueing system for modeling a smart green base station, in: European Workshop on Performance Engineering, Springer, 2015, pp. 3–18.

[56] M. Abu Alsheikh, D. T. Hoang, D. Niyato, H.-P. Tan, S. Lin, Markov Decision Processes With Applications in Wireless Sensor Networks: A Survey, IEEE Communications Surveys and Tutorials 17 (3) (2015) 1239–1267.

[57] V. S. Rao, R. V. Prasad, I. G. Niemegeers, Optimal task scheduling policy in energy harvesting wireless sensor networks, in: 2015 IEEE Wireless Communications and Networking Conference (WCNC), IEEE, 2015, pp. 1030–1035.

[58] L. Lei, Y. Kuang, X. S. Shen, K. Yang, J. Qiao, Z. Zhong, Optimal Reliability in Energy Harvesting Industrial Wireless Sensor Networks, IEEE Transactions on Wireless Communications 15 (8) (2016) 5399–5413.

[59] D. Zordan, T. Melodia, M. Rossi, On the Design of Temporal Compression Strategies for Energy Harvesting Sensor Networks, IEEE Transactions on Wireless Communication. 15 (2) (2016) 1336–1352.

[60] M. Mitici, J. Goseling, M. de Graaf, R. J. Boucherie, Energy-efficient data collection in wireless sensor networks with time constraints, Performance evaluation 102 (2016) 34–52.

[61] D. Williams, Probability with martingales, Cambridge university press, 1991.

[62] A. E. Susu, A. Acquaviva, D. Atienza, G. De Micheli, Stochastic modeling and analysis for environmentally powered wireless sensor nodes, in: 2008 6th International Symposium on Modeling and Optimization in Mobile, Ad Hoc, and Wireless Networks and Workshops, IEEE, 2008, pp. 125–134.

[63] M. F. Neuts, Matrix-geometric solutions in stochastic models: an algorithmic approach, Courier Corporation, 1994.

[64] A. Seyedi, B. Sikdar, Performance modelling of transmission schedulers capable of energy harvesting, Proceedings of the ICC, Cape Town.

[65] A. Seyedi, B. Sikdar, Energy efficient transmission strategies for body sensor networks with energy harvesting, IEEE Transactions on Communications 58 (7) (2010) 2116–2126.

[66] G. Park, T. Rosing, M. D. Todd, C. R. Farrar, W. Hodgkiss, Energy harvesting for structural health monitoring sensor networks, Journal of Infrastructure Systems 14 (1) (2008) 64–79.

[67] C. Alippi, C. Galperti, An adaptive system for optimal solar energy harvesting in wireless sensor network nodes, IEEE Transactions on Circuits and Systems I: Regular Papers 55 (6) (2008) 1742–1750.

[68] C. Blondia, O. Casals, Statistical multiplexing of vbr sources: A matrix-analytic approach, Performance Evaluation 16 (1–3) (1992) 5–20.

[69] S. R. Chakravarthy, A disaster queue with markovian arrivals and impatient customers, Applied Mathematics and Computation 214 (1) (2009) 48–59.

[70] J. Yick, B. Mukherjee, D. Ghosal, Wireless sensor network survey, Computer Networks 52 (12) (2008) 2292–2330.

[71] X. Lu, P. Wang, D. Niyato, D. I. Kim, Z. Han, Wireless Networks With RF Energy Harvesting: A Contemporary Survey, IEEE Communications Surveys and Tutorials 17 (2) (2015) 757–789.

[72] J. M. Jornet, I. F. Akyildiz, Joint energy harvesting and communication analysis for perpetual wireless nanosensor networks in the terahertz band, IEEE Transactions on Nanotechnology 11 (3) (2012) 570–580.

[73] Y. Dong, F. Farnia, A. Özgür, Near Optimal Energy Control and Approximate Capacity of Energy Harvesting Communication, IEEE Journal on Selected Areas in Communications 33 (3) (2015) 540–557.

[74] J. Ventura, K. Chowdhury, Markov modeling of energy harvesting body sensor networks, in: The 22th Annual IEEE International Symposium on Personal, Indoor and Mobile Radio Communications., IEEE, 2011, pp. 2168–2172.

[75] M. Mitici, J. Goseling, M. de Graaf, R. J. Boucherie, Data retrieval time for energy-harvesting wireless sensor networks, Ad Hoc Networks 53 (2016) 32–40.

[76] V. Raghunathan, C. Schurgers, S. Park, M. B. Srivastava, Energy-aware wireless microsensor networks, IEEE Signal Processing Magazine 19 (2) (2002) 40–50.

[77] M. A. Razzaque, C. Bleakley, S. Dobson, Compression in Wireless Sensor Networks: A Survey and Comparative Evaluation, ACM Transactions on Sensor Networks 10 (1) (2013) 5:1—-5:44.

[78] V. Sharma, U. Mukherji, V. Joseph, S. Gupta, Optimal energy management policies for energy harvesting sensor nodes, IEEE Transactions on Wireless Communications 9 (4) (2010) 1326–1336.

[79] R. Morsi, D. S. Michalopoulos, R. Schober, On-off transmission policy for wireless powered communication with energy storage, in: 2014 48th Asilomar Conference on Signals, Systems and Computers, IEEE, 2014, pp. 1676–1682.

[80] K. Tutuncuoglu, A. Yener, Optimum transmission policies for battery limited energy harvesting nodes, IEEE Transactions on Wireless Communications 11 (3) (2012) 1180–1189.

[81] F. M. Ozcelik, G. Uctu, E. Uysal-Biyikoglu, Optimal Packet Scheduling on an Energy Harvesting Fading Channel, CoRR.

[82] O. Ozel, K. Tutuncuoglu, J. Yang, S. Ulukus, A. Yener, Transmission with energy harvesting nodes in fading wireless channels: Optimal policies, IEEE Journal on Selected Areas in Communications 29 (8) (2011) 1732–1743.

[83] J. Fernandez-Bes, J. Cid-Sueiro, A. G. Marques, An mdp model for censoring in harvesting sensors: Optimal and approximated solutions, IEEE Journal on Selected Areas in Communications 33 (8) (2015) 1717–1729.

[84] A. Aprem, C. R. Murthy, N. B. Mehta, Transmit Power Control Policies for Energy Harvesting Sensors With Retransmissions, IEEE Journal of Selected Topics in Signal Processing 7 (5) (2013) 895–906.

[85] A. Aprem, C. R. Murthy, N. B. Mehta, Transmit power control with arq in energy harvesting sensors: A decision-theoretic approach, in: In 2012 IEEE Global Communications Conference (GLOBECOM), IEEE, 2012, pp. 3388–3393.

[86] T. H. F. Khan, D. S. Kumar, Mobile collector aided energy reduced (mcer) data collection in agricultural wireless sensor networks, in: 2016 IEEE 6th International Conference on Advanced Computing (IACC), 2016, pp. 629–633.

[87] C. Kim, H. Cho, S. Kim, T. Yang, S. H. Kim, Sink mobility support scheme for continuous object tracking in wireless sensor networks, in: 2016 IEEE 30th International Conference on Advanced Information Networking and Applications (AINA), 2016, pp. 452–457.

[88] Y. Yun, Y. Xia, Maximizing the Lifetime of Wireless Sensor Networks with Mobile Sink in Delay-Tolerant Applications, IEEE Transactions on Mobile Computing 9 (9) (2010) 1308–1318.

[89] Z. M. Wang, S. Basagni, E. Melachrinoudis, C. Petrioli, Exploiting sink mobility for maximizing sensor networks lifetime, in: Proceedings of the 38th annual Hawaii international conference on system sciences, IEEE, 2005, pp. 287a–287a.

[90] L. He, J. Pan, J. Xu, A progressive approach to reducing data collection latency in wireless sensor networks with mobile elements, IEEE Transactions on Mobile Computing 12 (7) (2013) 1308–1320.

[91] A. Mehrabi, K. Kim, Maximizing Data Collection Throughput on a Path in Energy Harvesting Sensor Networks Using a Mobile Sink, IEEE Transactions on Mobile Computing 15 (3) (2016) 690–704.

[92] X. Ren, W. Liang, The use of a mobile sink for quality data collection in energy harvesting sensor networks, in: 2013 IEEE Wireless Communications and Networking Conference (WCNC), IEEE, 2013, pp. 1145–1150.

[93] X. Ren, W. Liang, Delay-tolerant data gathering in energy harvesting sensor networks with a mobile sink, in: 2012 IEEE Global Communications Conference (GLOBECOM), IEEE, 2012, pp. 93–99.

[94] C. M. Angelopoulos, S. Nikoletseas, Aggregated mobility-based topology inference for fast sensor data collection, Computer Communications 34 (13) (2011) 1570–1579.

[95] Y. Li, L. E. Parker, A spatial-temporal imputation technique for classification with missing data in a wireless sensor network, in: 2008 IEEE/RSJ International Conference on Intelligent Robots and Systems, 2008, pp. 3272–3279.

[96] D. P. Bertsekas, S. E. Shreve, Stochastic Optimal Control: The Discrete-Time Case, Academic Press, 1978.

[97] G. Latouche, V. Ramaswami, Introduction to Matrix Analytic Methods in Stochastic Modeling, ASA-SIAM Series on Statistics and Applied Probability, Society for Industrial and Applied Mathematics, 1999.

[98] L. B. White, A New Policy Evaluation Algorithm for Markov Decision Processes with Quasi Birth-Death Structure, Stochastic Modelling 21 (2-3) (2005) 785–797.

[99] J. N. Al-Karaki, A. E. Kamal, Routing techniques in wireless sensor networks: a survey, Wireless personal communications 11 (6) (2004) 6–28.

[100] W. B. Powell, Approximate Dynamic Programming: Solving the curses of dimensionality, Vol. 703, John Wiley & Sons, 2007.

[101] D. P. de Farias, B. Van Roy, The linear programming approach to approximate dynamic programming, Operations Research 51 (6) (2003) 850–865.

[102] K. Chen, Y. Zhou, J. He, A localization scheme for underwater wireless sensor networks, International Journal of Advanced Science and Technology 4.

[103] J.-Y. Le Boudec, D. McDonald, J. Mundinger, A generic mean field convergence result for systems of interacting objects, in: Fourth international conference on the quantitative evaluation of systems (QEST 2007), IEEE, 2007, pp. 3–18.

[104] C. Namislo, Analysis of mobile radio slotted ALOHA networks, IEEE Journal on Selected Areas in Communications 2 (4) (1984) 583–588.

[105] M. Talebi, J. F. Groote, J.-P. M. Linnartz, Continuous approximation of stochastic models for wireless sensor networks, in: 2015 IEEE Symposium on Communications and Vehicular Technology in the Benelux (SCVT), IEEE, 2015, pp. 1–6.

[106] F. Cecchi, Mean-field analysis of CSMA wireless networks, in: 2016 IEEE Conference on Computer Communications Workshops (INFOCOM WKSHPS), 2016, pp. 540–541.

[107] N. Gast, B. Gaujal, J.-Y. Le Boudec, Mean field for Markov decision processes: from discrete to continuous optimization, IEEE Transactions on Automatic Control 57 (9) (2012) 2266–2280.

[108] H. Tembine, S. Lasaulce, M. Jungers, Joint power control-allocation for green cognitive wireless networks using mean field theory, in: 2010 Proceedings of the Fifth International Conference on Cognitive Radio Oriented Wireless Networks and Communications, IEEE, 2010, pp. 1–5.

[109] F. Mériaux, S. Lasaulce, H. Tembine, Stochastic differential games and energy-efficient power control, Dynamic Games and Applications 3 (1) (2013) 3–23.

[110] W. F. Feehery, P. I. Barton, Dynamic optimization with state variable path constraints1, Computers & Chemical Engineering 22 (9) (1998) 1241–1256.

[111] R. W. L. Coutinho, A. Boukerche, L. F. M. Vieira, A. A. F. Loureiro, Design guidelines for opportunistic routing in underwater networks, IEEE Communications Magazine 54 (2) (2016) 40–48.

[112] H. Yan, Z. J. Shi, J.-H. Cui, Dbr: depth-based routing for underwater sensor networks, in: International conference on research in networking, Springer, 2008, pp. 72–86.

[113] G. Tuna, V. C. Gungor, A survey on deployment techniques, localization algorithms, and research challenges for underwater acoustic sensor networks, International Journal of Communication Systems 30 (17) (2017) e3350.

[114] Z. Guan, T. Melodia, D. Yuan, Stochastic channel access for underwater acoustic networks with spatial and temporal interference uncertainty, in: Proceedings of the Seventh ACM International Conference on Underwater Networks and Systems, ACM, 2012, pp. 18:1—-18:8.

[115] F. Pignieri, F. De Rango, F. Veltri, S. Marano, Markovian approach to model underwater acoustic channel: Techniques comparison, in: MILCOM 2008-2008 IEEE Military Communications Conference, IEEE, 2008, pp. 1–7.

[116] Z. Zhou, Z. Peng, J.-H. Cui, Z. Shi, Efficient multipath communication for time-critical applications in underwater acoustic sensor networks, IEEE/ACM Transactions on Networking 19 (1) (2011) 28–41.

[117] M. Faheem, G. Tuna, V. C. Gungor, LRP: Link quality-aware queue-based spectral clustering routing protocol for underwater acoustic sensor networks, International Journal of Communication Systems 30 (12).

[118] A. Stefanov, M. Stojanovic, Design and performance analysis of underwater acoustic networks, IEEE Journal on Selected Areas in Communications 29 (10) (2011) 2012–2021.

[119] F. A. de Souza, B. S. Chang, G. Brante, R. D. Souza, M. E. Pellenz, F. Rosas, Optimizing the number of hops and retransmissions for energy efficient multi-hop underwater acoustic communications, IEEE Sensors Journal 16 (10) (2016) 3927–3938.

[120] D. Marinakis, K. Wu, N. Ye, S. Whitesides, Network optimization for lightweight stochastic scheduling in underwater sensor networks, IEEE Transactions on Wireless Communications 11 (8) (2012) 2786–2795.

[121] L. M. Brekhovskikh, Lysanov, Fundamentals of ocean acoustics, Springer, 2003.

[122] D. Li, J. Du, L. Liu, A data routing algorithm based on markov model in underwater wireless sensor networks, in: 2016 IEEE International Conference on Ubiquitous Wireless Broadband (ICUWB), IEEE, 2016, pp. 1–4.

[123] M. Jafri, A. Marin, A. Torsello, M. Ghaderi, On the optimality of opportunistic routing protocols for underwater sensor networks, in: Proceedings of the 21st ACM International Conference on Modeling, Analysis and Simulation of Wireless and Mobile Systems, 2018, pp. 207–215.

[124] H. Yu, N. Yao, T. Wang, G. Li, Z. Gao, G. Tan, WDFAD-DBR: Weighting depth and forwarding area division DBR routing protocol for UASNs, Ad Hoc Networks 37 (2016) 256–282.

[125] M. A. Rahman, Y. Lee, I. Koo, EECOR: an energy-efficient cooperative opportunistic routing protocol for underwater acoustic sensor networks, IEEE Access 5 (2017) 14119–14132.

[126] C.-M. Chao, C.-H. Jiang, W.-C. Li, DRP: An energy-efficient routing protocol for underwater sensor networks, International Journal of Communication Systems 30 (15).

[127] S. Basagni, C. Petrioli, R. Petroccia, D. Spaccini, Carp: A channel-aware routing protocol for underwater acoustic wireless networks, Ad Hoc Networks 34 (2015) 92–104.

[128] P. Xie, Z. Zhou, Z. Peng, J.-H. Cui, Z. Shi, SDRT: A reliable data transport protocol for underwater sensor networks, Ad Hoc Networks 8 (7) (2010) 708–722.

[129] N. Nowsheen, G. Karmakar, J. Kamruzzaman, Pradd: A path reliability-aware data delivery protocol for underwater acoustic sensor networks, Journal of Network and Computer Applications 75 (2016) 385–397.

[130] M. R. Jafri, S. Ahmed, N. Javaid, Z. Ahmad, R. J. Qureshi, Amctd: Adaptive mobility of courier nodes in threshold-optimized dbr protocol for underwater wireless sensor networks, in: 2013 Eighth International Conference on Broadband and Wireless Computing, Communication and Applications, IEEE, 2013, pp. 93–99.

[131] M. Stojanovic, On the relationship between capacity and distance in an underwater acoustic communication channel, ACM SIGMOBILE Mobile Computing and Communications Review 11 (4) (2007) 34–43.

[132] P. S. Duke, Direct-sequence spread-spectrum modulation for utility packet transmission in underwater acoustic communication networks, Tech. rep., Naval Postgraduate school Monterey CA, USA (2002).

[133] L. Freitag, M. Grund, S. Singh, J. Partan, P. Koski, K. Ball, The whoi micro-modem: an acoustic communications and navigation system for multiple platforms, in: Proceedings of OCEANS 2005 MTS/IEEE, 2005, pp. 1086–1092 Vol. 2.

[134] Y. Noh, U. Lee, P. Wang, B. S. C. Choi, M. Gerla, VAPR: void-aware pressure routing for underwater sensor networks, IEEE Transactions on Mobile Computing 12 (5) (2013) 895–908.

[135] S. Asmussen, P. W. Glynn, Stochastic Simulation: Algorithms and Analysis, Springer, 2007.